

NAVAL POSTGRADUATE SCHOOL

Monterey, California



THESIS

OPTIMAL IMPULSE CONDITIONS FOR DEFLECTING EARTH CROSSING ASTEROIDS

by

Jeffrey T. Elder

June, 1997

Thesis Advisors:

I. Michael Ross
David Cleary

Approved for public release; distribution is unlimited.

19980102/28

INFO QUALITY INSPECTED 4

REPORT DOCUMENTATION PAGE			Form Approved OMB No. 0704-0188	
Public reporting burden for this collection of information is estimated to average 1 hour per response, including the time for reviewing instruction, searching existing data sources, gathering and maintaining the data needed, and completing and reviewing the collection of information. Send comments regarding this burden estimate or any other aspect of this collection of information, including suggestions for reducing this burden, to Washington Headquarters Services, Directorate for Information Operations and Reports, 1215 Jefferson Davis Highway, Suite 1204, Arlington, VA 22202-4302, and to the Office of Management and Budget, Paperwork Reduction Project (0704-0188) Washington DC 20503.				
1. AGENCY USE ONLY (Leave blank)	2. REPORT DATE June 1997	3. REPORT TYPE AND DATES COVERED Master's Thesis		
4. TITLE AND SUBTITLE OPTIMAL IMPULSE CONDITIONS FOR DEFLECTING EARTH CROSSING ASTEROIDS.		5. FUNDING NUMBERS		
6. AUTHOR Elder, Jeffrey T.				
7. PERFORMING ORGANIZATION NAME(S) AND ADDRESS(ES) Naval Postgraduate School Monterey CA 93943-5000		8. PERFORMING ORGANIZATION REPORT NUMBER		
9. SPONSORING/MONITORING AGENCY NAME(S) AND ADDRESS(ES)		10. SPONSORING/MONITORING AGENCY REPORT NUMBER		
11. SUPPLEMENTARY NOTES The views expressed in this thesis are those of the author and do not reflect the official policy or position of the Department of Defense or the U.S. Government.				
12a. DISTRIBUTION/AVAILABILITY STATEMENT Approved for public release; distribution is unlimited.			12b. DISTRIBUTION CODE	
13. ABSTRACT (maximum 200 words) An analysis of the effects of small impulses on Earth impacting asteroids is presented. The analysis is performed using a numerical routine for an exact, two-body, analytic solution. The solution is based on two-dimensional, two-body, Earth intersecting elliptical orbits. Given the asteroid eccentricity, time prior to impact and impulse magnitude and direction, an analysis of impulse-to-minimum-separation distance is generated. Impulse times prior to impact from zero to a few orbits are considered. The analysis is presented as three-dimensional plots of minimum separation distance as a function of impulse magnitude, direction, and time prior to impact. The general result is that for long lead times the optimal impulse occurs at the perihelia of the asteroid's orbit in the direction of the velocity vector, in the orbital plane. For short lead times the optimal impulse direction becomes more normal to the velocity vector, in the orbital plane, as the asteroid approaches the Earth.				
14. SUBJECT TERMS Asteroid, Comet, Earth Crossing Asteroid, Impact Hazard, Impulse , Near Earth Object, Optimum, Perturbation			15. NUMBER OF PAGES 114	
			16. PRICE CODE	
17. SECURITY CLASSIFICATION OF REPORT Unclassified	18. SECURITY CLASSIFICATION OF THIS PAGE Unclassified	19. SECURITY CLASSIFICATION OF ABSTRACT Unclassified	20. LIMITATION OF ABSTRACT UL	

NSN 7540-01-280-5500

Standard Form 298 (Rev. 2-89)
Prescribed by ANSI Std. Z39-18 298-102

Approved for public release; distribution is unlimited.

**OPTIMAL IMPULSE CONDITIONS FOR DEFLECTING EARTH CROSSING
ASTEROIDS**

Jeffrey T. Elder
Lieutenant, United States Navy
B.S., Iowa State University, 1988

Submitted in partial fulfillment
of the requirements for the degrees of

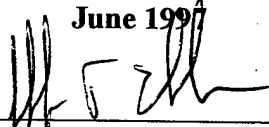
**MASTER OF SCIENCE IN ASTRONAUTICAL ENGINEERING
AND
MASTER OF SCIENCE IN APPLIED PHYSICS**

from the


NAVAL POSTGRADUATE SCHOOL

June 1997

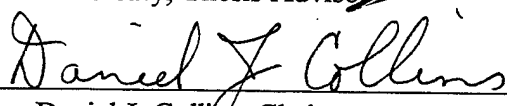
Author:

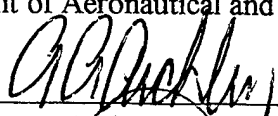

Jeffrey T. Elder

Approved by:


I. M. Ross, Thesis Advisor


D. Cleary, Thesis Advisor


Daniel J. Collins, Chairman
Department of Aeronautical and Astronautical Engineering


Anthony Atchley, Chairman
Department of Physics

ABSTRACT

An analysis of the effects of small impulses on Earth impacting asteroids is presented. The analysis is performed using a numerical routine for an exact, two-body, analytic solution. The solution is based on two-dimensional, two-body, Earth intersecting elliptical orbits. Given the asteroid eccentricity, time prior to impact and impulse magnitude and direction, an analysis of impulse-to-minimum-separation distance is generated. Impulse times prior to impact from zero to a few orbits are considered. The analysis is presented as three-dimensional plots of minimum separation distance as a function of impulse magnitude, direction, and time prior to impact. The general result is that for long lead times the optimal impulse occurs at the perihelia of the asteroid's orbit in the direction of the velocity vector, in the orbital plane. For short lead times the optimal impulse direction becomes more normal to the velocity vector, in the orbital plane, as the asteroid approaches the Earth.

TABLE OF CONTENTS

I. INTRODUCTION	1
II. SOLAR SYSTEM OBJECT ORIGINS.....	5
A. SOLAR SYSTEM FORMATION	5
B. PLANETARY FORMATION	5
C. ASTEROID AND COMET FORMATION	5
D. ASTEROIDS	6
E. COMETS	10
III. IMPACT RECORD.....	13
A. LUNAR IMPACT RECORD.....	13
B. TERRESTRIAL IMPACT RECORD	13
C. OTHER PLANETARY IMPACTS.....	15
D. IMPACT SCALE	15
IV. ORBITS.....	19
A. CONIC SECTIONS	19
B. COORDINATE FRAMES.....	19
C. ORBITAL ELEMENTS	20
D. KEPLER'S SECOND LAW	21
V. PROBLEM FORMULATION AND SOLUTION	23
A. STATEMENT.....	23
B. ASSUMPTIONS	23
C. TEMPORAL CONSIDERATION	23
D. METHOD OF SOLUTION	23
VI. PROGRAM VALIDATION.....	33
A. NUMERICAL SIMULATION	33
B. APPROXIMATE ANALYTIC SOLUTIONS.....	34
VII. ANALYSIS AND RESULTS	37
A. ANALYSIS.....	37
B. RESULTS	40
VIII. APPLICATION TO A REAL CASE	43
A. IMPULSE ACHIEVABLE.....	43
B. TOUTATIS	44
IX. FURTHER CONSIDERATIONS.....	47
A. LONG RESPONSE TIME	47
B. THREE-DIMENSIONAL ANALYSIS.....	47
C. ECCENTRICITY VARIATIONS.....	47
D. SHORT RESPONSE TIME	47

REFERENCES	49
BIBLIOGRAPHY	53
APPENDIX A. DETAILED SOLUTION METHOD	55
APPENDIX B. ANALYTIC SOLUTION METHOD, MATLAB MODEL	75
APPENDIX C. NUMERICAL VALIDATION MODEL	81
APPENDIX D. ANALYTIC METHOD SCENARIO MODELS	83
INITIAL DISTRIBUTION LIST	105

I. INTRODUCTION

The possibility that a large asteroid may impact the Earth delivering an energy in excess of 30 MT of TNT is a very real threat. One only has to look at the Moon in the night sky to gain an appreciation for the magnitude and probability of such an impact. How the human race deals with the threat of such an impact is of significant interest to the planet Earth as a whole.

As discussed by Rather et. al. (1992), as early as 1705, when Edmund Halley wrote *A Synopsis of the Astronomy of Comets*, there has been speculation that an extraterrestrial object might impact the Earth. the possibility of such impacts was not perceived as a threat to life on Earth until the late 1940's when the Moon's craters were fully understood to be the result of impact events, not volcanism, and that the Earth is subject to the same impact hazard. Rather et. al (1992) also mention that the magnitude of the threat was not fully realized until the late 1970s to early 1980s. The perceived threat began to stand upon a solid foundation with the publication by Alvarez et. al. (1980) of a theory on the extinction of the dinosaurs due to the impact of a large asteroid or comet 65 million years ago. The theory put forth by Alvarez et. al. suggests that an impact by a 10 km diameter asteroid at the Chicxulub site off of the Yucatan peninsula indirectly caused the extinction of 60% of all life on the Earth, including the dinosaurs.

Since the awareness of the possibility of an asteroid impacting the Earth began developing in the mid 20th century, there have been several "near misses" recorded. Perhaps the most spectacular near miss was a large fireball created by an object racing across the daytime sky in a northerly direction that entered the Earth's atmosphere above Utah in the United States and exited above Alberta, Canada on the 10th of August, 1972. The object observed was determined to be an asteroid upwards of 30 meters in diameter as reported in *Sky and Telescope Magazine* (1972). Had this asteroid's trajectory been ever so slightly different, mankind would have had its first opportunity to observe a large object impact the Earth. Such an impacting object would carve out a crater 200 to 500 meters in diameter. Since then, several other asteroids and comets have been detected passing by the Earth at distances less than a few hundred thousand kilometers. Apollo Asteroid 1989FC, referenced by the AIAA Space Systems Technical Committee; Asteroid

1991BA, reference by Scotti et. al. (1991); and Asteroid 1996JA1 referenced by Jaroff (1996) are three asteroids discovered recently passing very close to Earth. On an astronomical scale, these close approaches are essentially impacts.

In April of 1990 the American Institute of Aeronautics and Astronautics issued the position paper entitled *Dealing with the Threat of an Asteroid Striking the Earth* that briefly described the implications of an asteroid impact. The AIAA found that "Earth-orbit-crossing asteroids clearly present a danger to the Earth and its inhabitants." It was recommended that a "systematic and open program" for detection of Earth crossing asteroids be established as well as a study to "define systems which can deflect or destroy, or significantly alter the orbits of, asteroids predicted to impact the Earth." A few search programs existed prior to the position paper and a few others have begun subsequently.

As a result of the awareness of the possibility of an asteroid or comet impacting the Earth, the National Aeronautics and Space Administration has sponsored two workshops to study the fundamentals of the impact and impact mitigation problem. The first workshop is summarized in the report entitled "The Spaceguard Survey: Report of the NASA-International Near-Earth-Object Detection Workshop." The second workshop is summarized in the report entitled "Near-Earth-Object Interception Workshop." The concentration of the workshops have been related to assessing the magnitude of the threat, impact effects and hazards to the Earth, as well as the political implications of developing an impact mitigation capability. Several books have been published on the matter, both technical and non-technical, and more than one Hollywood movie has been based on the subject. Two spacecraft exploration missions, Near Earth Asteroid Rendezvous (NEAR) and Clementine, have included intercepts of asteroids as a major part of their mission to study the nature of asteroids. However, little "astrodynamical analysis" has been performed on the feasibility of the impact mitigation problem.

The astrodynamical analysis of feasibility is where this thesis is intended to fit into the larger problem. Presented is an analysis of the impact and mitigation problem based on a two-dimensional and two-body analysis. It is intended to be a first order approximation for the solution of a larger problem. However, it is a more rigorous treatment of the astrodynamics of the hazard than previous published analyses, such as

Ahrens and Harris (1994). Included in the following analysis is the periodic nature of the problem as well as the near term effects. The analysis is not concerned with object detection or orbit prediction, but instead centers on how impulses applied to an asteroid at various points on the asteroid's orbit affect the outcome when there is a presumption of collision otherwise. Mission design for mitigation is not a goal of the following analysis; however, the analysis tool presented may be utilized in determining a first order estimate for optimizing the time and position of asteroid intercept for impact mitigation.

Presented first is an astronomical development of the existence of an asteroid impact problem from the origins of the solar system to the record of past impacts on the Earth followed by a brief description of two-body orbits. The problem is then presented with governing assumptions and a method of solution. The solution method is then assessed and validated followed by an analysis of an asteroid impact scenario with a discussion of the results. The analysis method is then applied to the asteroid Toutatis which will make several close approaches to the Earth over the next decade.

II. SOLAR SYSTEM OBJECT ORIGINS

A. SOLAR SYSTEM FORMATION

Current theories of formation of the Solar System stem from the post initial expansion universe environment of gas, dust, radiation, and magnetic fields in a nonuniform distribution. Bouyed by the interplay of gravitational, magnetic, and pressure forces local mass concentrations began to form. This interplay of forces on the non-uniform environment sets up initial angular momentum conditions for very large three-dimensional structures. These large rotating structures began to coalesce into accretion disks around central masses. These central masses eventually reached critical mass for fusion to occur and stars emerged. We call our local star the Sun.

B. PLANETARY FORMATION

In a similar fashion to the stellar formation, the accretion disk around the Sun provided the environment for smaller mass concentrations and accretion disks to form thus producing small scale structures called planetismals composed of the basic chemical elements in varying quantities. Gravitational attraction and relative motion of these planetismals caused them to collide with one another and cohesive forces enabled some to remain attached forming larger structures. After enough of these interactions occurred, the planets began to form. Unlike for the stellar conditions, the planets do not possess the critical mass to initiate and sustain a fusion reaction. This allows for large scale assembly of solid, aqueous and gaseous structures to take place in quantities and composition proportional the relative percentages of chemical elements present in the planetismals. These structures are more familiar on the Earth as the crust, the oceans and the atmosphere. Analysis of the elements present from the impact delivery mechanism and current known compositions of asteroids and comets suggests that this was the mechanism of organic and non-organic material delivery that formed the Earth as proposed by Chyba et. al. (1994).

C. ASTEROID AND COMET FORMATION

However, not all of the accretion disk surrounding the Sun coalesced into either the Sun, the Planets or their satellites. The remainder of the planetismals continue to be dispersed throughout the Solar System in the form of asteroids and comets. The asteroids

being located primarily within the inner Solar System, and the comets existing in the outer Solar System and beyond.

The asteroids are mainly concentrated in the asteroid belt located between the orbits of Mars and Jupiter. The remainder of the asteroids are dispersed throughout the solar system in elliptical orbits lying mainly inside the orbit of Jupiter. There are several theories of how the asteroid belt came to exist. These ideas include the destruction of a planet, or the inability of a planet to form, due to the tidal forces of Jupiter. There are several theories accounting for the formation of the asteroids not located in the asteroid belt. These ideas range from planetismals that have never collided and attached themselves to another planetary body, to cast off remnants of massive collisions of planetary bodies with very large planetismals, to objects from the asteroid belt that may have been perturbed by a passing object into a smaller orbit. All of the ideas have some amount of merit that give them validity.

Comets are believed to originate from the Oort Cloud of cometary material orbiting the Sun at a distance of some 50,000AU. From this cloud, comets are believed to be injected into the solar system by orbital perturbations due to the gravitational field of passing stars. Once injected into the solar system, gravitational encounters with the Sun and Jupiter may further perturb the comets' orbit and either "capture" the comet, so it remains within the solar system, or "assist" the comet on its way to interstellar space. Additionally, there is believed to exist a band of icy objects that extends from the orbit of Neptune at 30 AU out to as much as 100 AU. These objects are said to be located in the Kuiper Belt, so named after Gerard Kuiper, who first proposed their existence in 1951. The objects that form the Kuiper belt range in size and orbital characteristics to the extent that it is believed that Pluto may actually be a member of this group as discussed by Jewitt and Luu (1995).

D. ASTEROIDS

1. Location

The asteroids are of particular interest as potential impact hazards in that they have a greater mass density than comets and are more likely to reach the surface of the Earth in a given impact scenario. The majority of the asteroids are located in the asteroid belt

between the orbits of Mars and Jupiter. Very few asteroids have been detected beyond the orbit of Jupiter. This lack of detection may only be an effect of the limited capability of current detection sensors. However, a significant number of asteroids in orbits smaller than that of the typical asteroid belt object have been identified. These are the objects of primary concern for the problem of mitigation.

2. Quantities

Literally thousands of asteroids have been observed and identified orbiting the Sun. Of those, more than 300 are considered near Earth asteroids (NEA's) and pose a threat as a potential impacting object. Of greater concern are the subset of NEA's dubbed Earth crossing asteroids (ECA's) which are currently about 200 in number. The orbits of the ECA's are such that they allow for the possibility of impact with the Earth at some future date. These ECA's range in size from 10 km down to 0.1 km, which is currently the limit of detection of asteroids by Earth based sensors. Estimates for ECA's near and above 10 km in diameter indicate that all of the asteroids have been identified and that for the ECA's of 1 km in diameter or less, the identified asteroids represent only about 10% of those that are believed to exist, as stated by Grieve and Shoemaker (1994).

3. Classification

Classification of the ECA's are determined with respect to the Earth's orbital extrema. The Earth's perihelion and aphelion distances are 0.9833 and 1.0167 AU respectively. The orbits of the ECA's all have perihelia less than the aphelion of the Earth orbit and aphelia greater than the perihelion of the Earth orbit. The ECA's have been subdivided into three classes, the Atens, Apollos and Amors, based on their orbital characteristics as discussed by Rabinowitz et. al. (1994). Table 1 summarizes the distinction between the three classes. Figures 1, 2 and 3 depict typical orbits of each of the three classes.

Class Name	Semi-Major Axis a (AU)	Perihelion Distance q (AU)	Aphelion Distance Q (AU)
Aten	< 1	-	> 0.9833
Apollo	> 1	< 1.0167	-
Amor	-	$1.0167 < q < 1.3$	-

Table 1. ECA Classes

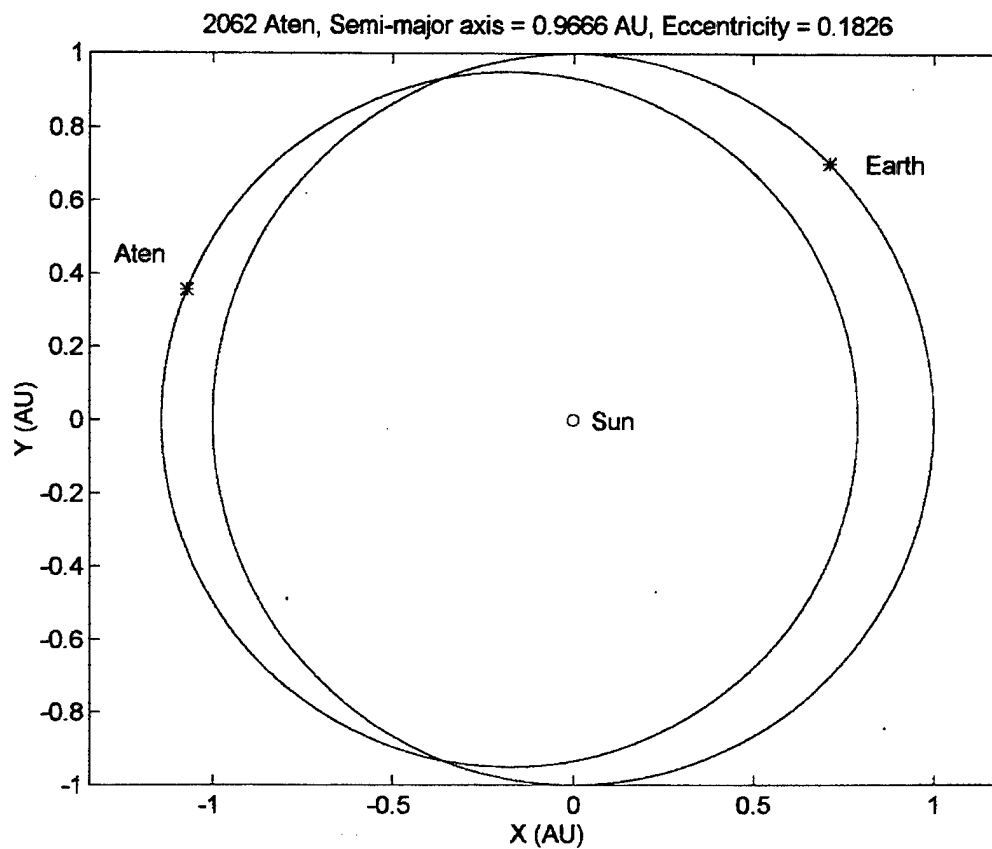


Figure 1. Typical Aten Orbit

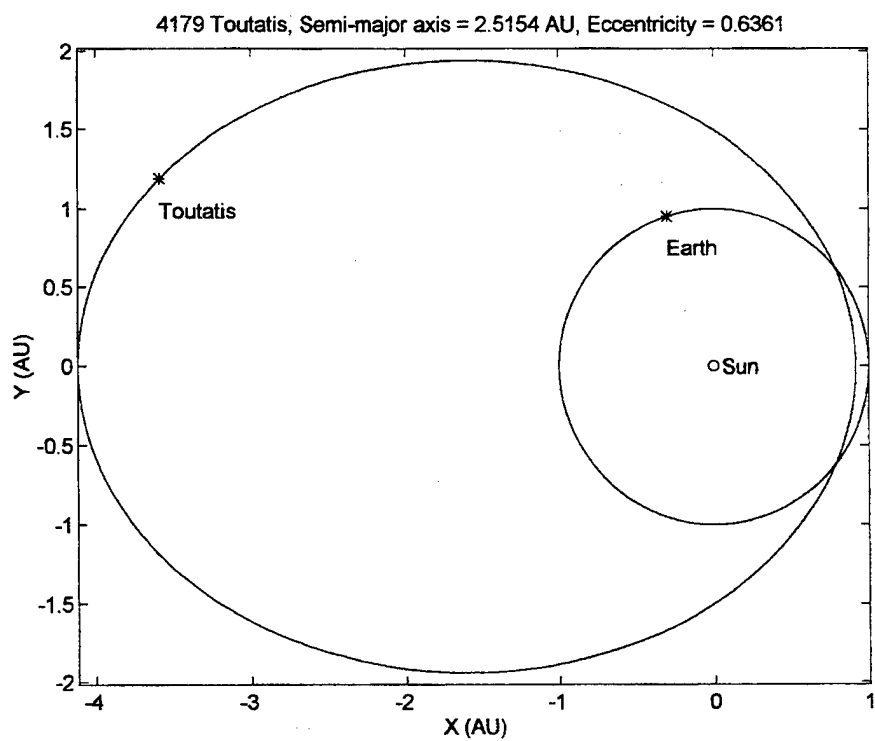


Figure 2. Typical Apollo Orbit

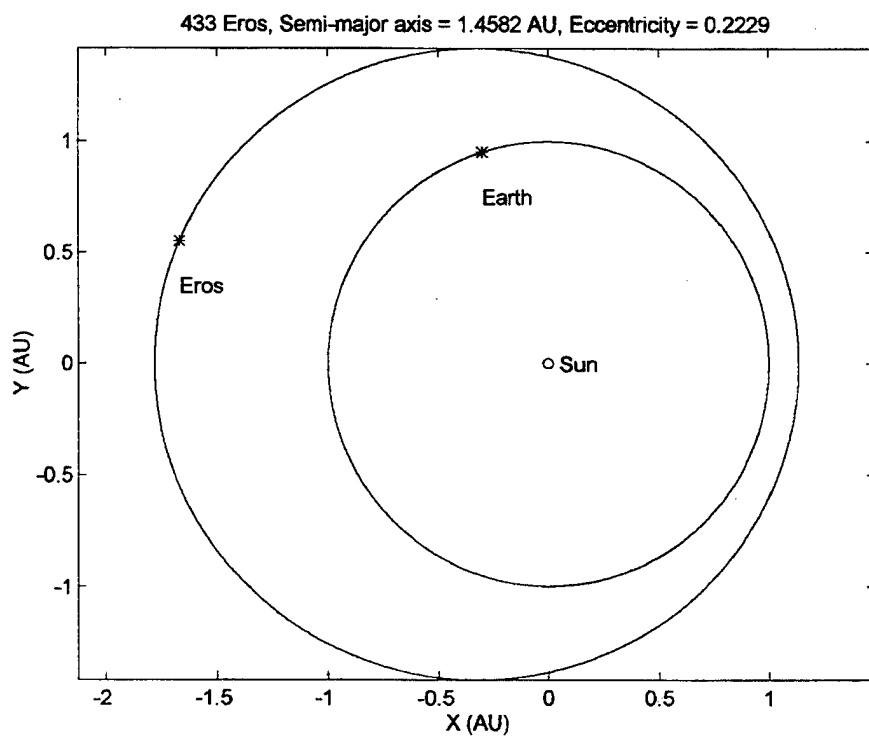


Figure 3. Typical Amor Orbit

4. Physical Properties

The physical properties of the asteroids are generally that of “rocky”, irregularly shaped spinning objects. Estimates of asteroid densities range from a more cometary density of $2 \times 10^3 \text{ kg m}^{-3}$ to a dense asteroid of $5 \times 10^3 \text{ kg m}^{-3}$ with a mean density of about $3 \times 10^3 \text{ kg m}^{-3}$. Asteroids have been observed that are composed of a single solid mass as well as multiple mass centers either physically connected or gravitationally bound at a contact surface. As stated by Winters (1996), some of the asteroids may actually be aggregates of numerous smaller bodies that are gravitationally bound together. This hypotheses is further supported by analysis of object spin motion. It appears the many asteroids spin at angular rates sufficiently slow as to permit gravitational binding. The case of the comet Shoemaker-Levy 9 supports these theories in that it was gravitationally separated by tidal forces from a previous passage of Jupiter prior to its 1994 impact.

E. COMETS

1. Location

Early in the 20th century, Jan Oort hypothesized that virtually all of the comets originate in a cloud of cometary matter beginning some 50,000AU from the Sun. The so called Oort cloud is assumed to be a uniformly distributed spherical shell that surrounds the solar system and extends to approximately half of the distance to the nearest star, Alpha Centauri. From this cloud, comets are injected into the solar system by orbital perturbations of passing stars. Once inside the solar system the comets may be further perturbed by the planets. The planetary perturbations may “capture” the comet in the interior of the solar system or it may assist the comet on its way ejecting it from the solar system for all time.

2. Quantities

The number of comets in the Oort cloud is believed to be diminishing, however the remaining number is believed to be on the order of 10^{12} . The quantity of comets that exist within the solar system is far smaller, only 100 or fewer have been identified.

3. Classification

The “captured” comets are classified as periodic comets and are subdivided into two groups as summarized by Shoemaker et. al. (1994). Members of “Jupiter’s Family”

have aphelia close to Jupiter's mean orbital distance from the Sun and have periods of less than 20 years. Members of the "Halley family" are the so called long period comets and have orbital periods greater than 20 years but less than 200 years.

4. Physical Properties

Comets are primarily composed of "rock" and "ice." As such they have been sometimes called "dirty snowballs" or "icy dirtballs" depending on their relative composition. The icy material is believed to be composed of water, methane or ammonia. The rocky material is a variety of carbonaceous substances. Their mean density is less than that of the asteroids and is estimated to be about 1000 to 2000 kg m⁻³. As a comet "burns" off its icy material from repeated encounters with the Sun, the nucleus may in fact become an asteroid of a somewhat smaller dimension.

III. IMPACT RECORD

Occasionally an asteroid or a comet's orbit is such that it actually hits another object within solar system such as the event, widely celebrated in the media, of comet Shoemaker-Levy 9 impacting the planet Jupiter on the 16th of July, 1994. The very same mechanism that caused the solar system, in particular the Earth, to form and sustain life now threatens the very same life.

A. LUNAR IMPACT RECORD

One theory of the origin of the Moon, as mentioned by Chapman and Morrison (1994) describes it forming as the result of a Mars size object impacting the Earth early in its existence. The ejecta from the event is believed to have behaved in such a fashion as to remain in orbit and coalesce into what is now the Moon. Further evidence of such impacts is the cratered face of the lunar surface. The Moon displays literally millions of impact sites. Since the Moon has no atmosphere or large scale geologic processes there is no erosion of the impact record, unless by subsequent impact the previous impact structure is destroyed. Thus, the Moon serves as a reminder for all time of the nature of the impact hazard.

B. TERRESTRIAL IMPACT RECORD

On our planet Earth, the atmosphere, oceans, volcanism and plate tectonics tend to erode past impact sites. As discussed by Grieve and Shoemaker (1994) there are currently about 140 known impact craters around the world. The locations of these sites are displayed in Figure 4.

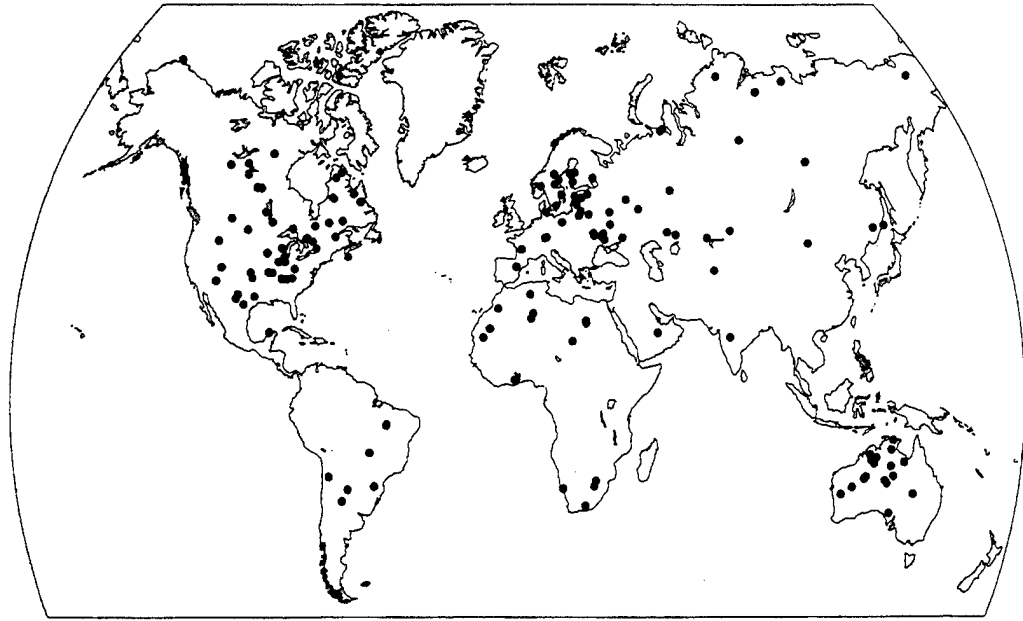


Figure 4. Known Impact Site Locations from Grieve and Shoemaker (1994)

These impact craters range in size from 1.5 km in up to 200 km in diameter. Perhaps the best example of a classic impact crater is the 1.5 km diameter Barringer Crater located in Arizona, see Figure 5. Barringer Crater is believed to be the most recent impact site on Earth having formed around 50,000 years ago.

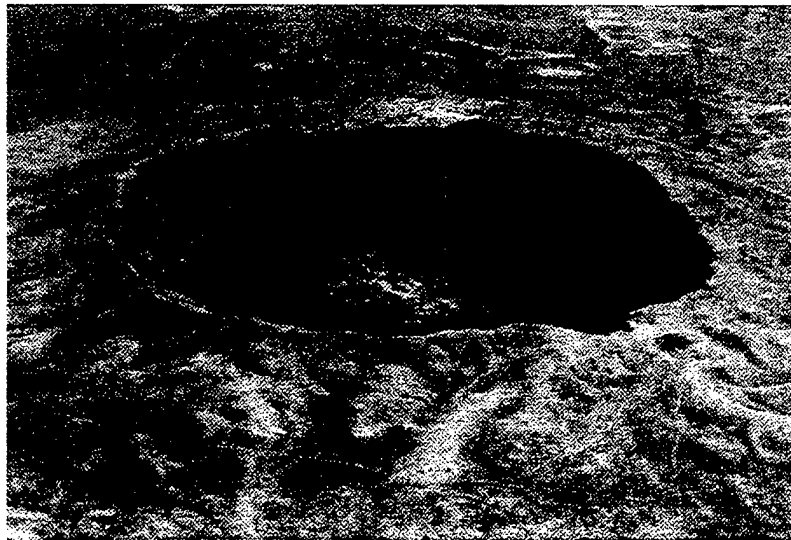


Figure 5. Barringer Crater from Grieve and Shoemaker (1994)

However, the most recent impact event to have resulted in surface damage is believed to be the Tunguska event which took place over northern Siberia in 1908. The

Tunguska event is believed to be the result of a 60 m diameter comet or light asteroid that exploded 10 km up in the atmosphere releasing some 30 MT of energy leveling 2500 square kilometers of forest. The Tunguska event is characteristic of a small scale impact occurrence. On the large scale end of the impact spectrum lies the K/T impact event so called by its occurrence in time at the boundary of the Cretaceous and Tertiary periods. It is believed that an enormous asteroid some 10 kilometers in diameter created the 200 km diameter Chicxulub impact site beneath the Gulf of Mexico off the coast of the Yucatan peninsula and is responsible for the extinction of 60% of the living species on Earth 65 million years ago.

There have been numerous recent close calls of asteroids impacting the Earth. Jaroff (1996) describes a near impact as recently as June of 1996 where an object roughly 600m in diameter passed within 450,000 kilometers (about 70 Earth radii) of the Earth.

C. OTHER PLANETARY IMPACTS

Numerous impact sites have been observed by planetary exploration spacecraft that have been sent to Venus and Mars. As mentioned above, Comet Shoemaker-Levy 9 impacted the planet Jupiter in July of 1994.

D. IMPACT SCALE

The energies released by the impact of asteroids on the Earth are quite large. It is conventional to express the impact energy in terms of megatons of TNT (MT), where $1\text{MT} = 4.2 \times 10^{15}\text{J}$. With the assumption of a mean asteroid density of 3000 kg m^{-3} a size versus impact velocity relation may be made for a given impact energy. Figure 6 displays an estimate of asteroid mass versus impact velocity for a range of impact energies from tens of megatons of TNT up to a petaton (10^{15}) of TNT. The diameter estimate assumes an effective spherical radius corresponding to the mass for the same impact energy and velocity.

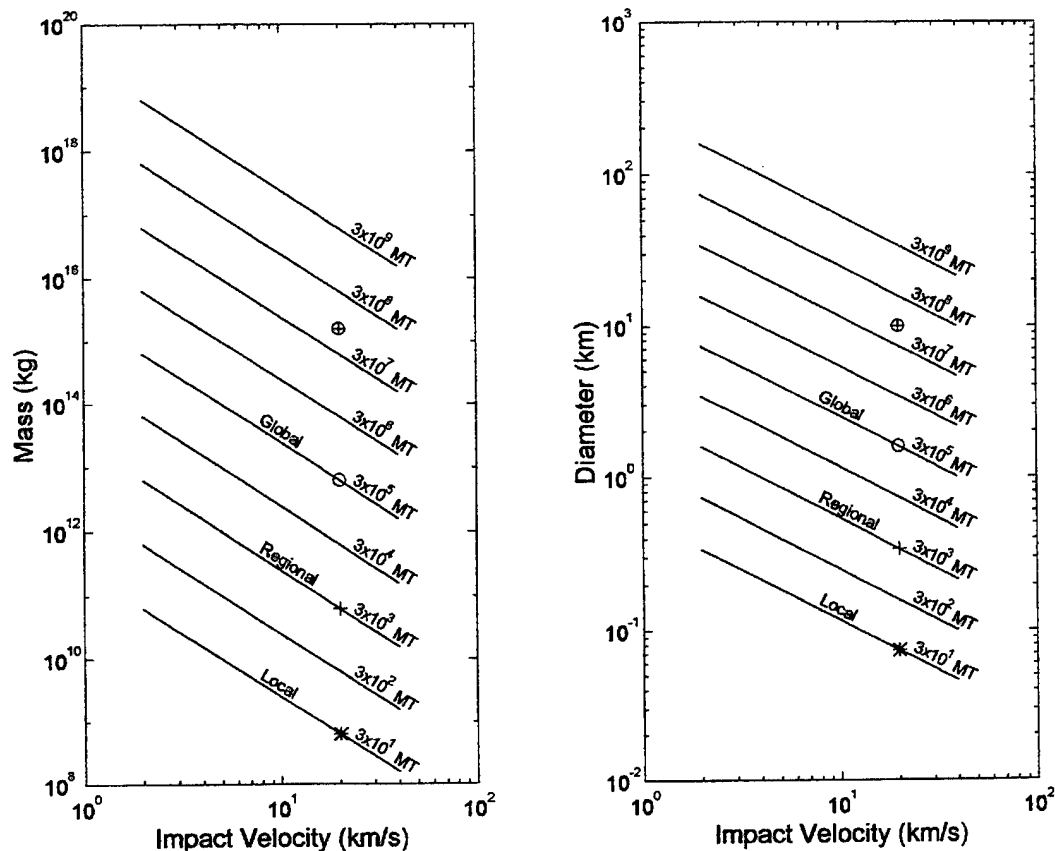


Figure 6. Impact Scale

Estimates of impact energy and terrestrial devastation have lead to the classification of impacts as local, regional, and global events as described in Morrison et. al. (1994). The distinction between these is somewhat blurred, however it is proposed that local events correspond to impact energies in the vicinity of 30 MT or less which will affect approximately 0.001% of the Earth's surface area or about the size of a large metropolitan area. Regional impact events are those that release energy in the vicinity of 300 MT to 3×10^4 MT and affect about 0.1% of the Earth's surface or about the size of a large state. Global events are considered to be impacts that release energies near and above 3×10^5 MT affecting approximately 10% of the Earth's surface area or about the size of a large country. These large events may cause such disruption of the ecological environment by particulate injection into the atmosphere that greater than 25% of the Earth's population may be eliminated. Figure 6 also shows several representative impact

scenarios for a typical impact velocity of 20 km s^{-1} . The Tunguska event is depicted by the '*' symbol. Tunguska represents a nearly classical local impact event of an object some 60 m in diameter. The recent May 1996 near miss is depicted by the '+' symbol and represents a regional event for an object some 600 m in diameter. A global impact is indicated by the 'o' symbol and corresponds to an asteroid some 1.5 km in diameter. The '⊕' symbol represents the K/T event that created the Chicxulub impact site and corresponds to a 10 km diameter object. It is noted that the K/T event is well above the threshold for global catastrophe.

IV. ORBITS

A. CONIC SECTIONS

In a simple inverse square gravitational field, orbits take the shape of conic sections. For an object that lacks sufficient energy to escape the gravitational attraction of the central body, the resultant orbit will take the shape of an ellipse. For an object with sufficient energy to escape the gravitational attraction of the central body, the resulting orbit will take the shape of a hyperbola. The transition from an elliptical to hyperbolic orbit occurs along an "escape" trajectory shaped as a parabola. Straight line orbits that lead to collision of the orbiting body with its mass center are special cases of elliptical, parabolic, and hyperbolic orbits.

B. COORDINATE FRAMES

1. Three-dimensional

To define the physical problem in time and space a reference frame needs to be established. For the general three-dimensional case a Cartesian Sun-centered inertial, or Heliocentric, coordinate frame is chosen. Figure 7 displays the orientation of the Heliocentric coordinate frame.

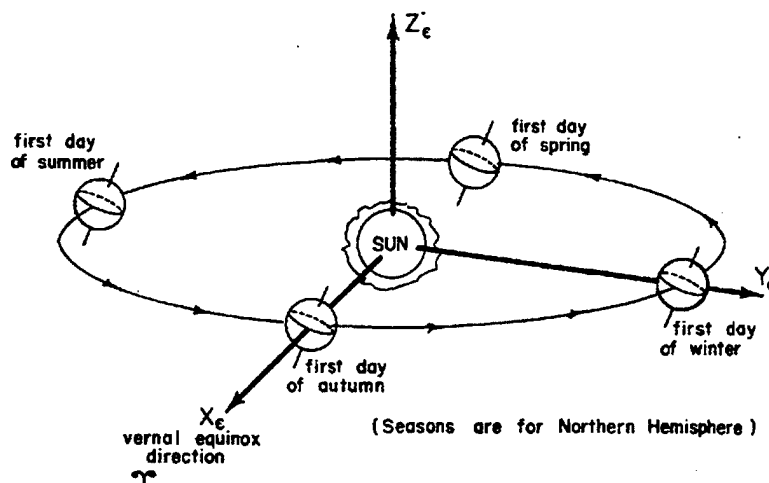


Figure 7. Heliocentric Coordinate System from Bate et. al. (1971)

The direction in the ecliptic plane from the Sun to the First point of Aries serves as the primary coordinate direction in the Heliocentric frame. The ecliptic normal serves as the “vertical” coordinate and is defined as positive in the northern half of the celestial sphere. The last coordinate direction is defined by taking the cross product of the previous two coordinate directions.

2. Two-dimensional

To simplify matters for the present analysis, a two-dimensional planar perifocal coordinate frame is chosen. The principal axis defining a two-dimensional elliptical orbit is the direction toward periapsis from the primary focus. It is from this primary axis that the true anomaly is measured in a counterclockwise sense. The secondary axis is normal to the primary axis in a right handed sense. The resultant coordinate system is shown in Figure 8.

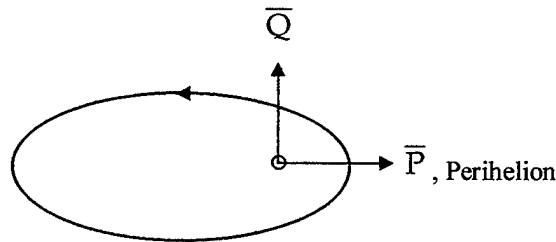


Figure 8. Perifocal Coordinate System

C. ORBITAL ELEMENTS

1. Three-dimensional

In the general three-dimensional case six orbital elements are required to define a particular location in space of an object in orbit. Those orbital elements are the semi-major axis (a), eccentricity (e), inclination to the ecliptic (i), longitude of ascending node (Ω), argument of periapsis (ω) and the time of periapsis passage (T). See Figure 9.

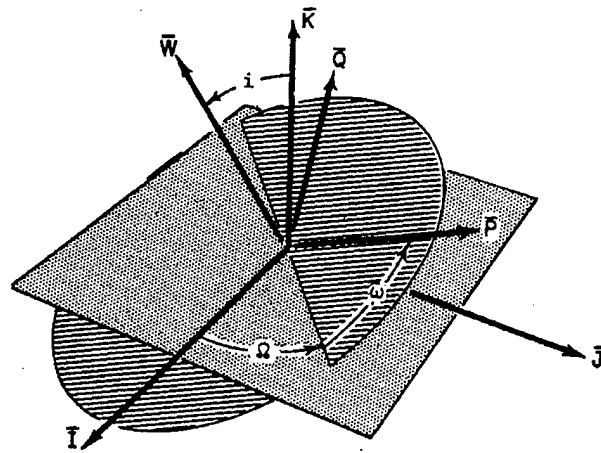


Figure 9. Three-dimensional Coordinates from Bate et. al. (1971)

2. Two-dimensional

In the perifocal coordinate system, only the semimajor axis (a), eccentricity (e), and true anomaly (v) are required to fix a position on an orbit. (Note the argument of periapsis is defined to be zero in this coordinate frame.). Other parameters of concern are the perihelion distance (q) and the aphelion distance (Q). Figure 10 displays the two-dimensional perifocal coordinate system.

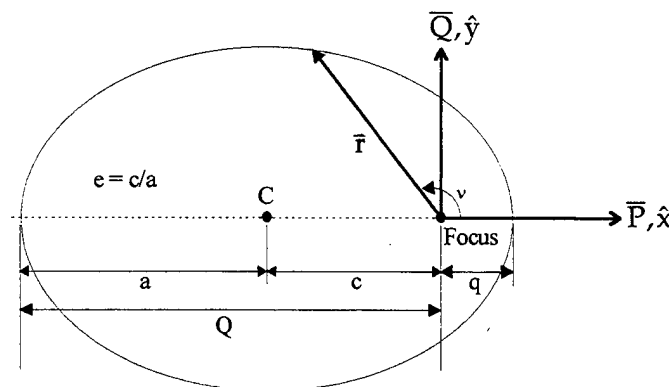


Figure 10. Perifocal Coordinates

D. KEPLER'S SECOND LAW

Motion of an object about the primary focus in an elliptical orbit is governed by Kepler's Second Law: the line joining the planet to the Sun sweeps out equal areas in equal times. This relation increases the difficulty in the problem solution in that there

exists a transcendental relationship between time and position. This relationship is called Kepler's Equation and takes the form:

$$t = \frac{E - e \sin E}{n}, \quad (1)$$

$$\text{where } \cos E = \frac{e + \cos v}{1 + e \cos v}. \quad (2)$$

V. PROBLEM FORMULATION AND SOLUTION

A. STATEMENT

Given an impending asteroid impact with the Earth, one would like to know if there is an optimum point on the asteroid's orbit where an impulse may be applied to yield the greatest achievable separation distance at the closest point of approach for a fixed impulse. Additionally, it is desirable to determine if there is an optimum direction associated with the applied impulse that further increases the separation distance.

B. ASSUMPTIONS

In order to proceed with an approximate solution method, simplifying assumptions were made. The first assumption was that of two-body motion. That is, the Sun is the mass center about which the asteroid and the Earth orbit. Furthermore, the asteroid and Earth do not gravitationally interact with each other. It was also assumed that there were no external perturbing effects on the orbits due to non-gravitational forces other than the applied perturbing impulse. All orbits were assumed to be coplanar, which yields a two-dimensional problem. The perturbing impulse is assumed to occur instantaneously. The asteroid is assumed to be one of the near Earth objects and hence in an elliptical orbit around the Sun. Hyperbolic and parabolic orbits were not considered for this analysis. Finally, it was assumed that the Earth is in a perfectly circular orbit at 1AU.

C. TEMPORAL CONSIDERATION

In determining the separation of a NEO from the Earth, time becomes the dominant factor in solving the problem. The relative phase of each of the orbiting bodies determines whether the bodies will collide. Hence, the Earth-to-NEO separation distance is the quantity of concern. Changing the orbital elements becomes secondary to changing the asteroid's orbital phase with respect to the Earth.

D. METHOD OF SOLUTION

Solution to the above problem may be achieved by use of a numerical simulation scheme where the orbital equations of motion are integrated from some initial condition forward in time. However, such a simulation is time consuming (on the order of several minutes per impact scenario) and therefore limits the scope of any analysis. The assumptions stated above allow for use of analytic elliptical orbit equations. Building a

solution based on these analytic two-body equations offers a greatly reduced time for solution (on the order of a couple seconds per impact scenario) and therefore a greater scope of analysis may be performed. A Mathworks MATLAB model was constructed to numerically execute the following method. A numerical integration simulation was also developed in order to validate the analytic method. The solution description below is quite general. For a detailed solution description see Appendix A. The MATLAB script that corresponds to the solution method is displayed in Appendix B.

1. Geometry

A general description of an elliptical orbit intersecting a circular orbit is used in the problem solution. This description suffices for all planar intercept scenarios. A rotation of the perifocal coordinates may be required to bring the model in alignment with the particular problem, but the relative geometry remains unchanged. Figure 11 demonstrates this equivalence.

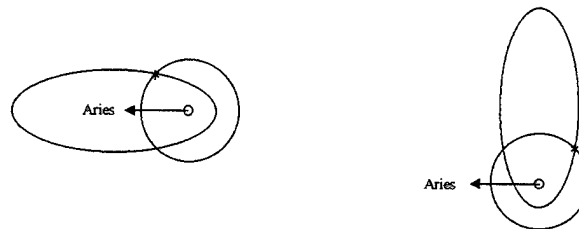


Figure 11. Equivalent Impact Scenarios

To uniquely fix an intercept scenario with the above assumptions, only the impact true anomaly and orbital eccentricity need to be defined. In the case of planar orbits, the perihelion direction, as defined by original asteroid elliptical orbit, defines the principal axis from which the impact true anomaly is measured. Implicit in the above impact location description is the assumption of an Earth orbital radius of 1 AU.

2. Solution Flowchart

Figure 12 depicts the steps in the problem solution method.

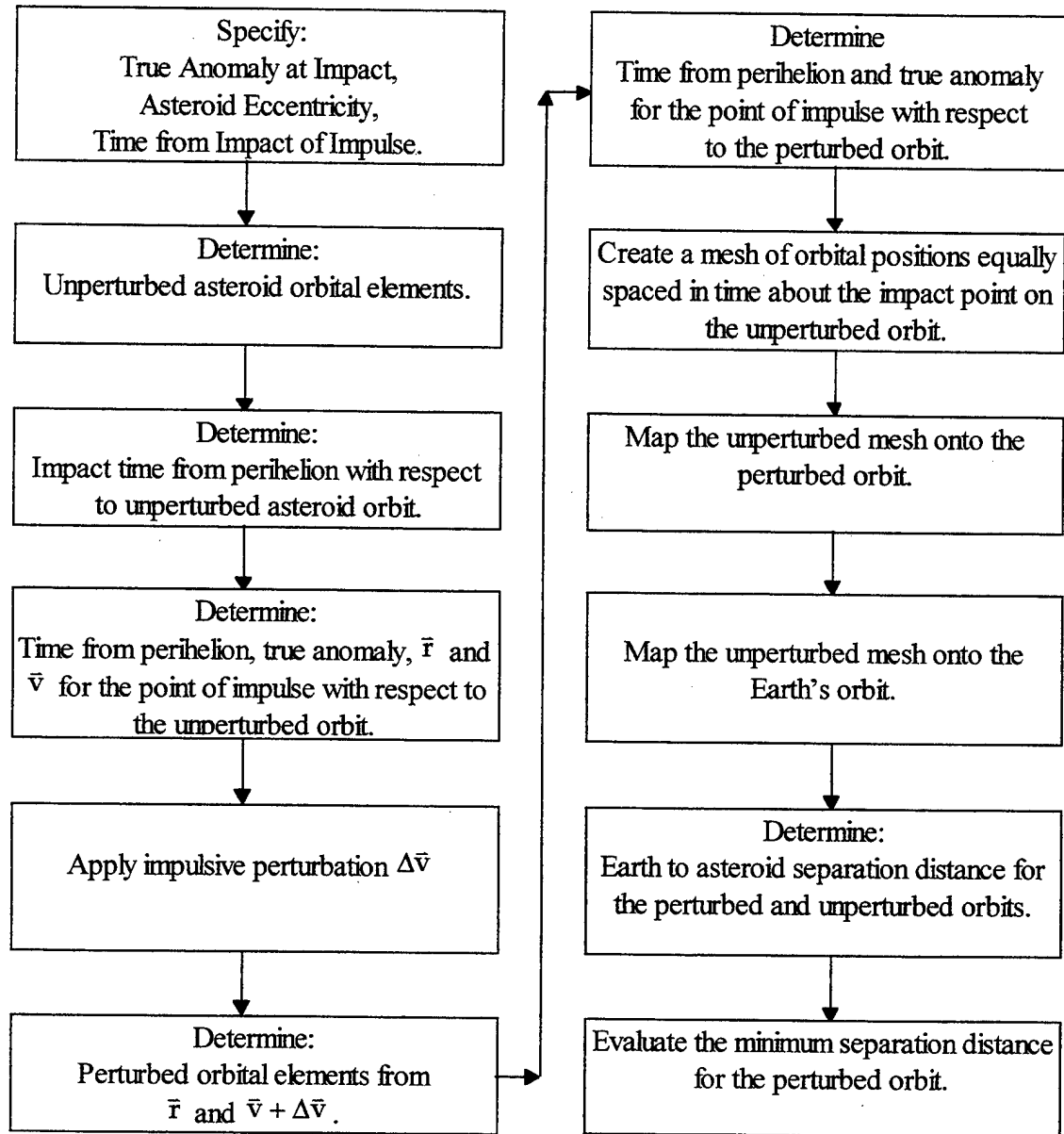


Figure 12. Solution Flowchart

3. Given Conditions

For a given impact scenario, it is assumed the impact true anomaly, asteroid orbital eccentricity are known and the desired impulse time prior to impact is specified. It should be noted here that specifying impact true anomaly and orbital eccentricity fixes the semi-major axis and hence, the orbital period. If either parameter is changed, the semi-major axis changes. That is, as impact true anomaly increases from 0 to π the semi-major axis decreases, thus decreasing the orbital period.

4. Unperturbed Orbital Elements

From the given conditions and the known Earth orbit the perihelion distance, semi-major axis, and orbital period for the unperturbed orbit may be determined by:

$$r_p = \frac{r_1(1 + e \cos v_1)}{1 + e},$$

$$a = \frac{r_p}{1 - e},$$

$$\text{and } P = \frac{2\pi}{n},$$

$$\text{where } n = \sqrt{\frac{\mu}{a^3}}.$$

5. Impact Condition

The time from perihelion of the impact with respect to the unperturbed orbit may be determined by Kepler's Equation as given in Equations (1) and (2).

6. Initial Impulse Condition

The time from perihelion of the impulse with respect to the unperturbed orbit may be determined by Figure 13 and the equation:

$$(\text{Impulse Time})_{\text{perihelion}} = (\text{Impact Time})_{\text{perihelion}} - (\text{Impulse Time})_{\text{Impact Time}}.$$

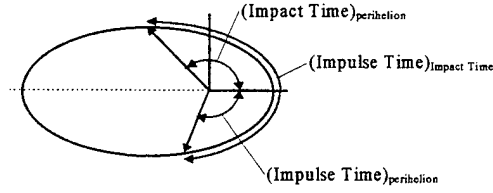


Figure 13. Impulse to Impact Time Relation

The true anomaly at impulse may be determined by inverting Kepler's Equation such that true anomaly becomes a function of time. This approach requires an iteration on eccentric anomaly.

The impulse position, \bar{r} , and velocity, \bar{v} , may now be found from:

$$r = \frac{a(1 - e^2)}{1 + e \cos v}, \quad (3)$$

$$\bar{r} = (r \cos v)\hat{x} + (r \sin v)\hat{y}, \quad (4)$$

$$\text{and } \bar{v} = \sqrt{\frac{\mu}{p}} [(-\sin v)\hat{x} + (e + \cos v)\hat{y}],$$

$$\text{where } p = a(1 - e^2).$$

7. Perturbation

An orbital perturbation, $\Delta\bar{v}$, is applied to the asteroid at the impulse position \bar{r} . This yields a perturbed orbital velocity $\bar{v} + \Delta\bar{v}$.

8. Perturbed Orbital Elements

From the impulse position \bar{r} and perturbed velocity $\bar{v} + \Delta\bar{v}$ the perturbed orbital elements may be determined from:

$$\bar{h} = \bar{r} \times (\bar{v} + \Delta\bar{v}),$$

$$p = \frac{h^2}{\mu},$$

$$\bar{e} = \frac{1}{\mu} \left[\left(|\bar{v} + \Delta\bar{v}|^2 - \frac{\mu}{|\bar{r}|} \right) \bar{r} - \{ \bar{r} \cdot (\bar{v} + \Delta\bar{v}) \} (\bar{v} + \Delta\bar{v}) \right],$$

and Equation (4).

9. Perturbed Impulse Condition

Substituting the perturbed orbital elements into Equation (3) enables the true anomaly at impulse to be determined with respect to the perturbed orbit. The time from perihelion of impulse with respect to the perturbed orbit may be found from Kepler's Equation.

10. Orbital Positions at Impact Time

To determine the separation distance of the perturbed asteroid from the Earth, the positions, and times, of the unperturbed asteroid orbit about the impact point must be mapped onto the corresponding positions and times of the perturbed asteroid orbit. That is, a one-for-one correlation between where the asteroid would have been if not for the perturbation and where the asteroid is due to the perturbation must be developed. This is the key step in determining the effect of the impulse perturbation.

The true anomalies and time from perihelion of the perturbed and unperturbed orbits are related by Kepler's Equation and not a simple function. The approach used to achieve the required mapping is as follows:

a) *Unperturbed Orbital Positions*

Develop an evenly spaced window, or mesh, of time about the impact position wide enough to include the perturbed orbits' minimum Earth separation. (A first estimate of the required width of this mesh is achieved by a numerical simulation. From the numerical simulation and model development an interval width of $\pm 1.5 \times \Delta v \times \text{Impulse Time}_{\text{Impact Time}}$ was used to provide a sufficiently wide mesh to obtain a solution without excessive computation time.) By inverting Kepler's Equation, the true anomalies of the mesh points may be determined. From the true anomalies of the mesh points the orbital positions may be found from Equations (3) and (4).

b) *Perturbed Orbital Positions*

From the relationship of the time of impact (known) with the time of impulse (also known) the center of the mesh may be determined for the perturbed orbit. Again, the true anomalies of the mesh points and the orbital positions for the perturbed orbit may be determined by use of Kepler's Equation and Equations (3) and (4). This now yields the asteroid orbital positions due to the perturbation.

c) Earth Orbital Positions

In the same fashion, the Earth orbital positions corresponding to the mesh points may be determined. However, since a circular Earth orbit was chosen, it is easier to relate the mesh times to orbital positions by use of the Earth's orbital mean motion.

11. Earth to Asteroid Separation Distance

With the perturbed asteroid's orbital positions and the corresponding Earth orbital positions known, it is a simple matter to determine the Earth to asteroid separation distance at each of the mesh points from:

$$R_{i,sep} = \sqrt{(x_{i,P} - x_{i,E})^2 + (y_{i,P} - y_{i,E})^2}.$$

12. Minimum Separation

From the above orbital separation distances, the minimum may be determined. It is useful to express this separation in terms of Earth radii. This enables a quick evaluation of whether a sufficient separation was achieved to cause a "miss". As with the analysis performed by Ahrens and Harris (1994) the resultant separation distances scale linearly with the applied impulse magnitude.

13. Sample Model Output

A sample of the MATLAB model output is shown in Figures 14 and 15. The impact scenario is for the case of an impact occurring at a true anomaly of 30° , an asteroid orbital eccentricity of $1/2$, and a perturbing impulse of 1 m s^{-1} in the direction of the velocity vector occurring 0.47 asteroid orbits prior to impact. Figure 14 displays the initial conditions of the scenario at the time of impulse. The impact position and the asteroid and Earth positions at the time of impulse are also displayed. Times prior to impact are displayed on the asteroid orbit in tenths of an orbital period.

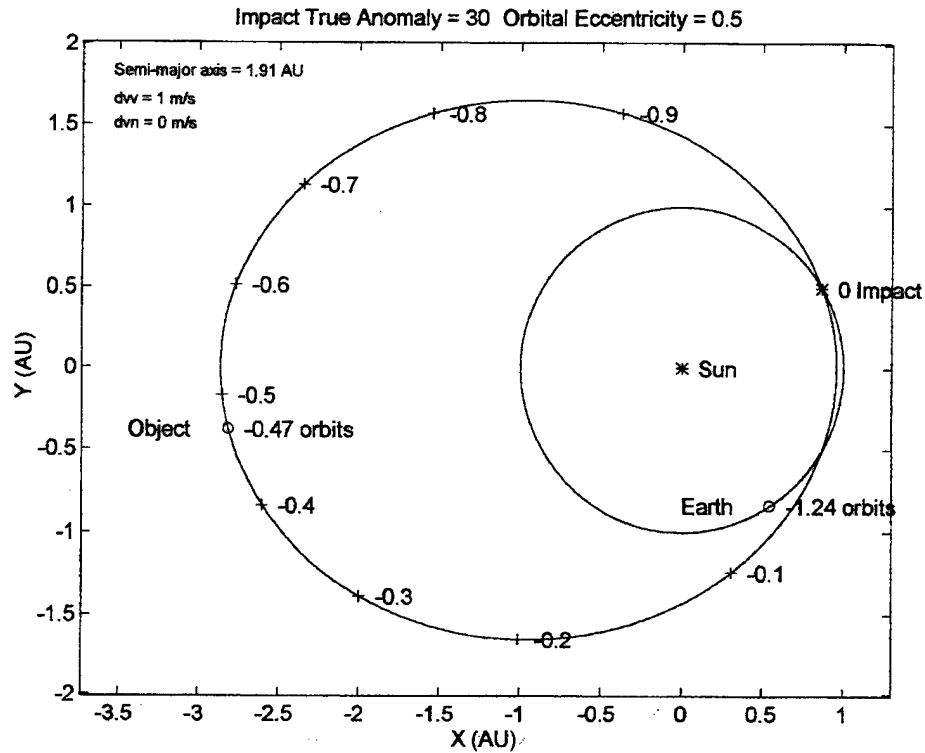


Figure 14. Initial Conditions

Figure 15 shows the effect of the impulse on the asteroid near the impact point. The unperturbed asteroid position is shown achieving impact conditions at zero Earth radii. The perturbed asteroid trajectory is shown approaching an impact condition, but instead reaches a minimum separation (indicated by the 'x') and then increases in separation.

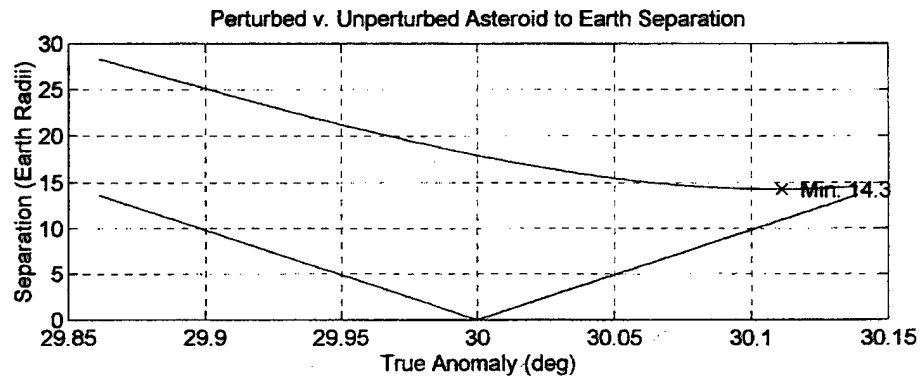


Figure 15. Perturbed Asteroid to Earth Separation

The minimum separation indicated in Figure 15 is the final output of the model. The figures were generated from the model working variables. This enables the model to be incorporated into a controlling routine allowing for repeated simulations that sweep over ranges of the input conditions.

VI. PROGRAM VALIDATION

Prior to making an analysis of various impact scenarios, the solution method and MATLAB model had to be validated. This validation was achieved by use of a simple numerical integration simulation and by comparison to approximate analytic solutions of nearly circular orbits.

A. NUMERICAL SIMULATION

The numerical integration simulation was developed using the Mathworks MATLAB and SIMULINK numerical processors. The SIMULINK diagram and MATLAB script files that support the SIMULINK model are displayed in Appendix C.

The two-body equation of motion integrated by the model is:

$$\ddot{\vec{r}} = \frac{-\mu}{r^3} \vec{r}.$$

Expressed as a two-dimensional system of linear differential equations in perifocal coordinate form:

$$\dot{v}_x = \frac{-\mu}{r^2} \frac{x}{r},$$

$$\dot{x} = v_x,$$

$$\dot{v}_y = \frac{-\mu}{r^2} \frac{y}{r},$$

$$\dot{y} = v_y.$$

Numerous orbital scenarios were run to ensure the numerical integration was performing correctly. A fourth order Runge-Kutta integration scheme was used for the simulation acting on a second order differential equation. This yields a solution that is analytically exact and accurate to the numerical precision of the computer microprocessor. For the present analysis, the computer microprocessor was a 100 MHz, 32 bit, Intel Pentium. For the cases chosen for orbital modeling verification, integrating around one orbit resulted in an ending position the same as the starting position with a relative error of 2×10^{-16} (3×10^{-7} km error at 1.5×10^8 km, 1 AU).

Once the numerical integration orbit models were validated, numerous perturbation simulations were made to provide a reference data base for the analytic method. It was found that the analytic method numerical model was in excellent agreement with the numerical simulations. Differences arose only from the difference in mesh size between the two solution methods, with the analytic solution having a finer mesh interval.

B. APPROXIMATE ANALYTIC SOLUTIONS

For circular orbits, Ahrens and Harris (1994) performed an approximate analysis that yields expressions for maximum orbital separation due to impulses applied both normal to and parallel to the orbital velocity vector. For the case where the impulse is applied normal to velocity vector, the maximum separation is found half an orbital period later with a magnitude $\delta_{\max} = 2\Delta v P / \pi$. This case is shown in Figure 16.

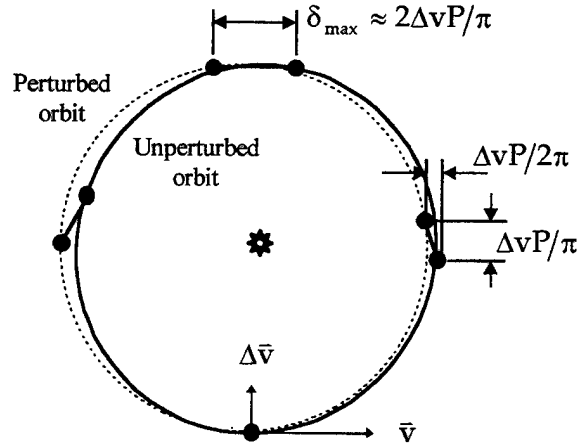


Figure 16. Impulse Normal to Velocity Vector

For the case where the impulse is applied parallel to velocity vector the separation a full orbital period later is found to be $\delta = 3\Delta v P$ per orbit. That is, for this case the separation increases by δ for every orbit after the single impulse. This case is shown in Figure 17.

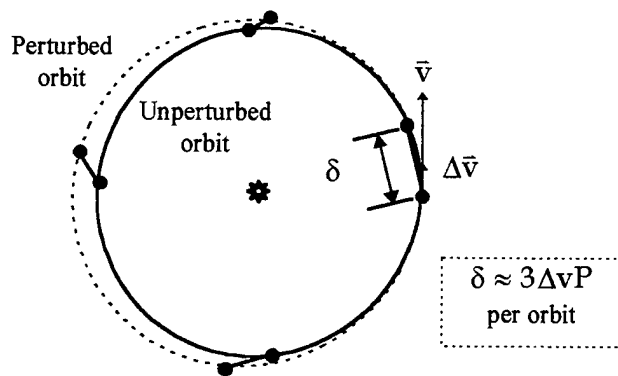


Figure 17. Impulse Parallel to Velocity Vector

Evaluation of these scenarios by numerical simulation verifies the above approximate solution. The separations between the perturbed and unperturbed orbits at the described locations does indeed agree very well with the approximate analytic solution. Further, evaluation of the above scenarios by the analytic method numerical model using an asteroid orbital eccentricity of 10^{-5} (nearly circular) and an impulse of 1 m s^{-1} yields virtually the same result as the approximate analytic solution. Table 2 summarizes the performance of the three solution methods for the circular orbit case.

Impulse Direction	Approximate Analytic Solution	Analytic Numerical Method	Numerical Simulation
Normal to \bar{v}	$3\Delta v P = 14.8$	14.8	14.8
Parallel to \bar{v}	$2\Delta v P / \pi = 3.15$	3.14	3.15

(Separation in Earth Radii)

Table 2. Validation of Solution Method

VII. ANALYSIS AND RESULTS

A. ANALYSIS

The preceding analytic numerical method for solution of the Earth to asteroid separation problem was incorporated as a function into a routine that sweeps over impulse direction and time of impulse. In this manner hundreds of solutions may be generated in a few minutes. Appendix D contains numerous analyses for impact scenarios that may occur around the Earth's orbit.

1. Long Time Response Behavior

For a perturbing impulse time well prior to impact the observed behavior resulting from the orbital dynamics is not linear. The Earth-to-asteroid separation achieved by an impulse is strongly dependent on the location of the impulse on the orbit as well as the direction of the impulse with respect to the orbital velocity. The typical behavior of an impulse is depicted in Figure 18. Each point on this plot represents the minimum separation point depicted on Figure 15. In Figure 18 the vertical axis represents the minimum Earth-to-asteroid separation (in Earth radii) that results from an impulse of 1 m s^{-1} . The two horizontal axes represent the direction of the impulse and the time prior to impact of the impulse. The axis representing direction of impulse is measured from 0° to 360° with respect to the forward direction of the velocity vector. The sense of the direction is that impulse directions between 0° and 180° point inward to the orbit and directions from 180° to 360° point outward from the orbit. The remaining axis represents impulse time prior to impact as a fraction of the asteroid's original orbital period (e.g., $t/P = 0.5$ corresponds to an impulse one half orbit prior to impact).

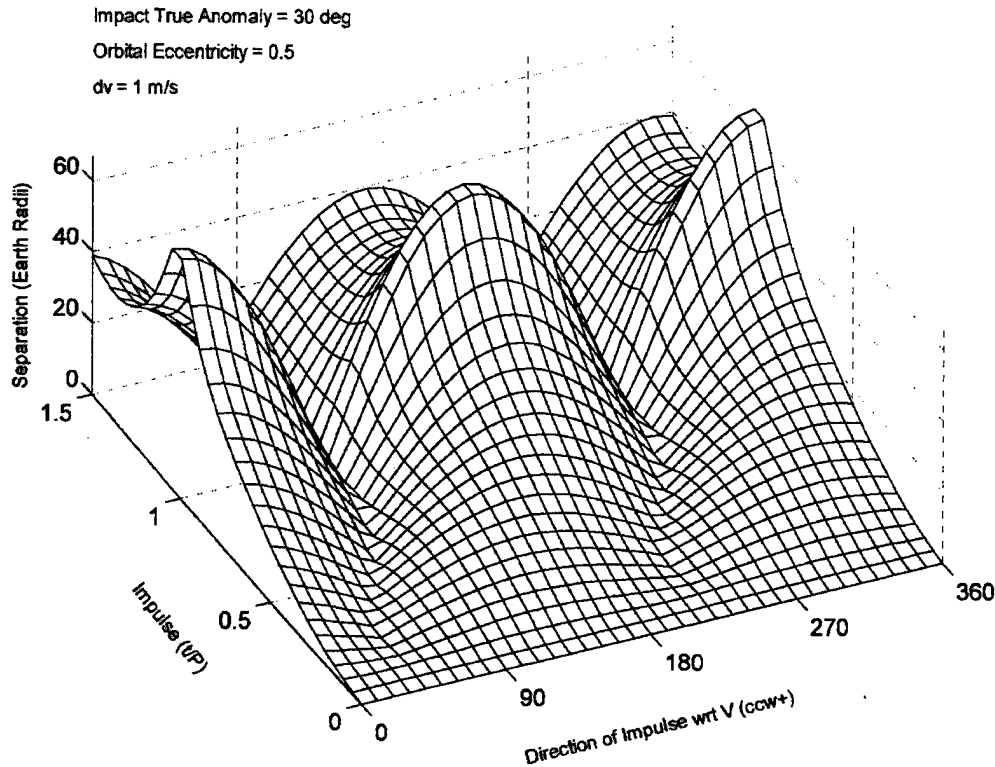


Figure 18. Earth to Asteroid Separation

2. Relative Maxima

Impulse times ranging from 0 to $1\frac{1}{2}$ asteroid orbits prior to impact yield two maxima points as shown in Figure 18. Inspection of these maxima points reveal that they occur at the time of perihelion passage for the asteroid approximately one orbit prior to impact for impulse directions parallel and anti-parallel to the orbital velocity vector. This relationship holds true for all cases considered.

3. Non-perihelion Impulse Direction

Closer inspection of Figure 18 reveals that for impulse times less than that corresponding to one orbit prior to impact, the maximum separation is achieved if the impulse direction is not aligned either parallel or anti-parallel to the velocity vector. This effect is better shown in Figure 19, which is a contour plot of Figure 18.

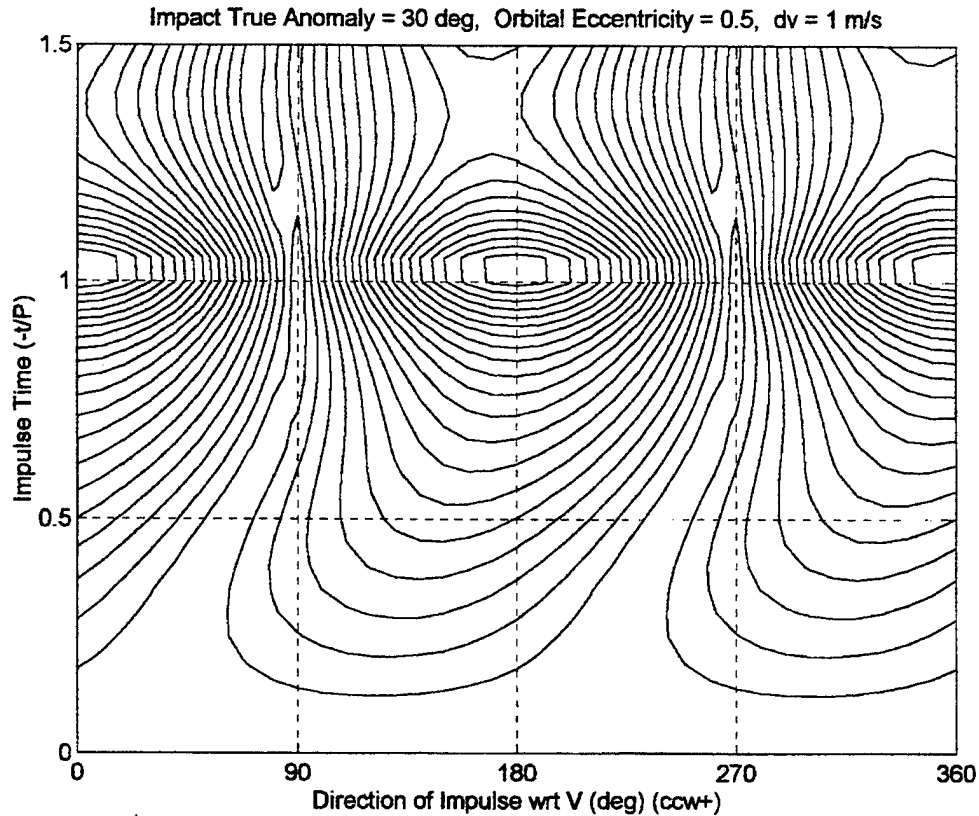


Figure 19. Contour Plot of Figure 18.

A distinct shift in the direction of impulse for maximum separation as the time of impulse becomes closer to impact can be seen. This shift in direction arises from the two ways in which to achieve the desired separation. If sufficient time prior to impact exists, changing the speed of the asteroid on its orbit will shift the phase of the asteroid with respect to the Earth and avoid the impact. If the time prior to impact is short, changing the direction of the asteroid laterally with respect to its approach to the Earth is necessary to avoid the impact. For times prior to impact between these the former and the latter, a tradeoff between changing the orbital speed and displacing the asteroid laterally on its orbital path exists and is the cause of the shift in the optimal impulse direction.

4. Periodic Growth

Thus far, only impulse times within approximately one asteroid orbital period of impact have been considered. Extending the analysis to beyond this time period

demonstrates the manner in which the separation grows as a function of impulse time. Figure 20 shows this behavior for the same impact scenario as discussed above. Of note is the periodic growth over time and the peak displacements occurring at each perihelion point. This particular figure represents a slice of Figure 18 along the 0° impulse direction extended from 0 to 10 orbits prior to impact.

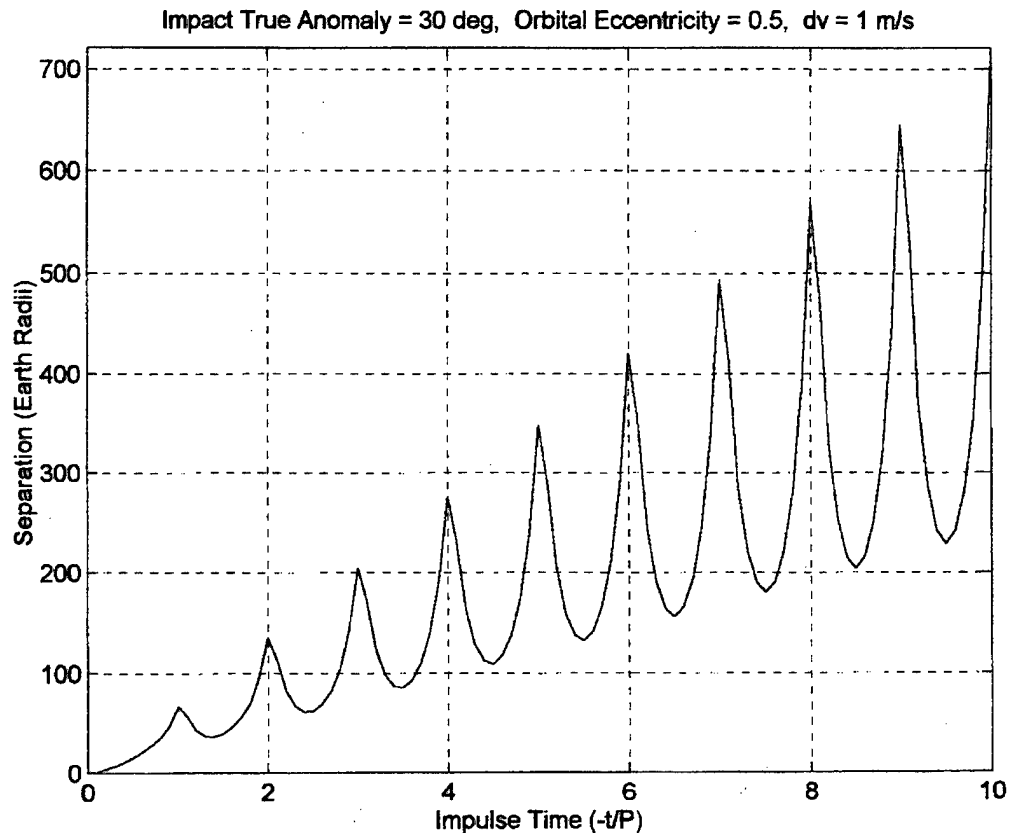


Figure 20. Periodic Growth of Separation Distance

B. RESULTS

The collection of the numerous impact scenarios modeled by the above method may be found in Appendix D. A study of these numerous model results yield the following general conclusion.

1. Optimum Impulse Condition

Assuming the optimum impulse condition is achievable in terms of a "real" mission sense (that is, the booster technology and energy delivery mechanism exist for asteroid mitigation), the optimum impulse point is located at the perihelion of the original asteroid orbit at least $\frac{1}{2}$ orbit prior to impact. If time prior to impact permits, impulse at perihelia

multiple orbits prior have an even greater effect on separating the asteroid from the Earth at the given impact time. However, impact prediction becomes a problem in such cases as the validity of orbital prediction models in a general n-body problem comes into question.

2. Optimum Impulse Direction

If, due to the late time of detection, it is not possible to achieve even the first relative maximum for the optimum impulse condition, then there exists an optimum impulse direction at the time of impulse that maximizes the Earth to object separation. For fractions of an orbit from $0.2 < (t/P) < 0.9$ there is a shift in the direction of impulse toward the orbital inward normal (for impulses that increase the orbital speed) and toward the orbital outward normal (for impulses that decrease the orbital speed) that yields a maximum in separation achievable.

3. Time of Arrival Consideration

Given the periodic nature of the impact problem, there exist conditions where it may be beneficial to delay a deflecting impulse until an optimal impulse condition occurs. For the scenario corresponding to Figure 20, if time permits delivery of an impulse two and one half asteroid orbits prior to impact, it would prove more advantageous to delay the impulse until only two orbits prior to impact in order to maximize the effect of the impulse.

4. Detection Consideration

The difficulty in realizing the use of an optimal impulse condition is that the detection of a colliding object may occur too late to achieve the most desirable condition. The earlier the detection the better the chance of deflection with a much smaller imparted energy. Unfortunately, the current search programs and record of detection have been yielding very short response times for NEO's having very close approaches. The current range of times for detection has been on the order of five days prior to closest approach to detection only after Earth passage.

VIII. APPLICATION TO A REAL CASE

A. IMPULSE ACHIEVABLE

The analysis of the energy coupling between an explosive yield and an asteroid performed by Ahrens and Harris (1994) shows that it may be feasible to deflect a NEO with an impulse magnitude from 1 cm s^{-1} to a few m s^{-1} for a globally threatening object of about 1 km in diameter. This impulse may be achieved using one of several methods. However, due to the relatively short warning times considered in this thesis, a nuclear blast appears to be the most efficient energy delivery mechanism. The blast may be a standoff detonation or surface detonation.

For the standoff detonation, the required explosive yield, W , may be determined by the approximate expression:

$$W = \frac{10^3 \Delta v D^3}{nA},$$

from Ahrens and Harris (1994), which has been modified to express yield in kT of equivalent TNT. The impulse, Δv , is expressed in m s^{-1} and the asteroid diameter, D , is in km. The efficiency of neutron production, n , from the nuclear blast lies between 0.03 and 0.3. The standoff blast efficiency factor, A , is taken for an optimum standoff distance of 0.4 asteroid radii with an efficiency of approximately 0.3. An order of magnitude analysis of the above approximation is presented in Table 3.

Impulse (m s^{-1})	0.1 km diameter	1 km diameter	10 km diameter
0.01	0.1-1 kT	100-1000 kT	100-1000 MT
0.1	1-10 kT	1-10 MT	1-10 GT
1.0	10-100 kT	10-100 MT	10-100 GT
10.0	100-1000 kT	100-1000 MT	100-1000 GT

Table 3. Impulse and Diameter v. Standoff Explosive Yield

For the surface detonation, the required explosive yield, W , may be determined from the approximate expression:

$$W = 4 \times 10^{-9} \Delta v M_{\text{NEO}},$$

also from Ahrens and Harris (1994) which again has been modified to express yield in kT of equivalent TNT. The impulse, Δv , is expressed in m s^{-1} and the asteroid mass, M_{NEO} , is in kg. An order of magnitude analysis of the above approximation is presented in Table 4.

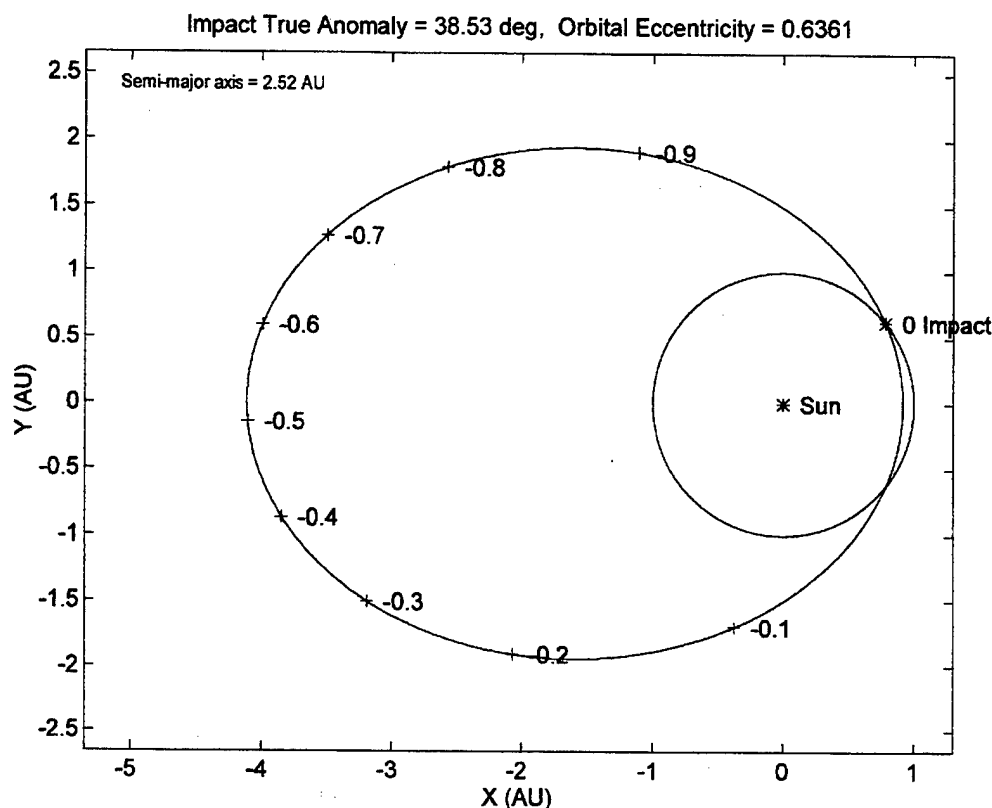
Impulse (m s^{-1})	0.1 km diameter	1 km diameter	10 km diameter
0.01	60 T	60 kT	60 MT
0.1	600 T	600 kT	600 MT
1.0	6 kT	6 MT	6 GT
10.0	60 kT	60 MT	60 GT

Table 4. Impulse and Diameter v. Surface Explosive Yield

B. TOUTATIS

Asteroid 4179 Toutatis will have multiple close approaches with the Earth over the next 15 years. It is of interest to apply the above analysis and methodology to Toutatis as if it were going to impact the Earth.

To perform this analysis it must be assumed that the orbit of Toutatis lies in the ecliptic plane. This is not far from the true geometry of Toutatis' orbit where the orbital inclination is 0.47° out of the ecliptic plane. From the catalog of NEA orbital elements listed compiled by Tholen (1995), the semi-major axis and eccentricity of Toutatis are currently listed as 2.5154 and 0.6361, respectively. Assuming that Toutatis and the Earth will collide and that the Earth is in a circular orbit at 1 AU yields an impact at $\pm 38.53^\circ$ with respect to the perihelion of Toutatis. This is determined by solving Equation (3) for true anomaly. Figure 21 depicts this relative orientation of Toutatis with respect to the Earth. For the following analysis, the $+38.53^\circ$ impact location is chosen for modeling purposes.



Modeling the Toutatis collision in the manner described above yields the results displayed in Figure 22. From the JPL and NASA Photo Caption (1993) and Press Release (1996), the size of Toutatis is estimated to be approximately that of two attached spheres having diameters of about 4 km and 2.5 km. If both masses are combined, the effective spherical diameter is approximately 4.3 km. Using a mean asteroid density of 3000 kg m^{-3} results in a mass for Toutatis near $1.25 \times 10^{14} \text{ kg}$. From the previous impulse analysis, an explosive yield of about 5 MT is required in the case of a surface detonation and an explosive yield from 9 to 90 MT, depending on neutron production, is needed for a standoff detonation to achieve a 1 cm s^{-1} change in orbital speed.

Using the 1 cm s^{-1} orbital speed change determined above, a maximum separation of 1.64 Earth radii is the result of an impulse delivered 1.02 orbits prior to impact (perihelion passage of the prior orbit). While the separation is sufficient to cause the Toutatis to miss the Earth in this scenario, a greater margin of safety would be desirable. A larger separation may be achieved by either delivering an impulse greater than 1 cm s^{-1}

or delivering the impulse at an earlier perihelion passage. Recognizing the extremely large explosive yield requirements for increased impulse magnitudes, it would appear preferable to deliver the impulse at an earlier time. This type of analysis demonstrates the necessity for detection of threatening asteroids many orbits prior to impact.

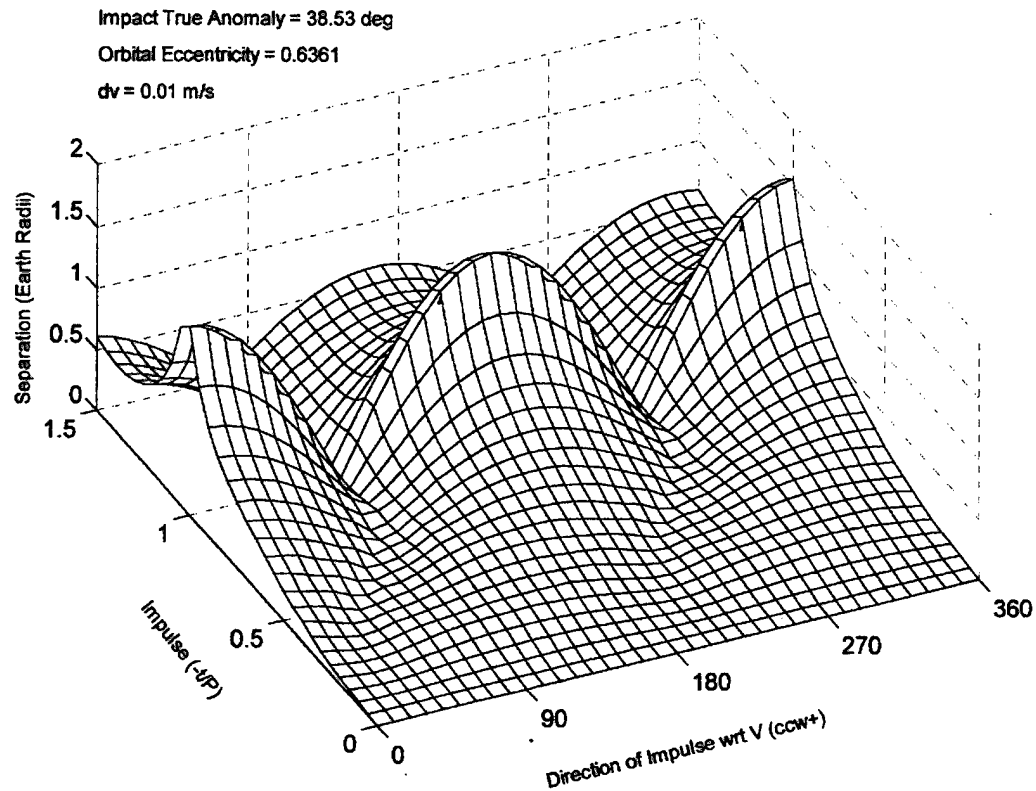


Figure 22. Impulse Effects on Toutatis-Earth Impact

IX. FURTHER CONSIDERATIONS

The above analysis shows promise as a tool for rapidly evaluating numerous scenarios for deflecting an asteroid that is going to impact the Earth. The possibility for further investigation utilizing this method presents itself in analyzing longer response times prior to impact, generalizing the method to a three-dimensional method and eccentricities other than $\frac{1}{2}$. Additionally, more work is needed in analysis of very short response time impulse effects.

A. LONG RESPONSE TIME

The analysis presented above and in Appendix D have been performed primarily for impulse times between 0 and $1\frac{1}{2}$ orbits prior to impact. A few models were made for one impulse direction at times ranging from 0 to 10 orbits prior to impact. However, this investigation needs to be pursued further in search of general trends other than maximum separations occurring at perihelion points.

B. THREE-DIMENSIONAL ANALYSIS

The current model and method apply only to two-dimensional scenarios. It is of interest and merit to further generalize the analysis to the three-dimensional case. This will allow for orbital inclinations out of the ecliptic plane and better simulate a variety of real scenarios.

C. ECCENTRICITY VARIATIONS

In the above analysis, other than for Toutatis, the orbital eccentricities have been maintained at $\frac{1}{2}$. An investigation into the effects of more circular orbits and highly eccentric orbits is in order.

D. SHORT RESPONSE TIME

The method presented is derived from a two-body representation of a more complicated physical system. This method is not valid for very short response times when the impacting object is within the Earth's sphere of influence. A further investigation is desirable to assess the effects of impulses in the three-body problem that arises when the object is detected close to the Earth.

REFERENCES

Ahrens, T. J., Harris, A. W., Deflection and Fragmentation of Near-Earth Asteroids, In *Hazards Due to Comets and Asteroids*, ed. T. Geherls, Univ. of Arizona Press, 1994, pp. 897-928.

Alvarez, L. W., Alvarez, W., Asaro, F. and Mitchell, H. V., 1980. Extraterrestrial Cause for the Cretaceous-Tertiary Extinction. *Science* 208: 1095-1108.

American Institute of Aeronautics and Astronautics Space Systems Technical Committee, Dealing with the Threat of an Asteroid Striking the Earth, AIAA Position Paper, April 1990.

Bate, R. R., Mueller, D. D., and White, J. E., Fundamentals of Astrodynamics, Dover Publications, 1971.

Chapman, C.R., Morrison, D., Impacts on the Earth by Asteroids and Comets: Assessing the Hazard, *Nature*, Vol. 367, 6 January 1994, pp. 33-40

Chyba, C. F., Owen, T. C., Ip, W. H., Impact Delivery of Volatiles and Organic Molecules to Earth, In *Hazards Due to Comets and Asteroids*, ed. T. Geherls, Univ. of Arizona Press, 1994, pp. 9-58.

Grieve, R. A., Shoemaker, E.M., The Record of Past Impacts on Earth, In *Hazards Due to Comets and Asteroids*, ed. T. Geherls, Univ. of Arizona Press, 1994, pp. 417-462.

Jaroff, L., "A Shot Across the Earth's Bow," *Time*, Vol. 147, No. 23, June 3, 1996, pp. 61-62.

Jet Propulsion Laboratory, National Aeronautical and Space Administration, Toutatis Radar Images Photo Caption, P-41525, 4 January 1993; from Asteroid 4179 Toutatis internet site <http://newproducts.jpl.nasa.gov/calendar/toutatus.html>.

Jet Propulsion Laboratory, National Aeronautical and Space Administration, Oddball Asteroid Captured on New Video Computer Simulation, Release: 96-249, 27 November 1996; from Asteroid 4179 Toutatis internet site <http://newproducts.jpl.nasa.gov/calendar/toutatus.html>.

Jewitt, D.C., Luu, J.X., The Solar System Beyond Neptune, *Astron. J.*, 109, pp.1867-1876.

Levy, E. H., Early Impacts: Earth Emergent From Its Cosmic Environment, In *Hazards Due to Comets and Asteroids*, ed. T. Geherls, Univ. of Arizona Press, 1994, pp. 3-8.

Morrison, D., Chapman, C. R., Slovic, P., The Impact Hazard. In *Hazards Due to Comets and Asteroids*, ed. T. Geherls, Univ. of Arizona Press, 1994, pp. 59-92.

Rabinowitz, D., Bowell, E., Shoemaker, E., Muinonen, K., The Population of Earth-Crossing Asteroids, In *Hazards Due to Comets and Asteroids*, ed. T. Geherls, Univ. of Arizona Press, 1994, pp. 285-312.

Rather, J.D.G, Rahe, J.H., Canavan, G., Summary Report of the Near-Earth-Object Interception Workshop, National Aeronautics and Space Administration, Los Alamos National Laboratory, 1992.

Scotti, J.V., Rabinowitz, D.L., Marsden, B.G., Near Miss of the Earth by a Small Asteroid, *Nature*, Vol. 354, 28 November 1991, pp. 287-289.

Shoemaker, E. M., Weissman, P. R., Shoemaker, C. S., The Flux of Periodic Comets Near Earth, In *Hazards Due to Comets and Asteroids*, ed. T. Geherls, Univ. of Arizona Press, 1994, pp. 313-336.

Sky and Telescope, Vol. 44, No. 4, October 1972, pp 269-272.

Tholen, D., from the Asteroid and Comet Impact Hazards internet site
http://ccf.arc.nasa.gov/sst/tables/asteroid_02.html, 21 Mar 1995.

Winters, J., "Flying Rubble," Discover, Vol. 18, No. 8, August 1996, p. 26.

BIBLIOGRAPHY

Abell, G. O., Exploration of the Universe, Saunders College Publishing 1982.

Brown, C. D., Spacecraft Mission Design, AIAA, 1992.

The Astronomical Almanac, U. S. Government Printing Office, 1996.

APPENDIX A. DETAILED SOLUTION METHOD

Given an Earth-asteroid collision with the following properties:

A circular Earth orbit with semi-major axis (radius), $a_E = 1\text{AU}$

(orbital eccentricity, $e_E = 0$);

an asteroid orbit with orbital eccentricity e_U ;

the true anomaly at time of impact, $v_{\text{impact},U} = v_{\text{impact},E}$;

and the time of the perturbing impulse, $\Delta\bar{v}$, prior to impact $\left(\frac{t}{P_U}\right)_{\Delta v}$.

Find the minimum separation of the asteroid from the Earth in the vicinity of the old impact point.

Nomenclature

Variables:

a	semi-major axis
E	eccentric anomaly
e	orbital eccentricity
h	specific angular momentum
F	fraction
N	number
n	orbital mean motion
P	orbital period
p	orbital parameter
R	asteroid to Earth separation distance, km
r	orbit to Sun radial distance
v	velocity
x	x-position
y	y-position
Δv	impulse quantity
α	angle w.r.t. x-coordinate axis
μ	gravitational mass parameter
ν	true anomaly
ρ	asteroid to Earth separation distance, Earth radii
$\Delta \nu$	shift in periapsis direction
$\left(\frac{t}{P}\right)$	fraction of orbit from periapsis

Subscripts:

days	number of days
E	Earth
i	i th element
inc	increment
impact	impact position
min	minimum
orbit	orbit count
P	perturbed asteroid orbit
p	periapsis
pos	position
Range	set of all i's
sep	separation
Sun	Sun parameter
U	unperturbed asteroid orbit
x	x-component
y	y-component
Δv	impulse
\parallel	parallel component
\perp	normal component

Symbols:

Δ	incremental amount
δ	incremental amount

Elliptical Orbit Relations

Mean motion:

$$n = \sqrt{\frac{\mu}{a^3}}$$

Period:

$$P = \frac{2\pi}{n}$$

Radial distance to gravitational focus (general):

$$r = \frac{a(1 - e^2)}{1 + e \cos v}$$

Periapsis radius

$$r_p = \frac{r_1(1 + e \cos v_1)}{1 + e}$$

Semi-major axis:

$$a = \frac{r_p}{1 - e}$$

Eccentric anomaly as a function of true anomaly:

$$\cos E = \frac{e + \cos v}{1 + e \cos v}$$

True anomaly as a function of eccentric anomaly:

$$\cos v = \frac{\cos E - e}{1 - e \cos E}$$

Time since periapsis:

$$t = \frac{E - e \sin E}{n}$$

True anomaly:

$$\cos v = \frac{a(1-e^2)}{re} - \frac{1}{e}$$

Position at a point in perifocal coordinates:

$$\bar{\mathbf{r}} = (r \cos v)\hat{\mathbf{x}} + (r \sin v)\hat{\mathbf{y}}$$

Velocity at a point in perifocal coordinates:

$$\bar{\mathbf{v}} = \sqrt{\frac{\mu}{p}} [(-\sin v)\hat{\mathbf{x}} + (e + \cos v)\hat{\mathbf{y}}]$$

Parameter of an orbit:

$$p = a(1-e^2) = \frac{h^2}{\mu}$$

Specific angular momentum:

$$\bar{\mathbf{h}} = \bar{\mathbf{r}} \times \bar{\mathbf{v}}$$

Eccentricity vector in perifocal coordinates:

$$\bar{\mathbf{e}} = \frac{1}{\mu} \left[\left(|\bar{\mathbf{v}}|^2 - \frac{\mu}{|\bar{\mathbf{r}}|} \right) \bar{\mathbf{r}} - (\bar{\mathbf{r}} \cdot \bar{\mathbf{v}}) \bar{\mathbf{v}} \right]$$

Constants

1AU = 1.4959787×10⁸ km, astronomical unit

G = 6.67259×10⁻²⁰ km³kg⁻¹s⁻², gravitational constant

M_{Sun} = 1.9891×10³⁰ kg, mass of the Sun

μ_{Sun} = GM_{Sun} = 1.327124399355×10¹¹ km³s⁻², Sun gravitational parameter

R_E = 6.37814×10³ km, Earth radius

Detailed Solution Method

I. Determine unperturbed asteroid orbital elements.

a. Perihelion radius:

$$r_{p,U} = \frac{a_E (1 + e_U \cos v_{\text{impact},U})}{1 + e_U}, \text{ km}$$

$$\text{where } r_{\text{impact},U} = a_E$$

b. Semi-major axis:

$$a_U = \frac{r_{p,U}}{1 - e_U}, \text{ km}$$

c. Mean motion:

$$n_U = \sqrt{\frac{\mu_{\text{Sun}}}{a_U^3}}, \text{ rad s}^{-1}$$

d. Period:

$$P_U = \frac{2\pi}{n_U}, \text{ s}$$

II. Determine the conditions at impact with respect to the unperturbed asteroid orbit.

a. Eccentric anomaly at impact:

$$E_{\text{impact},U} = \cos^{-1} \left(\frac{e_U + \cos v_{\text{impact},U}}{1 + e_U \cos v_{\text{impact},U}} \right)$$

$$(\cos^{-1} \text{ principle values are } 0 \leq \theta \leq \pi)$$

b. Fraction of orbit since (or prior to) perihelion of impact:

$$\left(\frac{t}{P_U} \right)_{\text{impact},p} = \frac{E_{\text{impact},U} - e_U \sin E_{\text{impact},U}}{2\pi}$$

$$\text{if } v_{\text{impact},U} < 0, \left(\frac{t}{P_U} \right)_{\text{impact},p} < 0$$

III. Determine the conditions at impulse with respect to the unperturbed orbit.

a. Fraction of orbit prior to (or since) perihelion of impulse:

$$\left(\frac{t}{P_U}\right)_{\Delta v,p} = \left(\frac{t}{P_U}\right)_{\text{impact},p} - \left(\frac{t}{P_U}\right)_{\Delta v,\text{impact}}$$

b. Eccentric anomaly at impulse (solve via Newton-Raphson iterative method):

$$\left(\frac{t}{P_U}\right)_{\Delta v,p} = \frac{E_{\Delta v,U} - e_U \cos E_{\Delta v,U}}{2\pi}$$

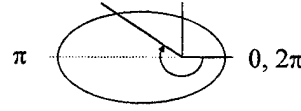
c. True anomaly at impulse measured with respect to unperturbed perifocal coordinates:

$$v_{\Delta v,U} = \cos^{-1} \left(\frac{\cos E_{\Delta v,U} - e_U}{1 - e_U \cos E_{\Delta v,U}} \right)$$

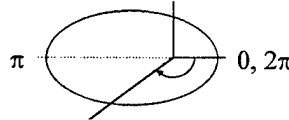
(\cos^{-1} principle values are $0 \leq \theta \leq \pi$)

$$\left(\frac{t}{P_U}\right)_{\Delta v,p} = N_{\text{orbit}} + F_{\text{orbit}}$$

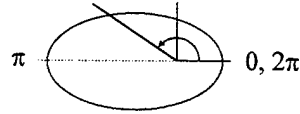
$$\text{if } -1 < F_{\text{orbit}} < -\frac{1}{2}, \text{ then } v_{\Delta v,U} = 2\pi(N_{\text{orbit}} - 1) + v_{\Delta v,U}$$



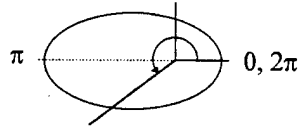
$$\text{if } -\frac{1}{2} \leq F_{\text{orbit}} < 0, \text{ then } v_{\Delta v,U} = 2\pi N_{\text{orbit}} - v_{\Delta v,U}$$



$$\text{if } 0 \leq F_{\text{orbit}} < \frac{1}{2}, \text{ then } v_{\Delta v,U} = 2\pi N_{\text{orbit}} + v_{\Delta v,U}$$



if $\frac{1}{2} \leq F_{\text{orbit}} < 1$, then $v_{\Delta v, U} = 2\pi(N_{\text{orbit}} + 1) - v_{\Delta v, U}$



d. Distance to focus (Sun) from impulse location:

$$r_{\Delta v, U} = \frac{a_U(1 - e_U^2)}{(1 + e_U \cos v_{\Delta v, U})}, \text{ km}$$

e. Velocity components at impulse with respect to unperturbed perifocal coordinates:

$$v_{x, \Delta v, U} = -\sqrt{\frac{\mu_{\text{Sun}}}{a_U^2(1 - e_U^2)}} \sin v_{\Delta v, U}, \text{ km s}^{-1}$$

$$v_{y, \Delta v, U} = \sqrt{\frac{\mu_{\text{Sun}}}{a_U^2(1 - e_U^2)}} (e_U + \cos v_{\Delta v, U}), \text{ km s}^{-1}$$

f. Velocity direction with respect to unperturbed perifocal coordinates

$$\alpha = \tan^{-1} \left(\frac{v_{y, \Delta v, U}}{v_{x, \Delta v, U}} \right)$$

(achieved utilizing "atan2(y,x)" numerical routine)

IV. Now perturb the asteroid with respect to velocity vector direction.

a. Impulse velocity components with respect to unperturbed perifocal coordinates:

$$\Delta v_x = \Delta v_{\parallel} \cos \alpha - \Delta v_{\perp} \sin \alpha, \text{ km s}^{-1}$$

$$\Delta v_y = \Delta v_{\parallel} \sin \alpha + \Delta v_{\perp} \cos \alpha, \text{ km s}^{-1}$$

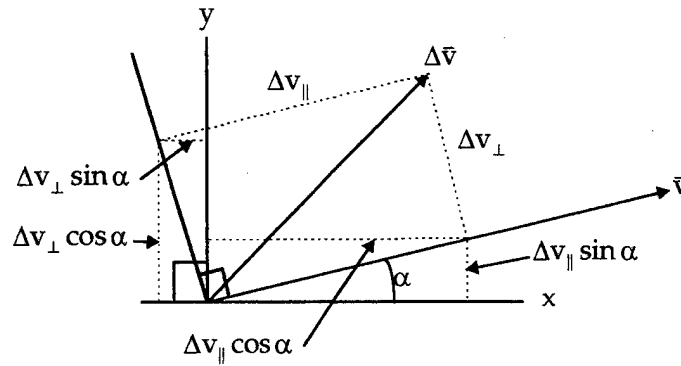
where, Δv_{\parallel} is in the direction of the velocity vector

and, Δv_{\perp} is normal to the velocity vector in a right hand sense

b. Velocity components after perturbation with respect to unperturbed perifocal coordinates:

$$v_{x,\Delta v,P} = v_{x,\Delta v,U} + \Delta v_x, \text{ km s}^{-1}$$

$$v_{y,\Delta v,P} = v_{y,\Delta v,U} + \Delta v_y, \text{ km s}^{-1}$$



V. Determine perturbed asteroid orbital elements from $\bar{\mathbf{r}}$ and $\bar{\mathbf{v}}$.

a. Position vector with respect to unperturbed perifocal coordinates:

$$\bar{\mathbf{r}}_{\Delta v,P} = \bar{\mathbf{r}}_{\Delta v,U} = r_{x,\Delta v,U} \hat{\mathbf{x}} + r_{y,\Delta v,U} \hat{\mathbf{y}} + 0 \hat{\mathbf{z}}, \text{ km}$$

$$\text{where, } r_{x,\Delta v,U} = r_{\Delta v,U} \cos v_{\Delta v,U}$$

$$\text{and, } r_{y,\Delta v,U} = r_{\Delta v,U} \sin v_{\Delta v,U}$$

b. Velocity vector with respect to unperturbed perifocal coordinates:

$$\bar{\mathbf{v}}_{\Delta v,P} = v_{x,\Delta v,P} \hat{\mathbf{x}} + v_{y,\Delta v,P} \hat{\mathbf{y}} + 0 \hat{\mathbf{z}}, \text{ km s}^{-1}$$

c. Specific angular momentum vector with respect to unperturbed perifocal coordinates:

$$\bar{\mathbf{h}}_P = \bar{\mathbf{r}}_{\Delta v,P} \times \bar{\mathbf{v}}_{\Delta v,P}, \text{ km}^2 \text{ s}^{-1}$$

d. Perturbed orbit parameter:

$$p_P = \frac{|\bar{\mathbf{h}}_P|^2}{\mu_{\text{Sun}}} = a_P (1 - e_P^2), \text{ km}$$

$$\text{where } |\bar{\mathbf{h}}_P|^2 = \bar{\mathbf{h}}_P \cdot \bar{\mathbf{h}}_P$$

e. Perturbed eccentricity vector with respect to unperturbed perifocal coordinates:

$$\bar{\mathbf{e}}_P = \frac{1}{\mu_{\text{Sun}}} \left[\left(|\bar{\mathbf{v}}_{\Delta v,P}|^2 - \frac{\mu_{\text{Sun}}}{|\bar{\mathbf{r}}_{\Delta v,P}|} \right) \bar{\mathbf{r}}_{\Delta v,P} - (\bar{\mathbf{r}}_{\Delta v,P} \cdot \bar{\mathbf{v}}_{\Delta v,P}) \bar{\mathbf{v}}_{\Delta v,P} \right]$$

$$\text{where } |\bar{\mathbf{v}}_{\Delta v,P}|^2 = \bar{\mathbf{v}}_{\Delta v,P} \cdot \bar{\mathbf{v}}_{\Delta v,P},$$

$$\text{and } |\bar{\mathbf{r}}_{\Delta v,P}| = r_{\Delta v,U}$$

f. Perturbed orbital eccentricity:

$$e_P = \sqrt{\bar{\mathbf{e}}_P \cdot \bar{\mathbf{e}}_P}$$

g. Perturbed orbit semi-major axis:

$$a_P = \frac{p_P}{1 - e_P^2}, \text{ km}$$

h. Perturbed orbit mean motion:

$$n_P = \sqrt{\frac{\mu_{\text{Sun}}}{a_P^3}}, \text{ rad s}^{-1}$$

i. Perturbed orbital period:

$$P_P = \frac{2\pi}{n_P}, \text{ s}$$

VI. Determine the angle between the perturbed and unperturbed orbital eccentricity vectors.

a. Unperturbed orbital eccentricity vector:

$$\bar{\mathbf{e}}_U = e_U \hat{\mathbf{x}} + 0\hat{\mathbf{y}} + 0\hat{\mathbf{z}}$$

b. Rotation of eccentricity vector due to impulse:

$$\Delta v = \cos^{-1} \left(\frac{\bar{\mathbf{e}}_P \cdot \bar{\mathbf{e}}_U}{e_P e_U} \right)$$

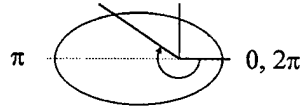
VII. Determine the impulse conditions with respect to the perturbed orbit.

a. True anomaly at impulse with respect to the perturbed orbit:

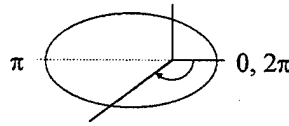
$$v_{\Delta v, P} = \cos^{-1} \left(\frac{a_P (1 - e_P^2)}{r_{\Delta v, P} e_P} - \frac{1}{e_P} \right)$$

(\cos^{-1} principle values are $0 \leq \theta \leq \pi$)

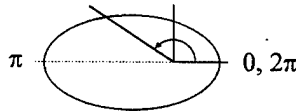
$$\text{if } -1 < F_{\text{orbit}} < -\frac{1}{2}, \text{ then } v_{\Delta v, P} = 2\pi(N_{\text{orbit}} - 1) + v_{\Delta v, P}$$



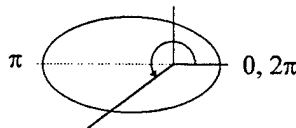
$$\text{if } -\frac{1}{2} \leq F_{\text{orbit}} < 0, \text{ then } v_{\Delta v, P} = 2\pi N_{\text{orbit}} - v_{\Delta v, P}$$



$$\text{if } 0 \leq F_{\text{orbit}} < \frac{1}{2}, \text{ then } v_{\Delta v, P} = 2\pi N_{\text{orbit}} + v_{\Delta v, P}$$



$$\text{if } \frac{1}{2} \leq F_{\text{orbit}} < 1, \text{ then } v_{\Delta v, P} = 2\pi(N_{\text{orbit}} + 1) - v_{\Delta v, P}$$



b. Eccentric anomaly at impulse with respect to perturbed orbit:

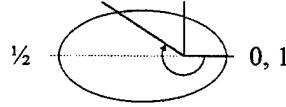
$$E_{\Delta v, P} = \cos^{-1} \left(\frac{e_p + \cos v_{\Delta v, P}}{1 + e_p \cos v_{\Delta v, P}} \right)$$

(\cos^{-1} principle values are $0 \leq \theta \leq \pi$)

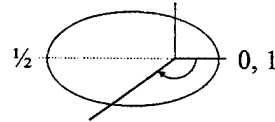
c. Fraction of orbit of prior to (or since) perihelion of impulse with respect to perturbed orbit:

$$\left(\frac{t}{P_p} \right)_{\Delta v, p} = \frac{E_{\Delta v, P} - e_p \sin E_{\Delta v, P}}{2\pi}$$

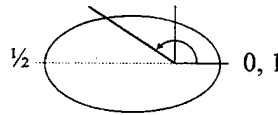
$$\text{if } -1 < F_{\text{orbit}} < -\frac{1}{2}, \text{ then } \left(\frac{t}{P_p} \right)_{\Delta v, p} = (N_{\text{orbit}} - 1) + \left(\frac{t}{P_p} \right)_{\Delta v, p}$$



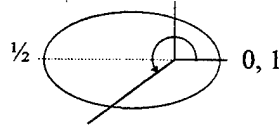
$$\text{if } -\frac{1}{2} \leq F_{\text{orbit}} < 0, \text{ then } \left(\frac{t}{P_p} \right)_{\Delta v, p} = N_{\text{orbit}} - \left(\frac{t}{P_p} \right)_{\Delta v, p}$$



$$\text{if } 0 \leq F_{\text{orbit}} < \frac{1}{2}, \text{ then } \left(\frac{t}{P_p} \right)_{\Delta v, p} = N_{\text{orbit}} + \left(\frac{t}{P_p} \right)_{\Delta v, p}$$



$$\text{if } \frac{1}{2} \leq F_{\text{orbit}} < 1, \text{ then } \left(\frac{t}{P_p} \right)_{\Delta v, p} = (N_{\text{orbit}} + 1) - \left(\frac{t}{P_p} \right)_{\Delta v, p}$$



VIII. Determine a range of times, and hence positions, of the unperturbed asteroid in the vicinity of the impact point on the unperturbed orbit for mapping to corresponding times, and positions, of the perturbed asteroid on the perturbed orbit.

a. Set time period:

$$N_{\text{days}} = \pm 2, \text{ days}$$

b. Set number of positions to map during time period:

$$n_{\text{pos}} = 201$$

c. Establish limits of time interval:

$$\Delta\left(\frac{t}{P_U}\right) = \left(\frac{N_{\text{days}}}{P_U}\right)\left(\frac{24 \text{ hrs}}{1 \text{ day}}\right)\left(\frac{3600 \text{ s}}{1 \text{ hr}}\right)$$

d. Number of increments in time period:

$$n_{\text{inc}} = n_{\text{pos}} - 1$$

e. Incremental time step:

$$\delta\left(\frac{t}{P_U}\right) = \Delta\left(\frac{t}{P_U}\right)\left(\frac{1}{n_{\text{inc}}}\right)$$

f. Now have n_{pos} positions from $-N_{\text{days}}$ to $+N_{\text{days}}$ in steps of $2N_{\text{days}}/n_{\text{inc}}$ parts of a day represented as fractions of a complete orbit.

$$\left(\frac{t}{P_U}\right)_{\text{Range}} = -\Delta\left(\frac{t}{P_U}\right) \leq \left(\frac{t}{P_U}\right)_i \leq +\Delta\left(\frac{t}{P_U}\right), \text{ in steps of } \delta\left(\frac{t}{P_U}\right)$$

g. Center this range of positions on the fraction of orbit since (or prior to) perihelion of impact:

$$\left(\frac{t}{P_U}\right)_{\text{Range, impact}} = \left(\frac{t}{P_U}\right)_{\text{Range}} + \left(\frac{t}{P_U}\right)_{\text{impact, p}}$$

h. Eccentric anomaly at each time coordinate (solve via Newton-Raphson iterative method):

$$\left(\frac{t}{P_U}\right)_{i, \text{Range, impact}} = \frac{E_{i,U} - e_U \cos E_{i,U}}{2\pi}$$

i. Determine the true anomalies at each time coordinate with respect to the unperturbed perifocal coordinates.

$$v_{i,U} = \cos^{-1} \left(\frac{\cos E_{i,U} - e_U}{1 - e_U \cos E_{i,U}} \right)$$

(\cos^{-1} principle values are $0 \leq \theta \leq \pi$)

$$\text{if } \left(\frac{t}{P_U}\right)_{i, \text{Range, impact}} < -\frac{1}{2}, \text{ then } v_{i,U} = -2\pi + v_{i,U}$$

$$\text{if } \left(\frac{t}{P_U}\right)_{i, \text{Range, impact}} < 0, \text{ then } v_{i,U} = -v_{i,U}$$

$$\text{if } \left(\frac{t}{P_U}\right)_{i, \text{Range, impact}} > \frac{1}{2}, \text{ then } v_{i,U} = 2\pi - v_{i,U}$$

j. Determine the radial distance to the focus (Sun) for these time coordinates:

$$r_{i,U} = \frac{a_U(1 - e_U^2)}{1 + e_U \cos v_{i,U}}, \text{ km}$$

k. Determine the distance components at each time coordinate with respect to the unperturbed perifocal coordinates:

$$x_{i,U} = r_{i,U} \cos v_{i,U}, \text{ km}$$

$$y_{i,U} = r_{i,U} \sin v_{i,U}, \text{ km}$$

IX. We now need to determine the true anomaly and fraction of orbit on the perturbed orbit that corresponds to the true anomaly and fraction of orbit at the impact position on the unperturbed orbit.

Determine the positions and orbit fractions on the perturbed orbit that correspond to the n_{pos} positions and orbit fractions of the unperturbed orbit.

a. Fraction of orbit since (or prior to) perihelion of the “impact” position with respect to the perturbed orbit:

$$\left(\frac{t}{P_P}\right)_{p, impact} = \left(\frac{t}{P_P}\right)_{\Delta v, P} + \left(\frac{t}{P_U}\right)_{\Delta v} \left(\frac{P_U}{P_P}\right)$$

b. Establish the n_{pos} orbital positions and fractions of orbit on the perturbed orbit that correspond exactly to the n_{pos} positions of the unperturbed orbit:

$$\left(\frac{t}{P_P}\right)_{Range, impact} = \left(\frac{t}{P_U}\right)_{Range} \left(\frac{P_U}{P_P}\right) + \left(\frac{t}{P_P}\right)_{impact, P}$$

c. Eccentric anomaly at each time coordinate (solve via Newton-Raphson iterative method):

$$\left(\frac{t}{P_P}\right)_{i, Range, impact} = \frac{E_{i, P} - e_P \cos E_{i, P}}{2\pi}$$

d. Determine the true anomalies at each time coordinate with respect to the perturbed perifocal coordinates.

$$v_{i, P} = \cos^{-1} \left(\frac{\cos E_{i, P} - e_P}{1 - e_P \cos E_{i, P}} \right)$$

(\cos^{-1} principle values are $0 \leq \theta \leq \pi$)

$$\text{if } \left(\frac{t}{P_P}\right)_{i, Range, impact} < -\frac{1}{2}, \text{ then } v_{i, P} = -2\pi + v_{i, P}$$

$$\text{if } \left(\frac{t}{P_P}\right)_{i, Range, impact} < 0, \text{ then } v_{i, P} = -v_{i, P}$$

$$\text{if } \left(\frac{t}{P_P} \right)_{i, \text{Range}, \text{impact}} > \frac{1}{2}, \text{ then } v_{i,P} = 2\pi - v_{i,P}$$

e. Shift true anomalies from perturbed coordinates to unperturbed coordinates:

$$v_{i,P,U} = v_{i,P} + \Delta v$$

e. Determine the radial distance to the focus (Sun) for these time coordinates:

$$r_{i,P} = \frac{a_P(1 - e_P^2)}{1 + e_P \cos v_{i,P}}, \text{ km}$$

f. Determine the distance components at each time coordinate with respect to the unperturbed perifocal coordinates:

$$x_{i,P} = r_{i,P} \cos v_{i,P,U}, \text{ km}$$

$$y_{i,P} = r_{i,P} \sin v_{i,P,U}, \text{ km}$$

X. Now we need the positions of the Earth at the same n_{pos} positions surrounding the impact position.

a. True anomaly of the Earth at each of the n_{pos} positions:

$$v_{\text{Range},E} = v_{\text{impact},E} + \left(\frac{t}{P_U} \right)_{\text{Range}} (P_U n_E)$$

b. Determine the distance components of the Earth at each time coordinate with respect to the unperturbed perifocal coordinates:

$$x_{i,E} = a_E \cos v_{i,E}, \text{ km}$$

$$y_{i,E} = a_E \sin v_{i,E}, \text{ km}$$

XI. Now must handle the special case of $\left(\frac{t}{P_U}\right)_{\Delta v} < \Delta\left(\frac{t}{P_U}\right)$.

For this case, set:

$$x_{i,P} = x_{i,U}$$

$$y_{i,P} = y_{i,U}$$

$$\text{while } \left(\frac{t}{P_U}\right)_{\Delta v} \leq \Delta\left(\frac{t}{P_U}\right)$$

XII. Define the separation distances of the perturbed and unperturbed asteroid orbital positions from the Earth orbital positions.

a. Perturbed asteroid to Earth separation distance:

$$R_{\text{sep},P} = \sqrt{(x_{i,P} - x_{i,E})^2 + (y_{i,P} - y_{i,E})^2}, \text{ km}$$

b. Unperturbed asteroid to Earth separation distance:

$$R_{\text{sep},U} = \sqrt{(x_{i,U} - x_{i,E})^2 + (y_{i,U} - y_{i,E})^2}, \text{ km}$$

c. Scale the separation distances by the radius of the Earth:

$$\rho_{\text{sep},P} = \frac{R_{\text{sep},P}}{R_E}, \text{ Earth radii}$$

$$\rho_{\text{sep},U} = \frac{R_{\text{sep},U}}{R_E}, \text{ Earth radii}$$

XIII. Finally, select the minimum value over the orbital position range as the minimum separation distance.

a. Minimum perturbed asteroid to Earth separation:

$$\left(\rho_{\text{sep},P}\right)_{\min} = \min\left(\rho_{\text{sep},P}\right), \text{ Earth radii}$$

b. Minimum unperturbed asteroid to Earth separation (By the definition of the problem this is zero, but this provides a good check of the method.):

$$\left(\rho_{\text{sep},U}\right)_{\min} = \min\left(\rho_{\text{sep},U}\right), \text{ Earth radii}$$

APPENDIX B. ANALYTIC SOLUTION METHOD, MATLAB MODEL

```
%%%%%%%%%%%%%%%%%%%%%%%%%%%%%%%%%%%%%%%%%%%%%%%%%%%%%%%%%%%%%%%%%%%%%%%%%
% Arbitrary Elliptical Orbit Intersecting Circular Earth Orbit
%
% MATLAB Script File Name: nwarborb.m
%
% Author: LT Jeffrey T. Elder
%   Naval Postgraduate School
%   November 1996
%
%%%%%%%%%%%%%%%%%%%%%%%%%%%%%%%%%%%%%%%%%%%%%%%%%%%%%%%%%%%%%%%%%%%%%%%%%

%%%%%%%%%%%%%%%%%%%%%%%%%%%%%%%%%%%%%%%%%%%%%%%%%%%%%%%%%%%%%%%%%%%%%%%%%
% Initialize computational workspace
clear

%%%%%%%%%%%%%%%%%%%%%%%%%%%%%%%%%%%%%%%%%%%%%%%%%%%%%%%%%%%%%%%%%%%%%%%%%
% Define constants
AU = 1.4959787e8;           % astronomical unit
musun = 1.327124399355e11; % gravitational parameter for the Sun
epsilon = 5e-6;            % Newton-Raphson tolerance

%%%%%%%%%%%%%%%%%%%%%%%%%%%%%%%%%%%%%%%%%%%%%%%%%%%%%%%%%%%%%%%%%%%%%%%%%
% Gather input data from user
nuimpactU = input('Enter True Anomaly for Impact (deg): ');
eU = input('Enter Asteroid eccentricity: ');
tPUdelv = input('Enter (t/P) of Impulse Prior to Impact: ');
delV = input('Enter the Magnitude of the Impulse dV, (m/s): ');
thet = input('Enter the Direction of the Impulse wrt V, ccw+ (deg): ');
dvvi = delV*cos(thet*pi/180);
dvni = delV*sin(thet*pi/180);

%%%%%%%%%%%%%%%%%%%%%%%%%%%%%%%%%%%%%%%%%%%%%%%%%%%%%%%%%%%%%%%%%%%%%%%%%
% Allow for model performance evaluation
%flops(0)
%tic

%%%%%%%%%%%%%%%%%%%%%%%%%%%%%%%%%%%%%%%%%%%%%%%%%%%%%%%%%%%%%%%%%%%%%%%%%
% Set Earth orbital elements
aE = 1.0*AU;
nE = sqrt(musun/aE^3);

%%%%%%%%%%%%%%%%%%%%%%%%%%%%%%%%%%%%%%%%%%%%%%%%%%%%%%%%%%%%%%%%%%%%%%%%%
% Convert impact true anomaly to radians
nuimpactU = nuimpactU*pi/180;

%%%%%%%%%%%%%%%%%%%%%%%%%%%%%%%%%%%%%%%%%%%%%%%%%%%%%%%%%%%%%%%%%%%%%%%%%
% Determine unperturbed asteroid orbital elements
rpU = aE*(1+eU*cos(nuimpactU))/(1-eU); % Perihelion radius
aU = rpU/(1-eU);                       % Semi-major axis
nU = sqrt(musun/aU^3);                 % Mean motion
PU = 2*pi/nU;                         % Period
```

```

%%%%%%%%%%%%%%%%%%%%%%%%%%%%%%%%%%%%%%%%%%%%%%%%%%%%%%%%%%%%%%%%%%%%%%%%
% Determine the conditions of impact wrt unperturbed orbit
EimpactU = ... % ... is line continuation
acos((eU+cos(nuimpactU))/...
/(1+eU*cos(nuimpactU))); % Impact eccentric anomaly
tPUimpact = ...
(EimpactU-eU*sin(EimpactU))/(2*pi); % t/P of impact wrt perihelion
if nuimpactU < 0
    tPUimpact = -tPUimpact;
end

%%%%%%%%%%%%%%%%%%%%%%%%%%%%%%%%%%%%%%%%%%%%%%%%%%%%%%%%%%%%%%%%%%%%%%%%
tPUimpulse = tPUimpact-tPUdely; % t/P of impulse wrt perihelion
Norbit = fix(tPUimpulse); % Number of whole orbits
Forbit = tPUimpulse - Norbit; % Fraction of orbits

%%%%%%%%%%%%%%%%%%%%%%%%%%%%%%%%%%%%%%%%%%%%%%%%%%%%%%%%%%%%%%%%%%%%%%%%
% Allow for numerical simulation validation
tao = tPUimpulse*PU; % Start time for simulation
tend = (tPUimpact+0.125)*PU; % End time for simulation

%%%%%%%%%%%%%%%%%%%%%%%%%%%%%%%%%%%%%%%%%%%%%%%%%%%%%%%%%%%%%%%%%%%%%%%%
% Determine true anomaly of impulse
EimpulseU = pi/4; % Guess eccentric anomaly
tptemp = Forbit;
if tPUimpulse < 0 % allow for +/- tPUimpulse
    tptemp = -Forbit;
end
true = 0;
while true == 0 % Newton-Raphson iteration
    fprime = 1 - eU*cos(EimpulseU);
    f = EimpulseU - eU*sin(EimpulseU) - 2*pi*tptemp;
    Elast = EimpulseU;
    EimpulseU = Elast - f/fprime;
    if abs(EimpulseU-Elast) < epsilon, true=1;, end
end % End N-R iteration
if tPUimpulse < 0, EimpulseU = -EimpulseU;, end
nuimpulseU = ...
acos((cos(EimpulseU)-eU)/...
(1-eU*cos(EimpulseU))); % True anomaly at impulse
% If t/P of impulse exceeds
% one orbit, determine true
% anomaly for multiple orbits
% Conditions to properly
% locate true anomaly

if (-1 < Forbit) & (Forbit < -0.5)
    nuimpulseU = ...
    2*pi*(Norbit-1)+nuimpulseU;
elseif (-0.5 <= Forbit) & (Forbit < 0)
    nuimpulseU = 2*pi*Norbit - nuimpulseU;
elseif (0 <= Forbit) & (Forbit < 0.5)
    nuimpulseU = 2*pi*Norbit + nuimpulseU;
elseif (0.5 <= Forbit) & (Forbit < 1)
    nuimpulseU = 2*pi*(Norbit+1) - nuimpulseU;
end

```

```

%%%%%%%%%%%%%%%%%%%%%%%%%%%%%%%%%%%%%%%%%%%%%%%%%%%%%%%%%%%%%%%%%%%%%%%%
% Determine orbital distances at time of impulse
rimpulseU = aU*(1-eU^2)/(1+eU*cos(nuimpulseU));
ximpulseU = rimpulseU*cos(nuimpulseU);
yimpulseU = rimpulseU*sin(nuimpulseU);

%%%%%%%%%%%%%%%%%%%%%%%%%%%%%%%%%%%%%%%%%%%%%%%%%%%%%%%%%%%%%%%%%%%%%%%%
% Perturb the asteroid
pU = aU*(1-eU*eU);
vximpulseU = ...
-sqrt(musun/pU)*sin(nuimpulseU);
vyimpulseU = ...
sqrt(musun/pU)*(eU+cos(nuimpulseU));
dvv = dvvi/1000.0;
dvn = dvni/1000.0;
alpha = atan2(vyimpulseU,vximpulseU);
vximpulseP = ...
vximpulseU+dvv*cos(alpha)-dvn*sin(alpha);
vyimpulseP = ...
vyimpulseU + dvv*sin(alpha) + dvn*cos(alpha);

%%%%%%%%%%%%%%%%%%%%%%%%%%%%%%%%%%%%%%%%%%%%%%%%%%%%%%%%%%%%%%%%%%%%%%%%
% Determine perturbed asteroid orbit elements from R and V
rimpulsePvec = [ximpulseU yimpulseU 0];
vimpulsePvec = [vximpulseP vyimpulseP 0];
hpvec = cross(rimpulsePvec,vimpulsePvec);
pP = hpvec*hpvec/musun;
ePvec = ( (vimpulsePvec*vimpulsePvec'-musun/rimpulseU)*rimpulsePvec...
- (rimpulsePvec*vimpulsePvec')*vimpulsePvec )/musun;
eP2 = ePvec*ePvec;
eP = sqrt(eP2);
aP = pP/(1-eP2);
nP = sqrt(musun/aP^3);
PP = 2*pi/nP;

%%%%%%%%%%%%%%%%%%%%%%%%%%%%%%%%%%%%%%%%%%%%%%%%%%%%%%%%%%%%%%%%%%%%%%%%
% Determine angle perturbed orbit perihelion makes wrt unperturbed orbit perihelion
dnu = acos( (ePvec*[eU 0 0])/(eP*eU) );
if ePvec(2) < 0, dnu = -dnu; end

%%%%%%%%%%%%%%%%%%%%%%%%%%%%%%%%%%%%%%%%%%%%%%%%%%%%%%%%%%%%%%%%%%%%%%%%
% Determine impulse true anomaly wrt perturbed orbit
cnuimpulseP = aP*(1-eP2)/(rimpulseU*eP) - 1/eP;
nuimpulseP = acos(cnuimpulseP);

if (-1 < Forbit) & (Forbit < -0.5)
    nuimpulseP = ...
    2*pi*(Norbit-1)+nuimpulseP;
elseif (-0.5 <= Forbit) & (Forbit < 0)
    nuimpulseP = 2*pi*Norbit - nuimpulseP;
elseif (0 <= Forbit) & (Forbit < 0.5)

% Parameter of orbit
% Unperturbed velocities
% Impulse parallel to V
% Impulse normal to V
% Angle of V wrt x-axis
% Perturbed velocities
% Position vector
% Velocity vector
% Angular momentum vec.
% Parameter of orbit
% Eccentricity vector
% Eccentricity
% Semi-major axis
% Mean motion
% Period
% True anomaly at impulse
% If t/P of impulse exceeds
% one orbit, determine true
% anomaly for multiple orbits
% Conditions to properly
% locate true anomaly

```

```

    nuimpulseP = 2*pi*Norbit + nuimpulseP;
elseif (0.5 <= Forbit) & (Forbit < 1)
    nuimpulseP = 2*pi*(Norbit+1) - nuimpulseP;
end

%%%%%%%%%%%%%%%%%%%%%%%%%%%%%%%%%%%%%%%%%%%%%%%%%%%%%%%%%%%%%%%%%%%%%%%%
% Determine impulse time wrt perturbed orbit
EimpulseP = acos( (eP+cnuimpulseP)/(1+eP*cnuimpulseP) );
tPPpimpulse = ...
    (EimpulseP-eP*sin(EimpulseP))/2/pi;

% t/P of impulse
% If t/P of impulse exceeds
% one orbit, determine t/P of
% impulse for multiple orbits
% Conditions to properly
% determine t/P of impulse

if (-1 < Forbit) & (Forbit < -0.5)
    tPPpimpulse = (Norbit-1)+tPPpimpulse;
elseif (-0.5 <= Forbit) & (Forbit < 0)
    tPPpimpulse = Norbit - tPPpimpulse;
elseif (0 <= Forbit) & (Forbit < 0.5)
    tPPpimpulse = Norbit + tPPpimpulse;
elseif (0.5 <= Forbit) & (Forbit < 1)
    tPPpimpulse = (Norbit+1) - tPPpimpulse;
end

%%%%%%%%%%%%%%%%%%%%%%%%%%%%%%%%%%%%%%%%%%%%%%%%%%%%%%%%%%%%%%%%%%%%%%%%
ndaycoef = 1.5;
Ndays = ndaycoef*tPUdelv*delV;

% npos & Ndays define initial
% mesh size
% Make two passes to ensure
% 'mesh' is properly sized
% to give accurate minimum

loop = 2;
while(loop >= 1)
    npos = max([201 fix(100*Ndays+1)]);

    nuU=[];
    nuP=[];

    % Initialize true anomaly
    % matrices

    %%%%%%%%%%%%%%%%%%%%%%%%%%%%%%%%%%%%%%%%%%%%%%%%%%%%%%%%%%%%%%%%%%%%%%%%%
    % Create a mesh of orbit positions about the impact point on the
    % unperturbed orbit
    deltPU = Ndays*24*3600/PU;
    tPURangeimpact = ...
        linspace(-deltPU,deltPU,npos)+tPUimpact;% located in t/P space
    for i = 1:npos
        true = 0;
        EU = tPURangeimpact(i)*pi;
        tptemp = tPURangeimpact(i);
        if tPURangeimpact(i) < 0, tptemp = -tPURangeimpact(i);, end
        while true == 0
            fprime = 1 - eU*cos(EU);
            f = EU - eU*sin(EU) - 2*pi*tptemp;
            Elast = EU;
            EU = EU - f/fprime;
            if abs(EU-Elast) < epsilon, true = 1; end
        end
        if tPURangeimpact(i) < 0, EU = -EU; end
        nuU(i) = ...

% Unperturbed mesh half width
% Unperturbed mesh properly

% Determine true anomaly of
% unperturbed mesh points

% Newton-Raphson iteration

% End N-R iteration

```

```

        acos((cos(EU)-eU)/(1-eU*cos(EU)));    % True anomalies of
                                                % unperturbed mesh points
    if tPURangeimpact(i) < -0.5                % Ensure true anomalies are
        nuU(i) = -2*pi + nuU(i);              % properly located
    elseif tPURangeimpact(i) < 0
        nuU(i) = -nuU(i);
    elseif tPURangeimpact(i) > 0.5
        nuU(i) = 2*pi - nuU(i);
    end
end
rU = aU*(1-eU^2) ./ (1+eU*cos(nuU));          % Positions of unperturbed
xU = rU.*cos(nuU);                            % mesh points wrt unperturbed
yU = rU.*sin(nuU);                           % coordinate frame

%%%%%%%%%%%%%%%%%%%%%%%%%%%%%%%%%%%%%%%%%%%%%%%%%%%%%%%%%%%%%%%%%%%%%%%%
% Map the mesh of orbit positions about the impact point onto the perturbed orbit
tPPpimpact = tPPpimpulse + tPUdelv*PU/PP;      % t/P of impact wrt perihelion
deltPP = Ndays*24*3600/PP;                   % Perturbed mesh half width
tPPRangeimpact = ...                          % Perturbed mesh properly
    linspace(-deltPP,deltPP,npos)+tPPpimpact;% located in t/P space
for i = 1:npos                                % Determine true anomaly
    true = 0;                                  % of perturbed mesh points
    EP = tPPRangeimpact(i)*pi;
    tptemp = tPPRangeimpact(i);
    if tPPRangeimpact(i) < 0, tptemp = -tPPRangeimpact(i);, end
    while true == 0                             % Newton-Raphson iteration
        fprime = 1 - eP*cos(EP);
        f = EP - eP*sin(EP) - 2*pi*tptemp;
        Elast = EP;
        EP = EP - f/fprime;
        if abs(EP-Elast) < epsilon, true = 1;,, end
    end                                         % End N-R iteration
    if tPPRangeimpact(i) < 0, EP = -EP;,, end
    nuP(i) = ...
        acos((cos(EP)-eP)/(1-eP*cos(EP)));    % True anomalies of perturbed
                                                % mesh points
    if tPPRangeimpact(i) < -0.5                % Ensure true anomalies are
        nuP(i) = -2*pi + nuP(i);              % properly located
    elseif tPPRangeimpact(i) < 0
        nuP(i) = -nuP(i);
    elseif tPPRangeimpact(i) > 0.5
        nuP(i) = 2*pi - nuP(i);
    end
end
nuPU = nuP + dnu;                             % Perturbed mesh true
                                                % anomalies wrt unperturbed
                                                % coordinate frame
rP = aP*(1-eP^2) ./ (1+eP*cos(nuP));          % Positions of perturbed mesh
xP = rP.*cos(nuPU);                           % points wrt unperturbed
yP = rP.*sin(nuPU);                           % coordinate frame

%%%%%%%%%%%%%%%%%%%%%%%%%%%%%%%%%%%%%%%%%%%%%%%%%%%%%%%%%%%%%%%%%%%%%%%%
% Map the mesh of orbit positions about the impact point on the Earth's orbit
delnuE = Ndays*24*3600*nE;                   % Earth mesh half width

```



```

nuRangeE = ...
    linspace(-delnuE,delnuE,npos)+nuimpactU;           % Earth mesh properly located
                                                    % in true anomaly space
xE = AU*cos(nuRangeE);                               % Positions of Earth mesh
yE = AU*sin(nuRangeE);                               % points wrt unperturbed
                                                    % coordinate frame

%%%%%%%%%%%%%%%%%%%%%%%%%%%%%%%%%%%%%%%%%%%%%%%%%%%%%%%%%%%%%%%%%%%%%%%%
% handle special case of tPUdelv < deltPU
if tPUdelv < deltPU
    [v,loc] = min(abs(tPPRangeimpact-tPUimpact+tPUdelv));
    xP(1:loc) = xU(1:loc);
    yP(1:loc) = yU(1:loc);
end

%%%%%%%%%%%%%%%%%%%%%%%%%%%%%%%%%%%%%%%%%%%%%%%%%%%%%%%%%%%%%%%%%%%%%%%%
% Determine the Earth to asteroid separation in Earth radii
rhosepU = ...
    sqrt((xU-xE).^2 + (yU-yE).^2)/6378.14;           % Unperturbed orbit
rhosepP = ...
    sqrt((xP-xE).^2 + (yP-yE).^2)/6378.14;           % Perturbed orbit
[rhosepUmin,inu] = min(rhosepU);                     % Minimum unperturbed
                                                    % separation (must be zero)
[rhosepPmin,inp] = min(rhosepP);                     % Minimum perturbed separation

%%%%%%%%%%%%%%%%%%%%%%%%%%%%%%%%%%%%%%%%%%%%%%%%%%%%%%%%%%%%%%%%%%%%%%%%
if Ndays == ndaycoef*tPUdelv*delV                   % Refine mesh
    Ndays = 1.25*abs(tPURangeimpact(inp)*PU/3600/24 ...
        -tPURangeimpact(inu)*PU/3600/24);
end
loop = loop - 1;                                       % Allow for loop exit
end                                                    % End while(test) loop

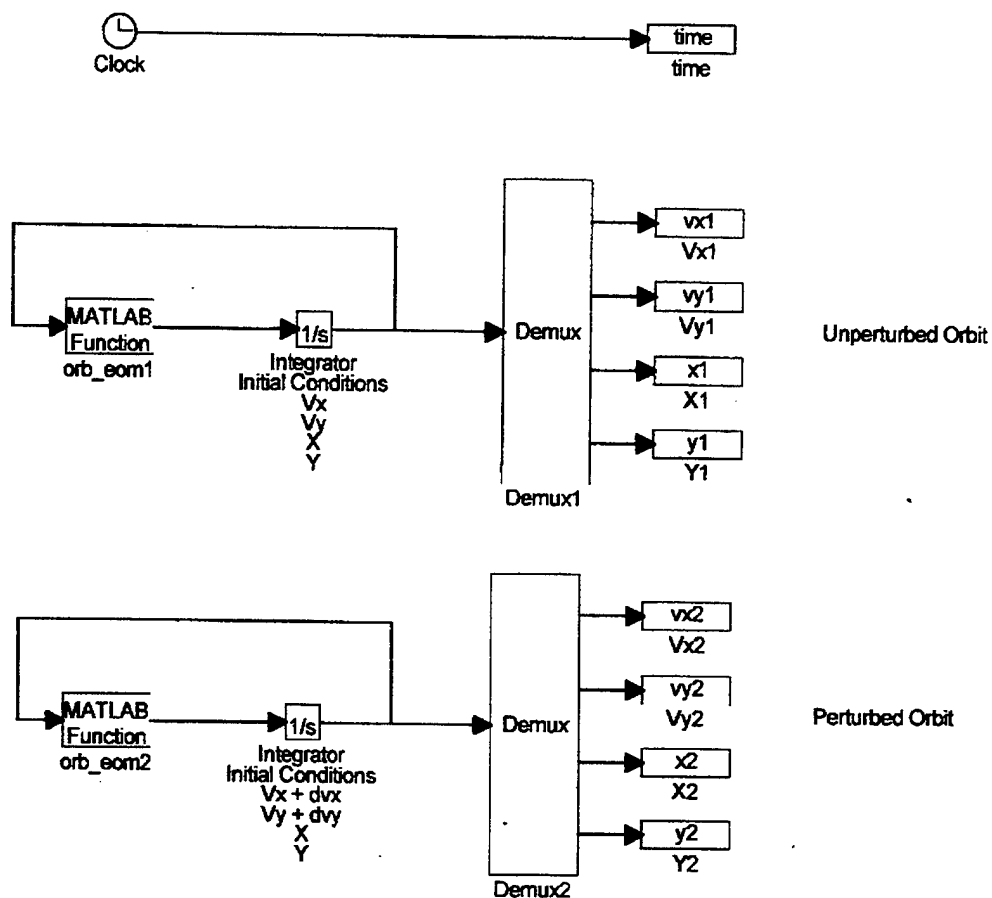
%%%%%%%%%%%%%%%%%%%%%%%%%%%%%%%%%%%%%%%%%%%%%%%%%%%%%%%%%%%%%%%%%%%%%%%%
rhosepPmin                                             % Display minimum separation

%%%%%%%%%%%%%%%%%%%%%%%%%%%%%%%%%%%%%%%%%%%%%%%%%%%%%%%%%%%%%%%%%%%%%%%%
%toc                                                  % Display model performance
%flops

```

APPENDIX C. NUMERICAL VALIDATION MODEL

SIMULINK MODEL



In order to run the SIMULINK numerical integration model, the analytic method model must first be run. The initial conditions for the integrators are specified by the working variables in the analytic model.

MATLAB SCRIPT SUPPORTING SIMULINK MODEL

```
%%%%%%%%%%%%%%%%%%%%%%%%%%%%%%%%%%%%%%%%%%%%%%%%%%%%%%%%%%%%%%%%%%%%%%%%%%%%%%
%
%
% orbeom2d.m
%
% Equations of motion for 2d orbit
%
% Author: LT Jeffrey T. Elder
%         Naval Postgraduate School
%         November 1996
%
%%%%%%%%%%%%%%%%%%%%%%%%%%%%%%%%%%%%%%%%%%%%%%%%%%%%%%%%%%%%%%%%%%%%%%%%%%%%%%
%

function xdot=orb_eom(x)

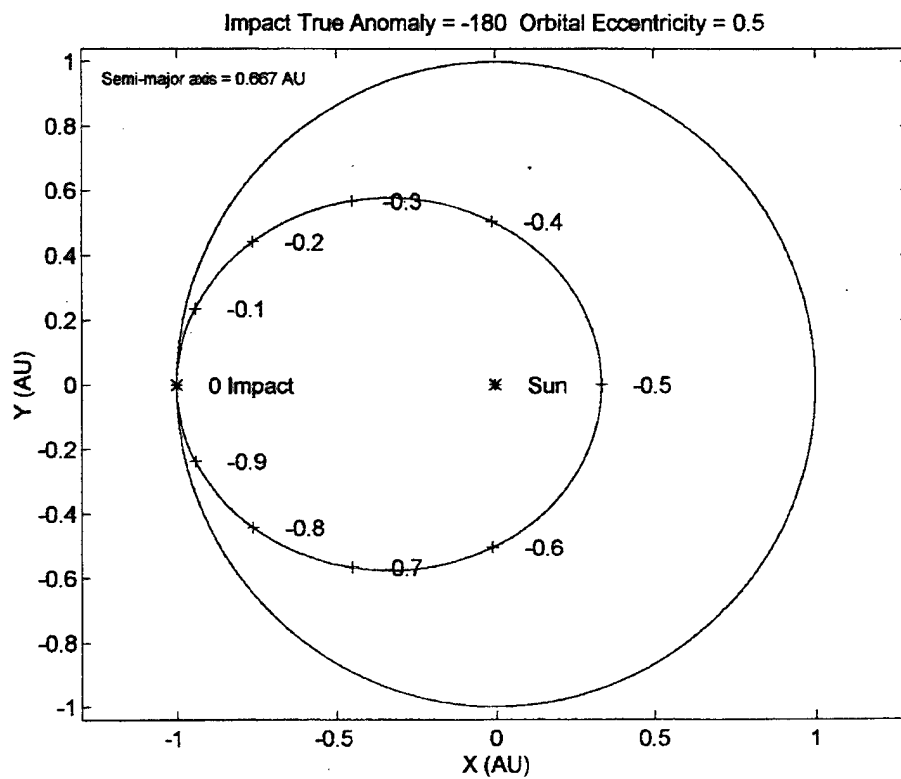
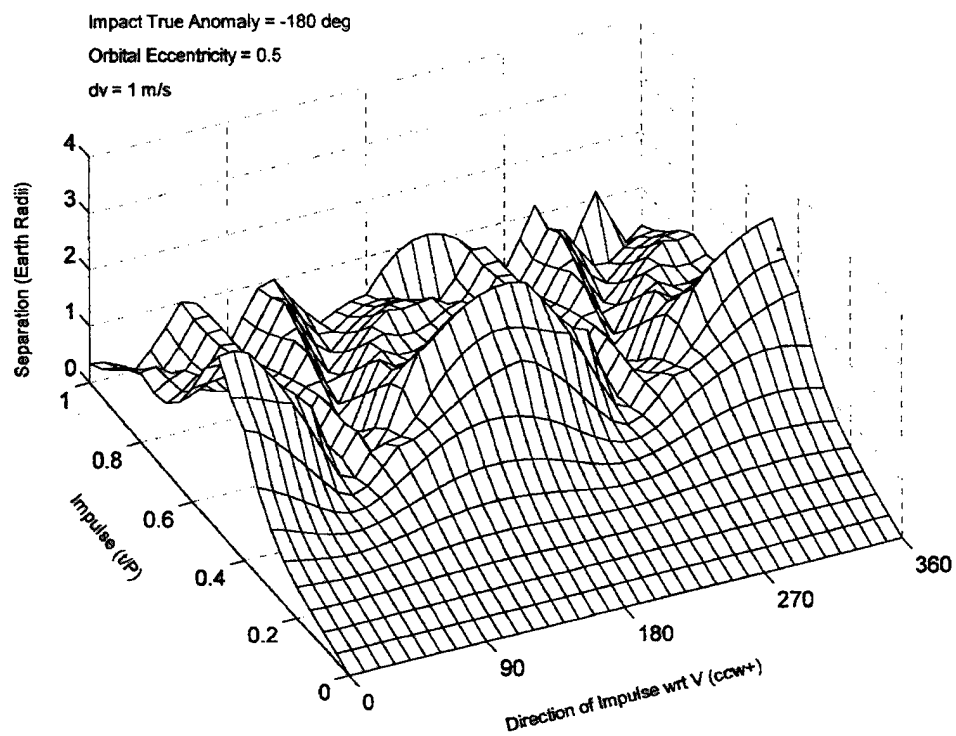
mu = 1.327124399355e11;          % Mass parameter for Sun
AU = 1.49597870e8;              % Astronomical unit
r2 = x(3)^2 + x(4)^2;          % Radial distance squared
mur2 = mu/r2;
r = sqrt(r2);                  % Radial distance

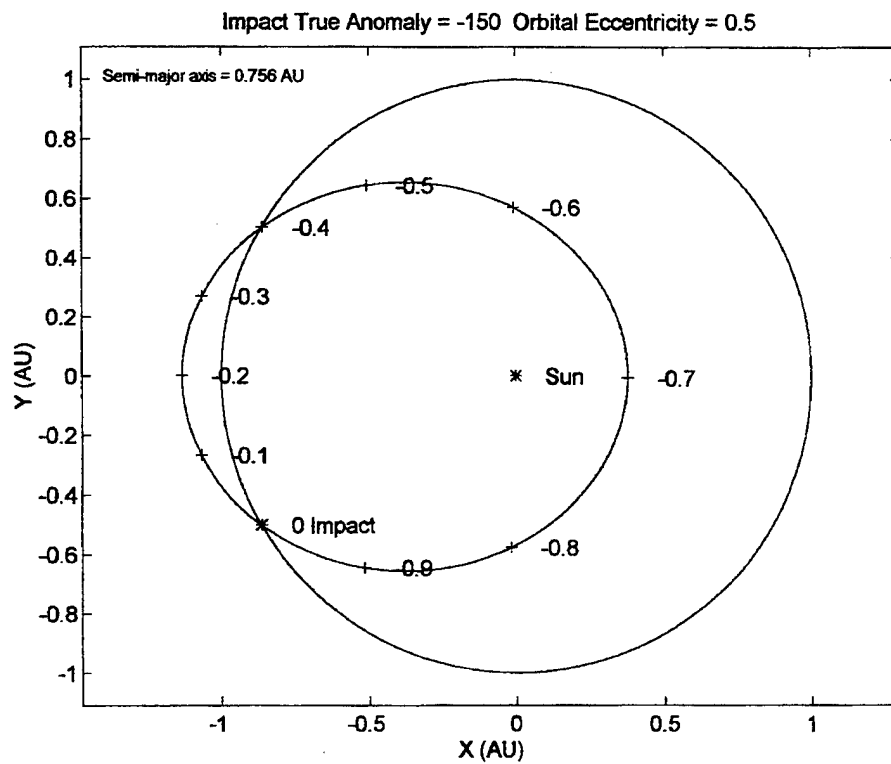
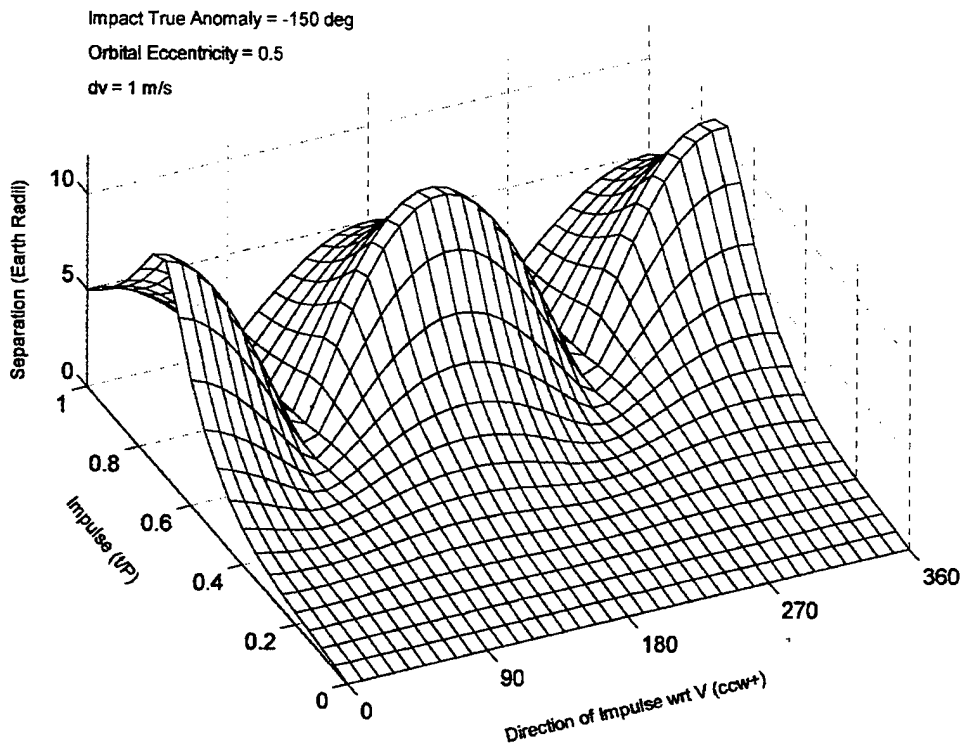
xdot(1) = -mur2*x(3)/r;        % vx 1st ODE
xdot(2) = -mur2*x(4)/r;        % vy 1st ODE
xdot(3) = x(1);                % x 1st ODE
xdot(4) = x(2);                % y 1st ODE
```

APPENDIX D. ANALYTIC METHOD SCENARIO MODELS

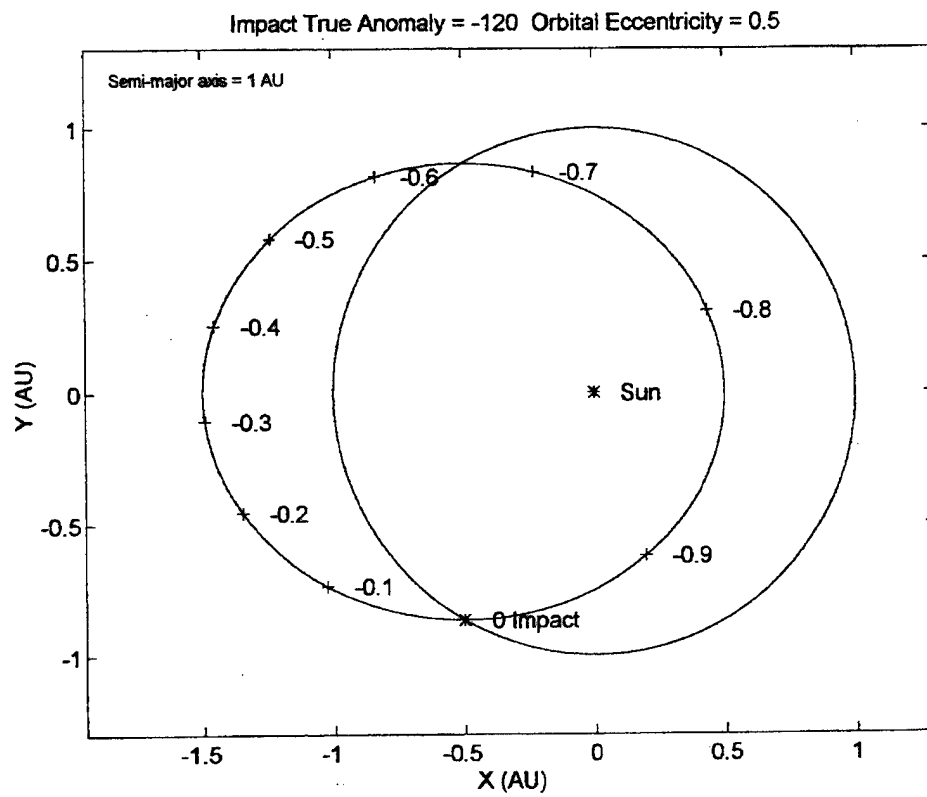
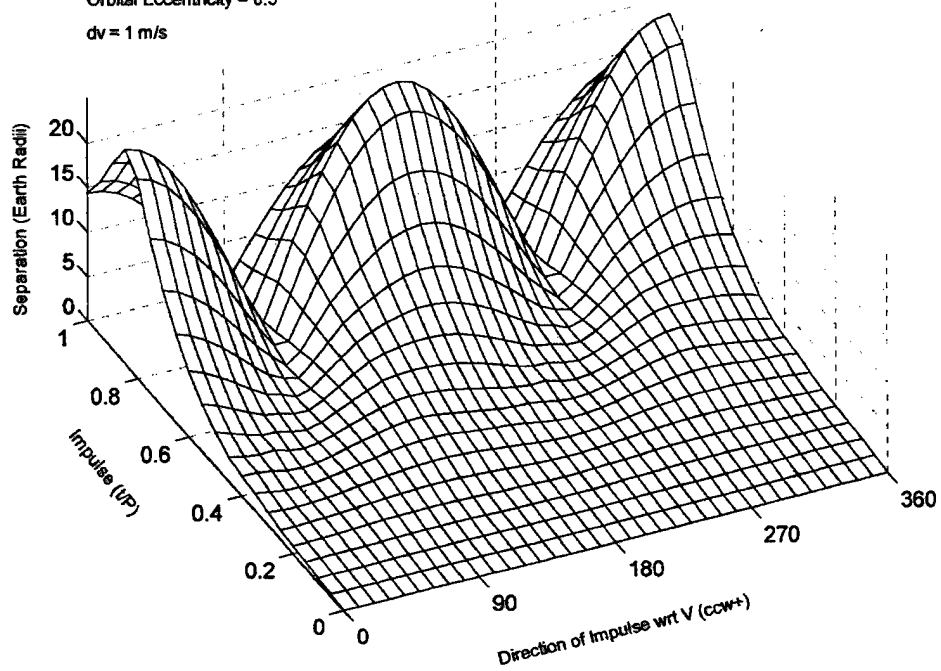
The following collection of figures represents the analysis performed using the numerical routine developed to perform the analytic solution. The scenarios are evaluated for impact true anomalies from -180° to $+180^\circ$ referenced to the asteroid orbit perihelion. The "steps" between impact scenarios is generally in 30° increments, however, for clarity purposes, the step size is reduced to 10° or even 1° intervals at times. The primary 30° increment figures occur where a "surface plot" and impact scenario plot appear together. At other increment values, two surface plots appear together.

For the surface plots at impact scenarios approaching $\pm 180^\circ$, the surface appears rough due to the coarseness of the step size in impulse time and impulse direction. At smaller step sizes the behavior is smooth and well behaved.





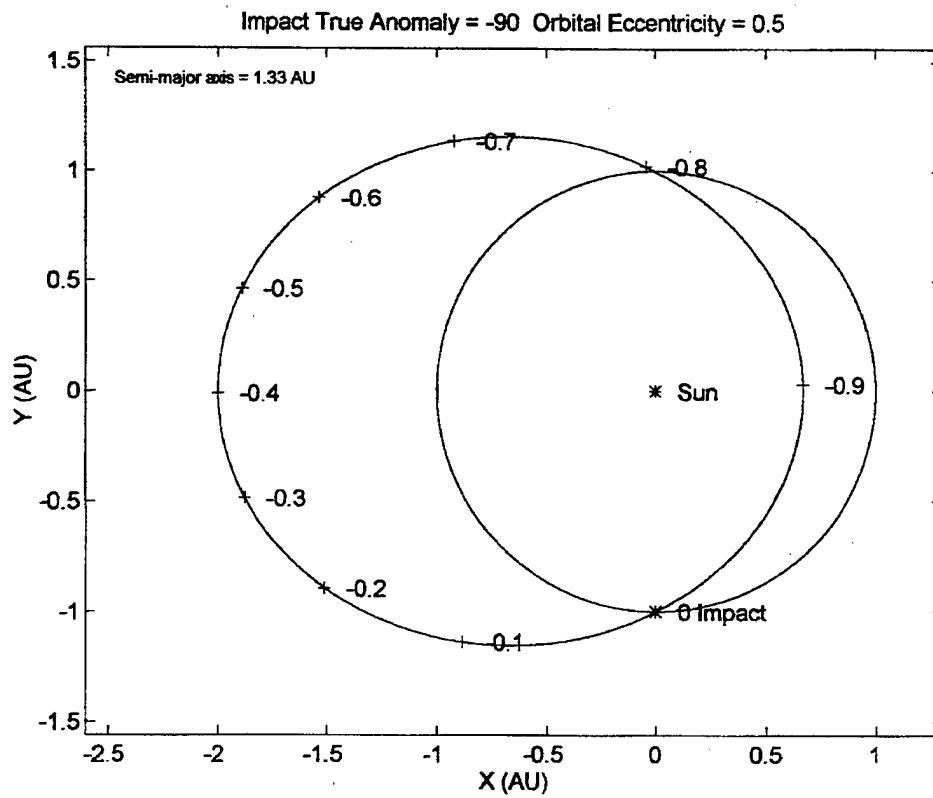
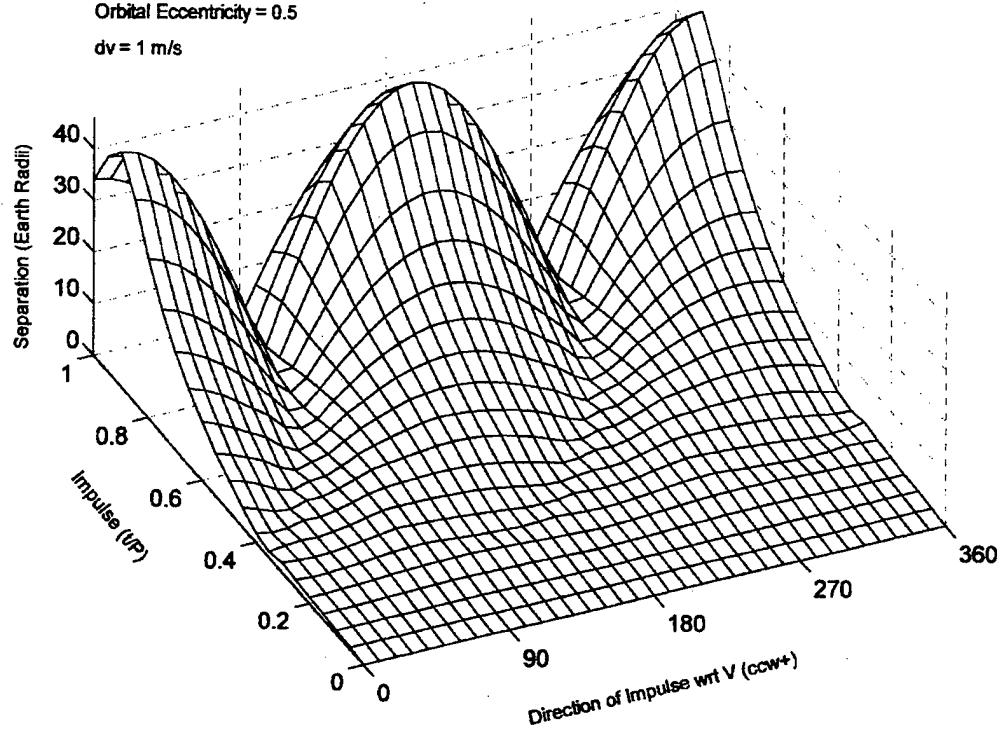
Impact True Anomaly = -120 deg
 Orbital Eccentricity = 0.5
 $dv = 1 \text{ m/s}$

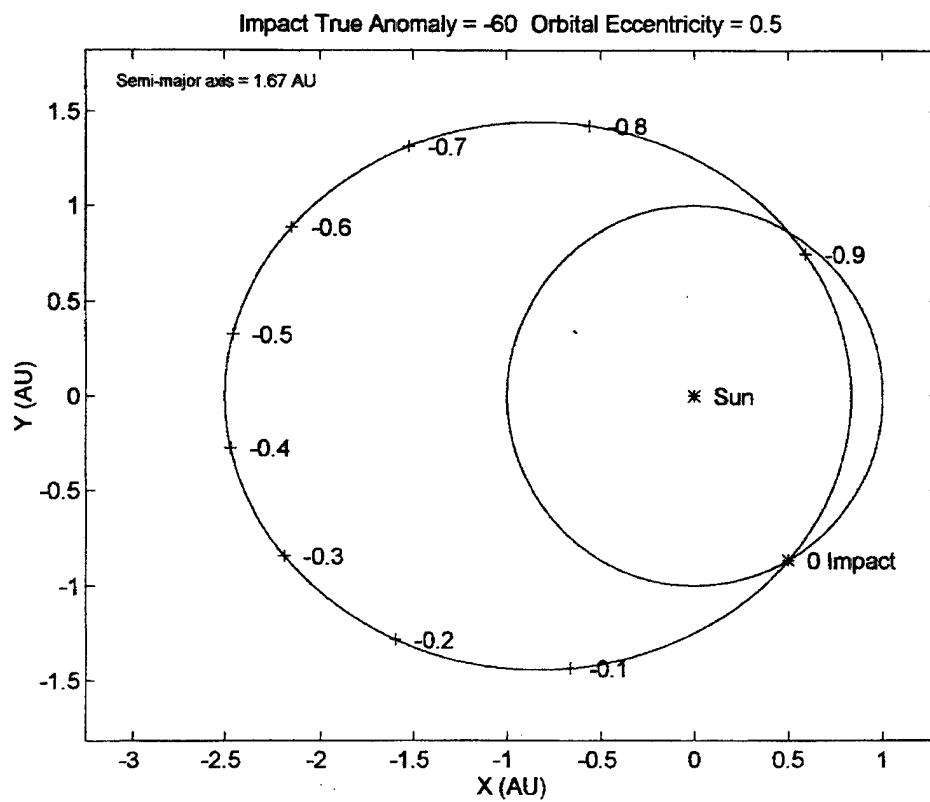
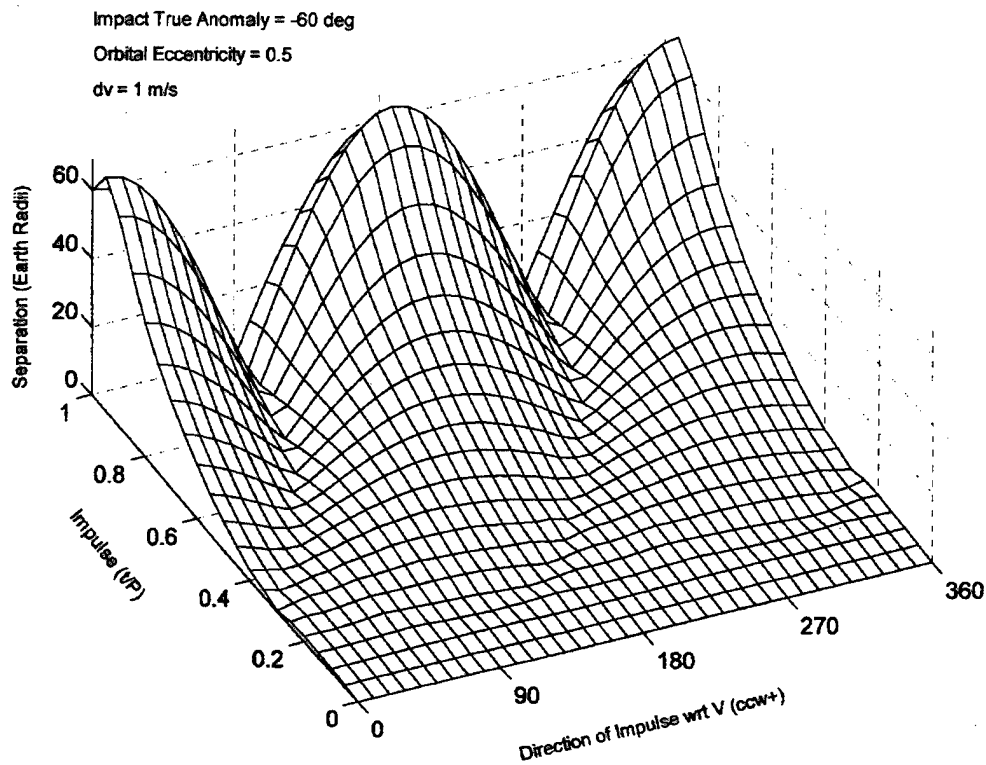


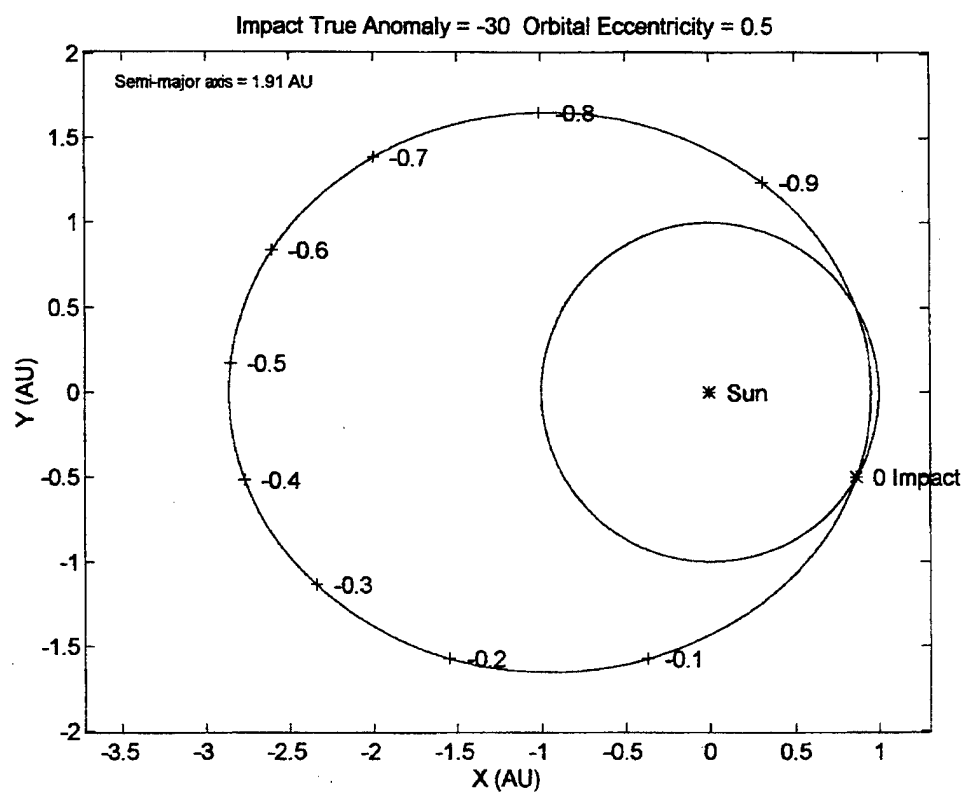
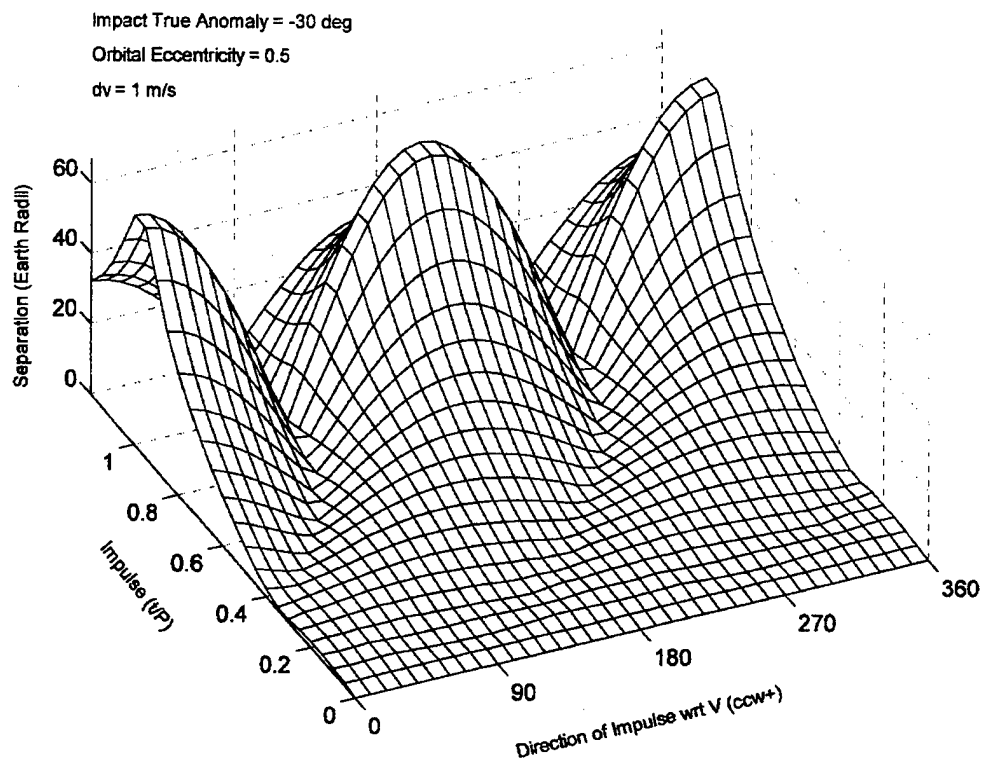
Impact True Anomaly = -90 deg

Orbital Eccentricity = 0.5

$dv = 1 \text{ m/s}$



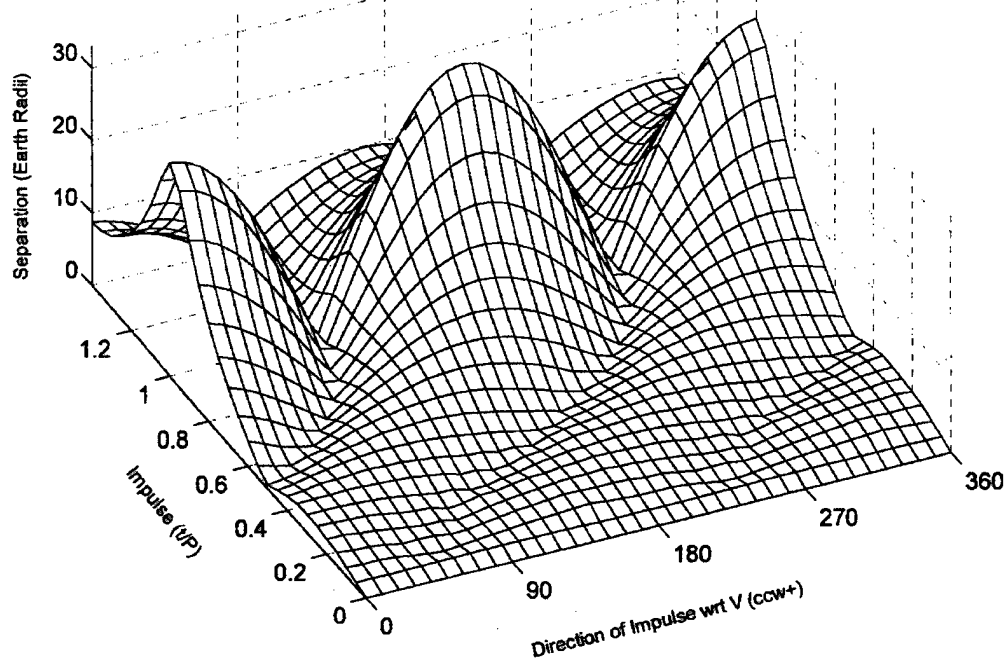




Impact True Anomaly = -10 deg

Orbital Eccentricity = 0.5

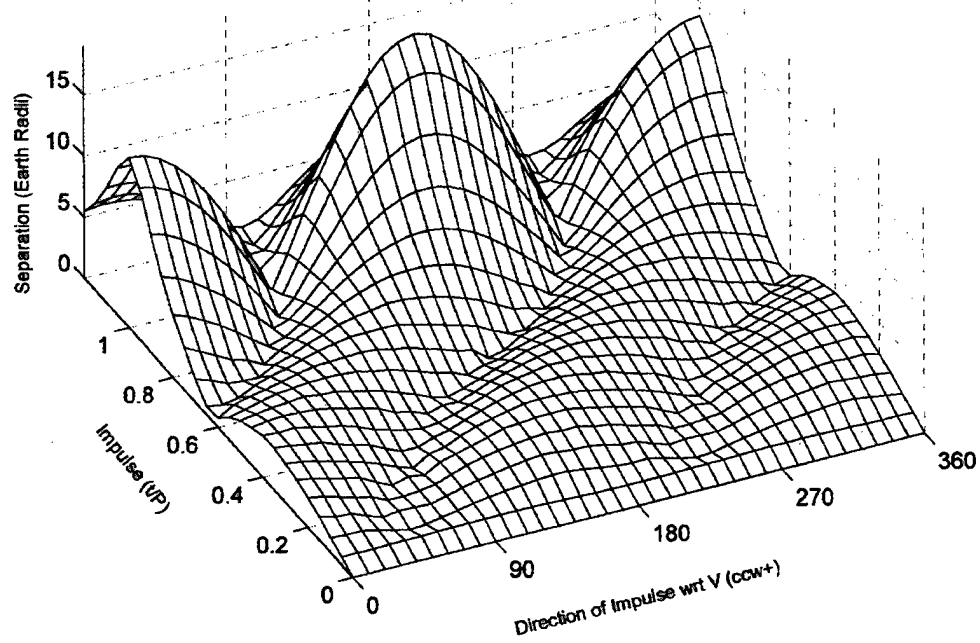
$dv = 1 \text{ m/s}$



Impact True Anomaly = -5 deg

Orbital Eccentricity = 0.5

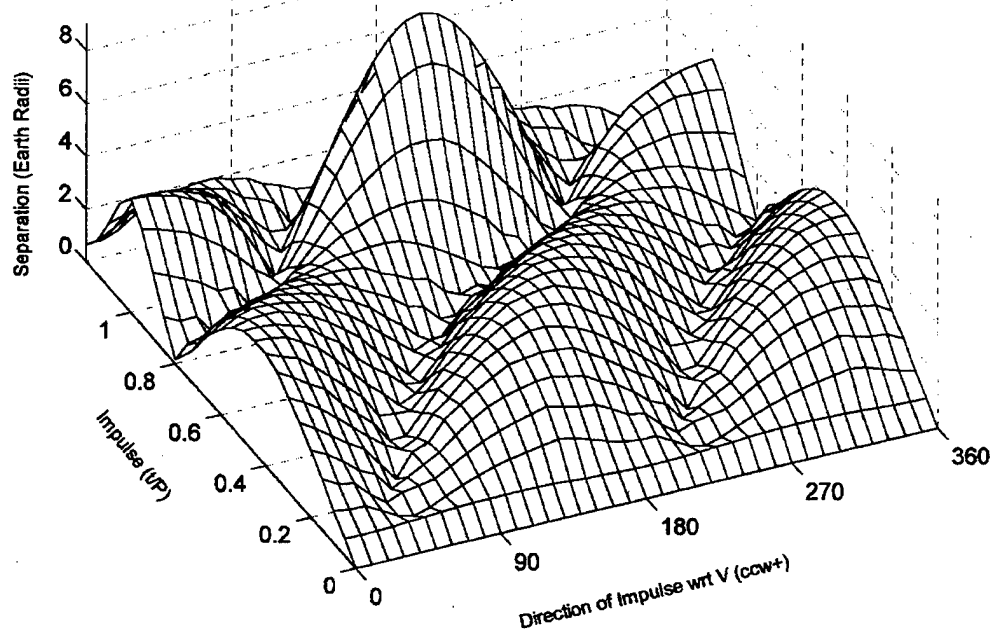
$dv = 1 \text{ m/s}$



Impact True Anomaly = -2 deg

Orbital Eccentricity = 0.5

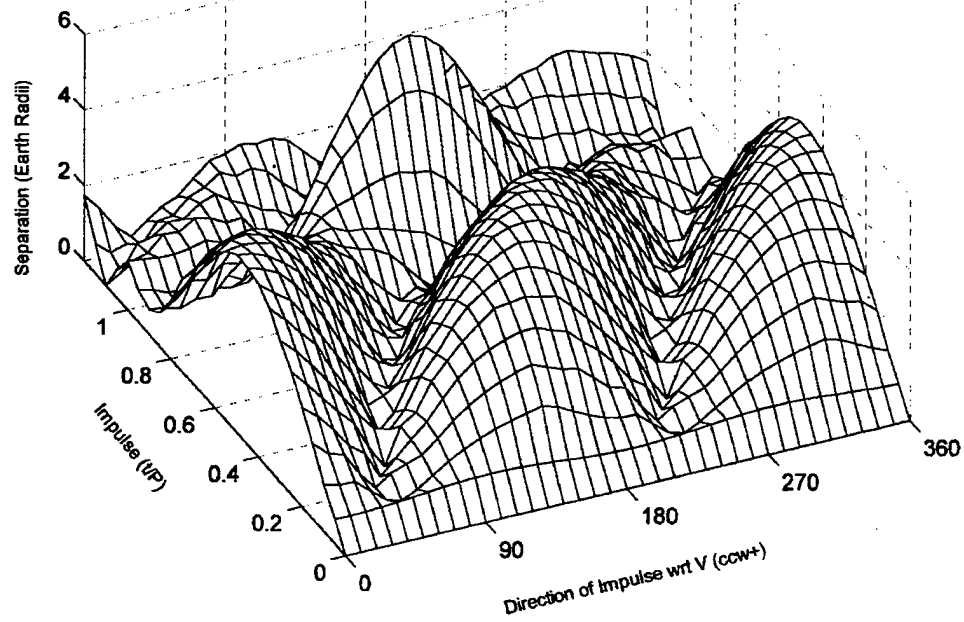
$dv = 1$ m/s

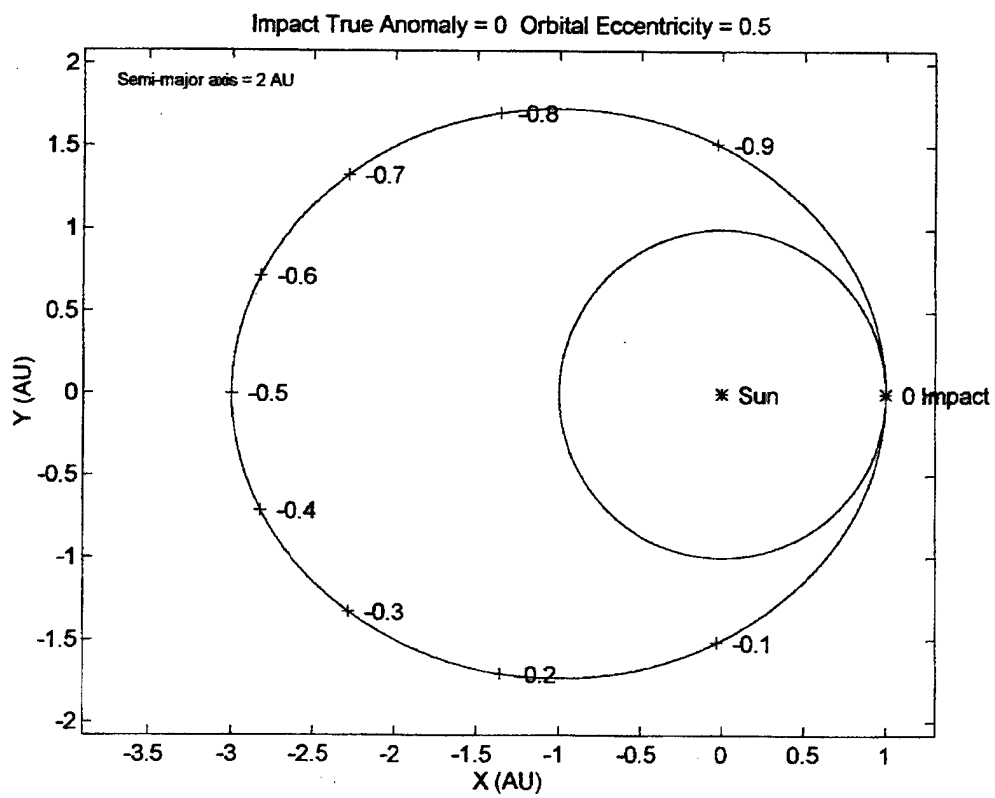
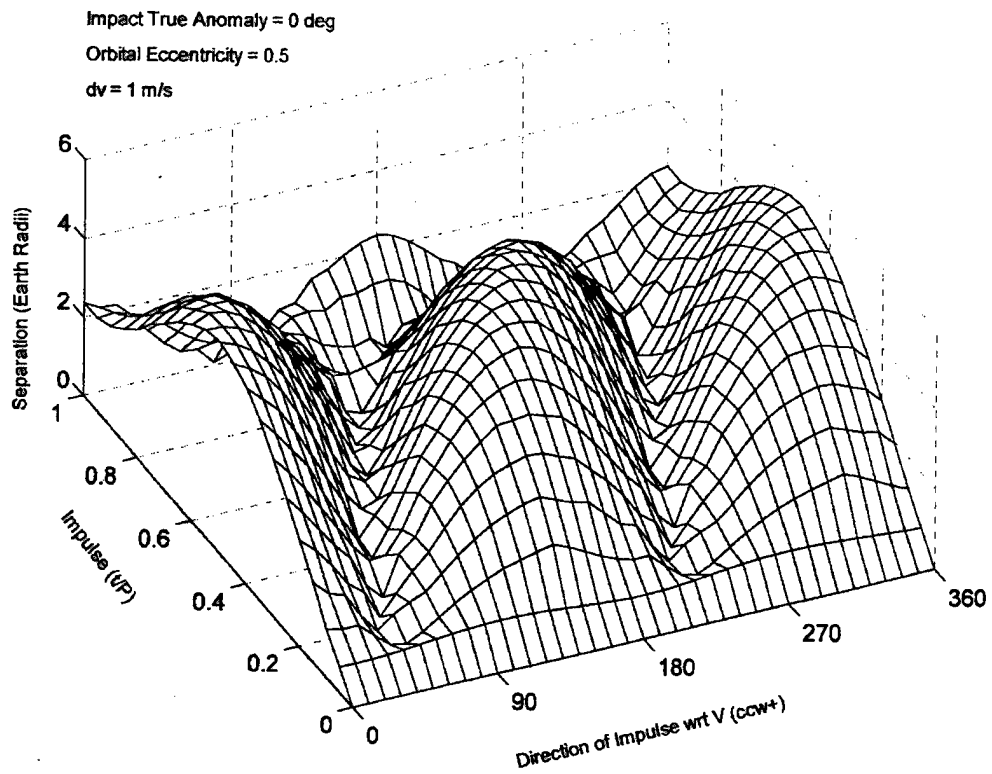


Impact True Anomaly = -1 deg

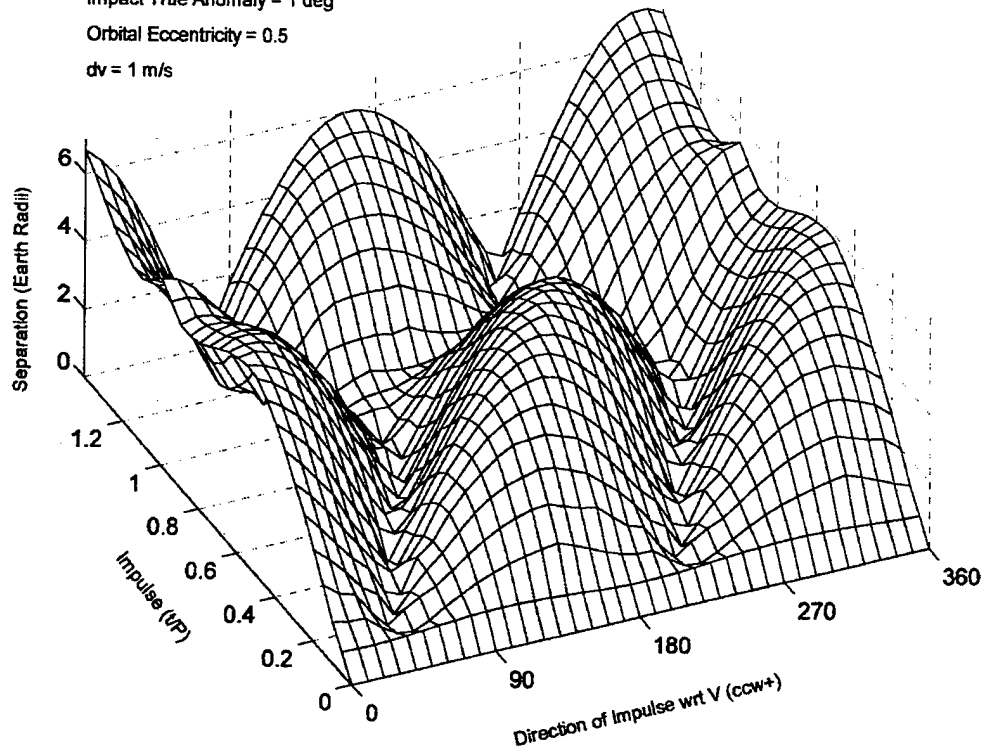
Orbital Eccentricity = 0.5

$dv = 1$ m/s

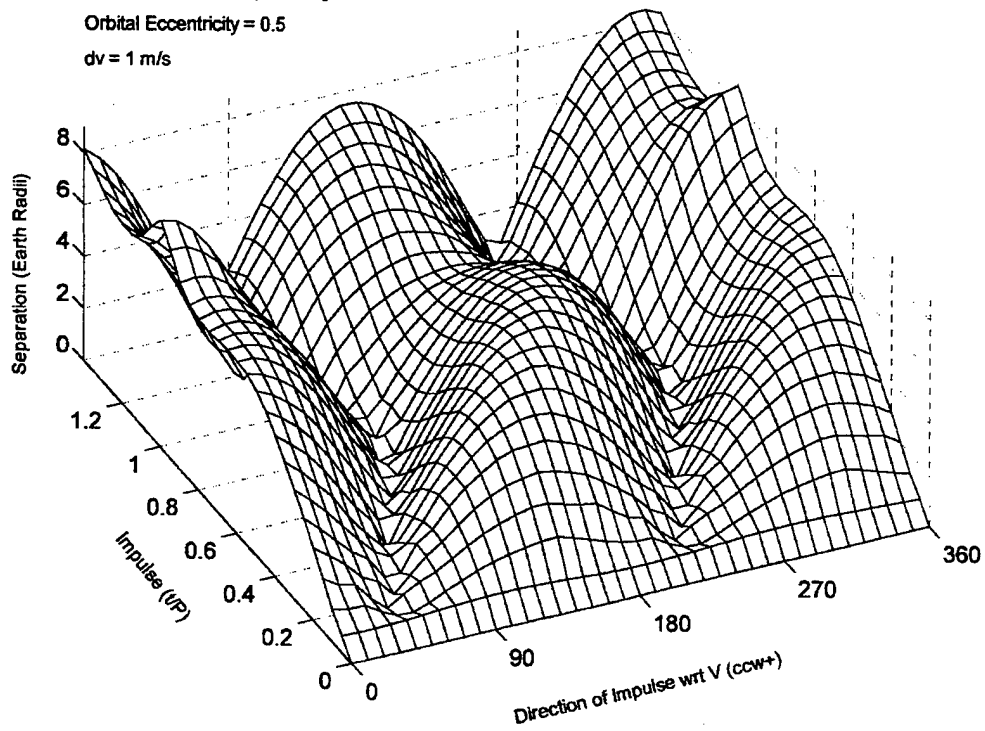




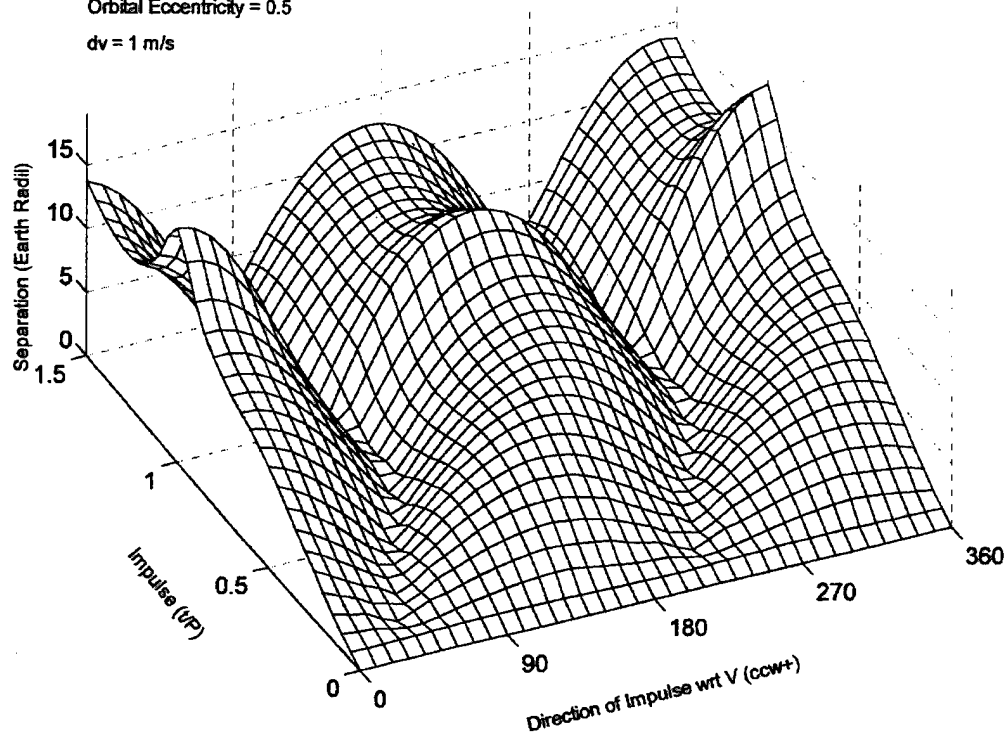
Impact True Anomaly = 1 deg
Orbital Eccentricity = 0.5
 $dv = 1 \text{ m/s}$



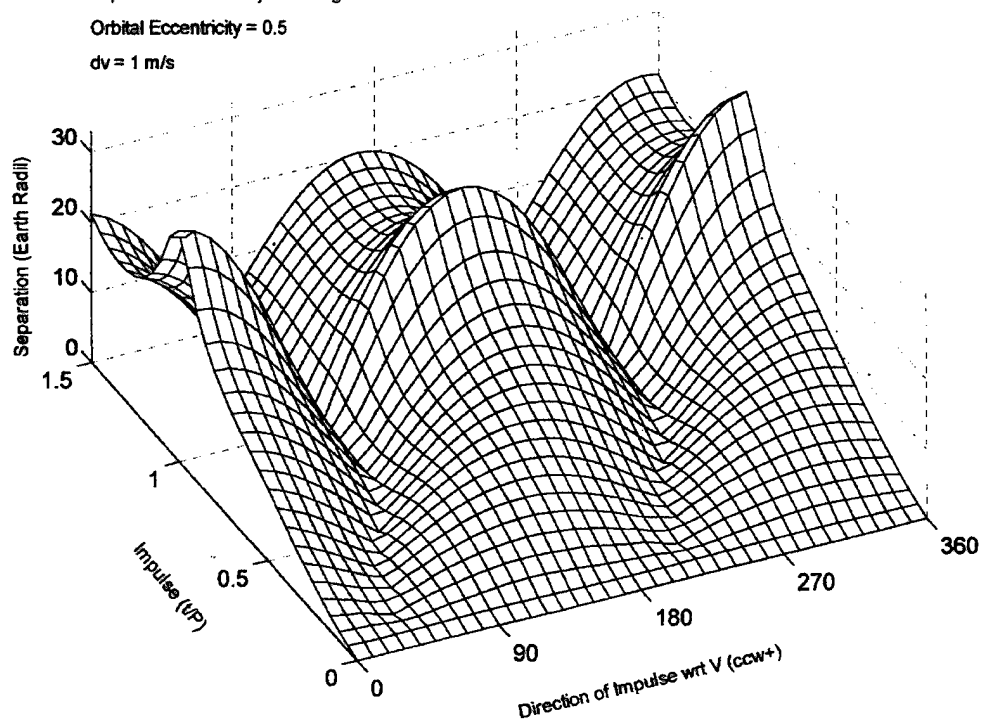
Impact True Anomaly = 2 deg
Orbital Eccentricity = 0.5
 $dv = 1 \text{ m/s}$



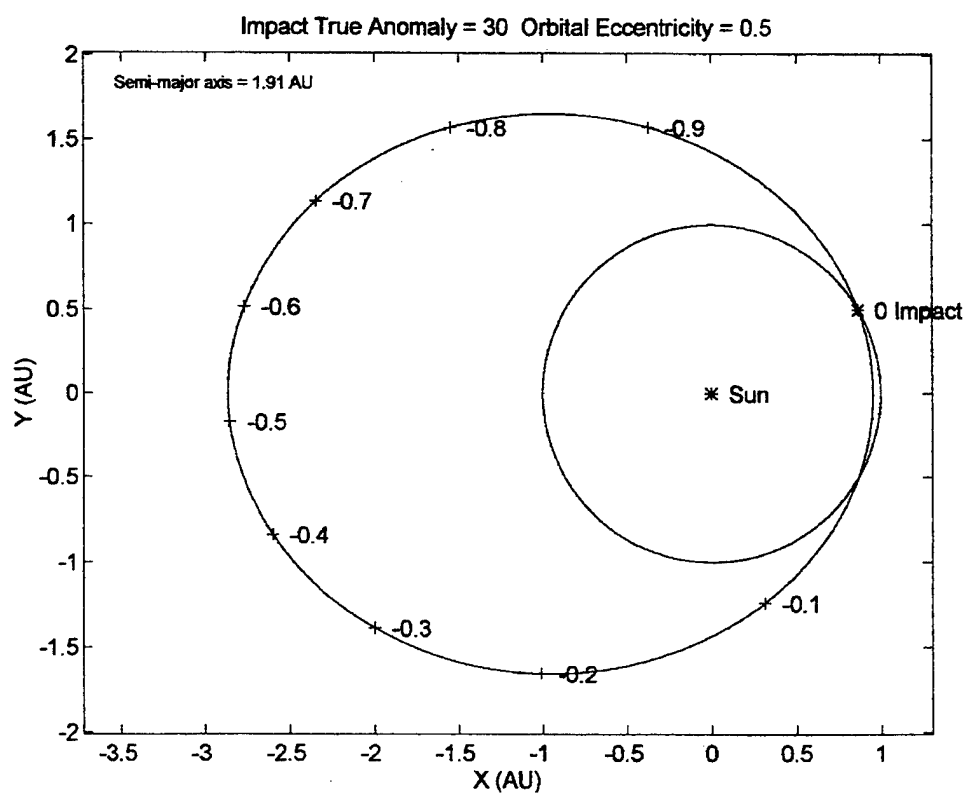
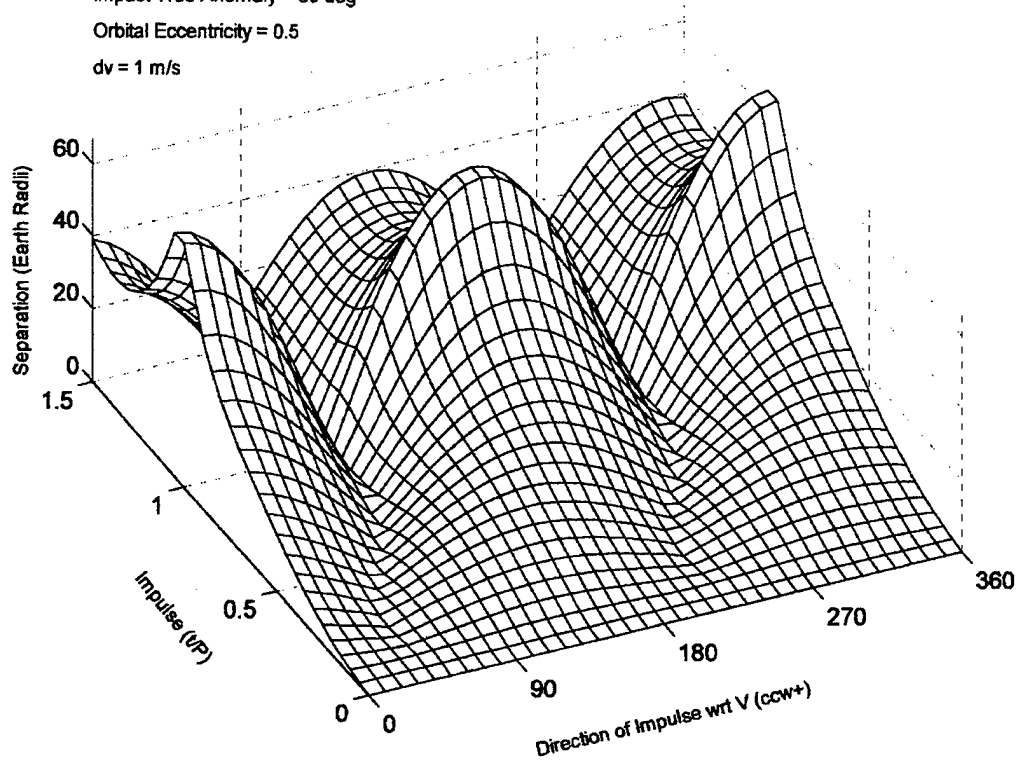
Impact True Anomaly = 5 deg
 Orbital Eccentricity = 0.5
 $dv = 1 \text{ m/s}$

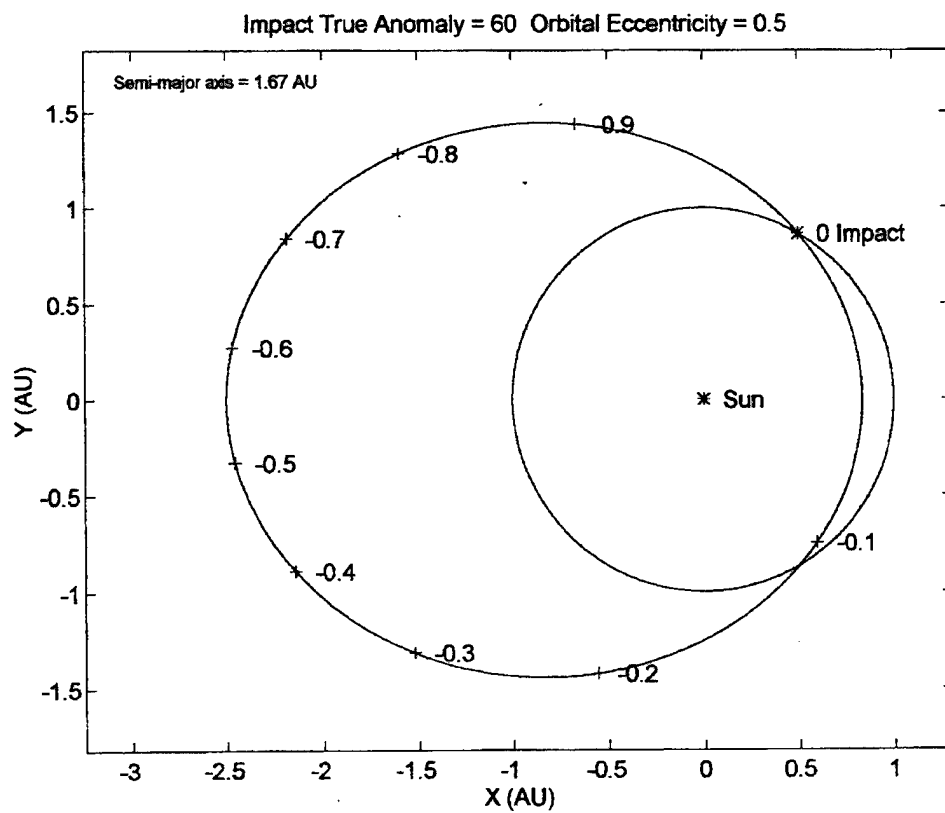
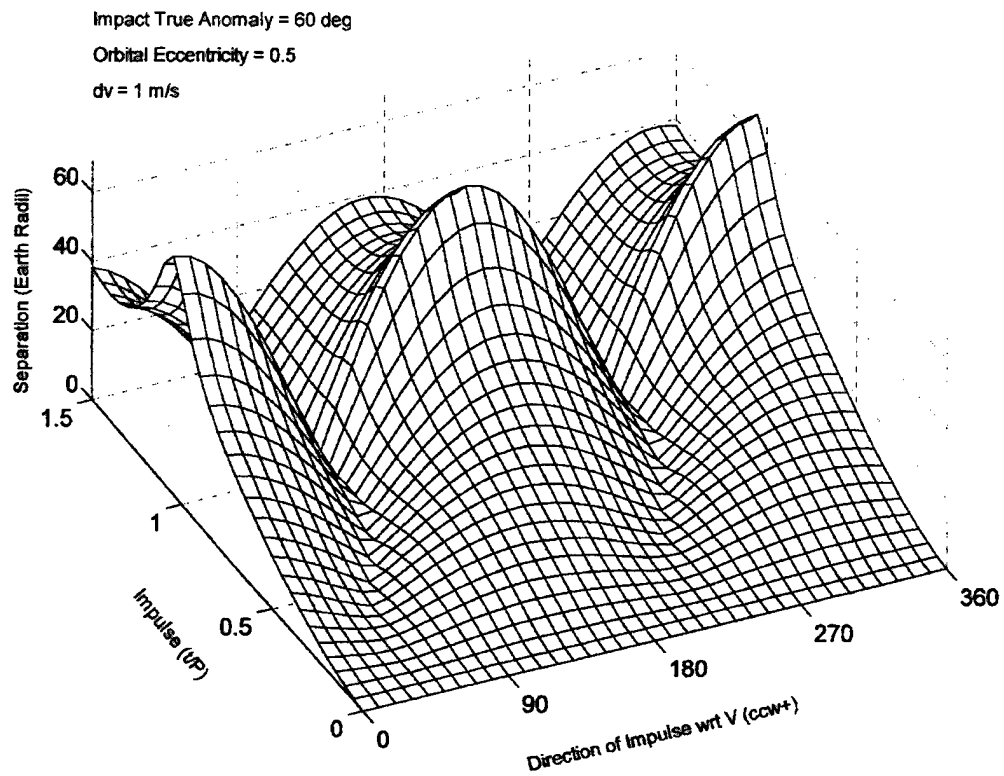


Impact True Anomaly = 10 deg
 Orbital Eccentricity = 0.5
 $dv = 1 \text{ m/s}$



Impact True Anomaly = 30 deg
 Orbital Eccentricity = 0.5
 $dv = 1 \text{ m/s}$

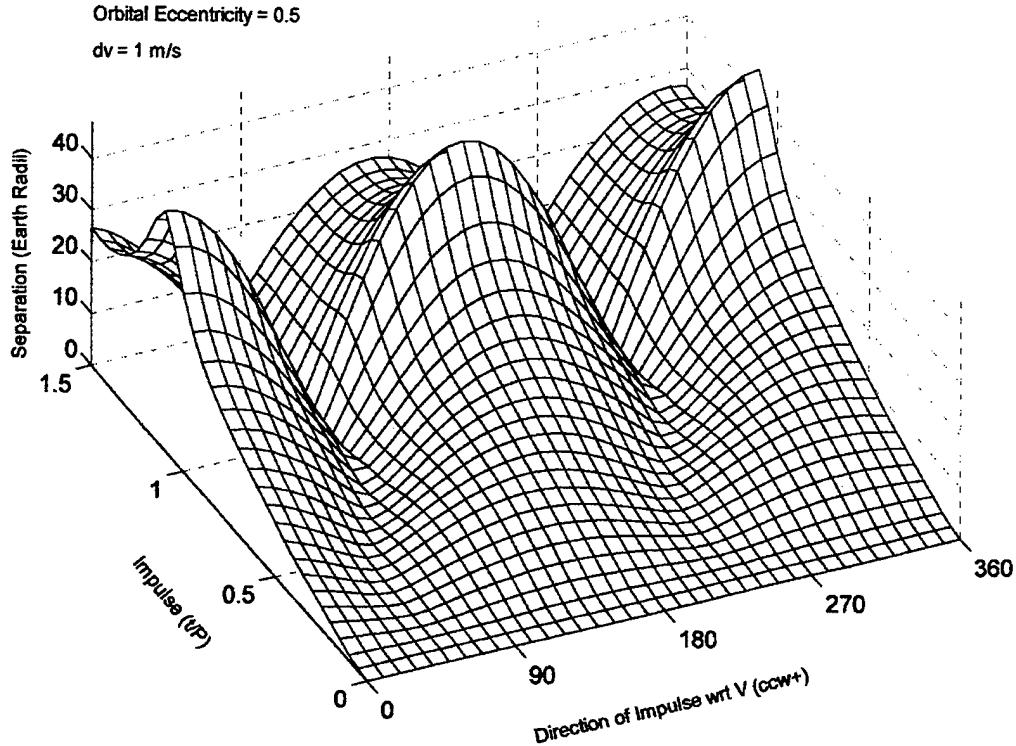




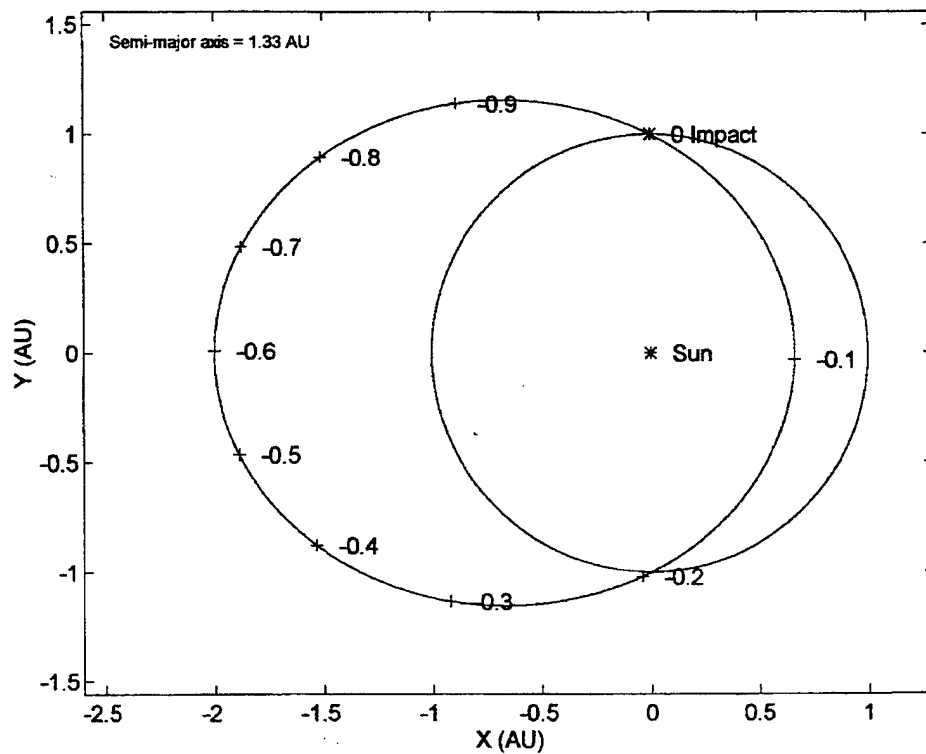
Impact True Anomaly = 90 deg

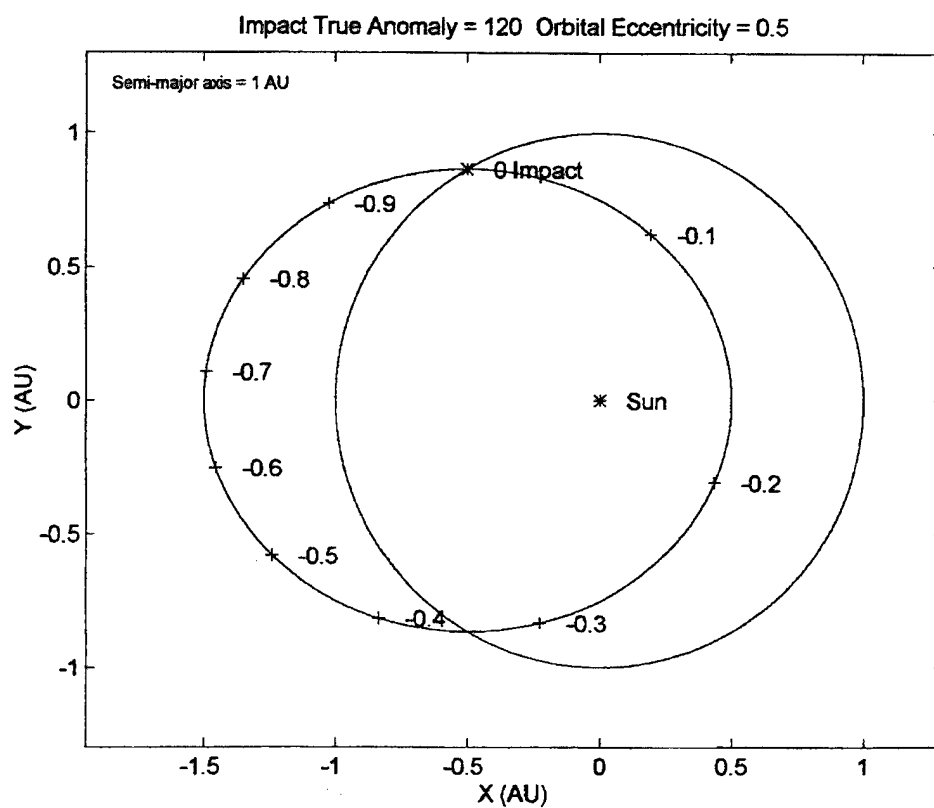
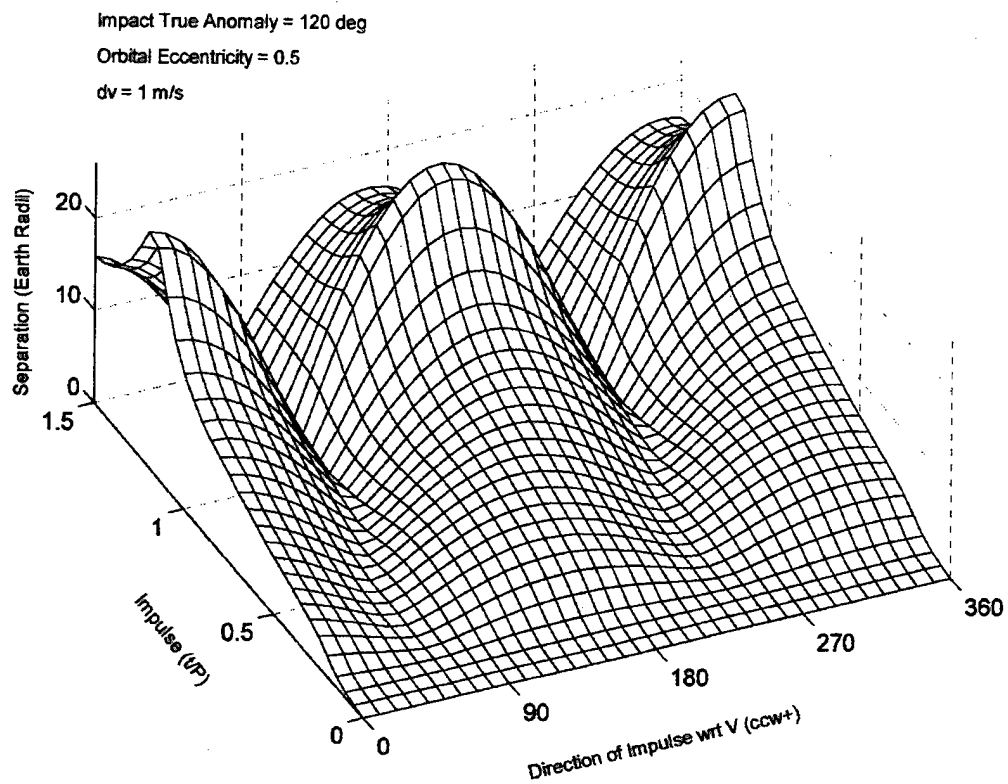
Orbital Eccentricity = 0.5

$dv = 1 \text{ m/s}$



Impact True Anomaly = 90 Orbital Eccentricity = 0.5

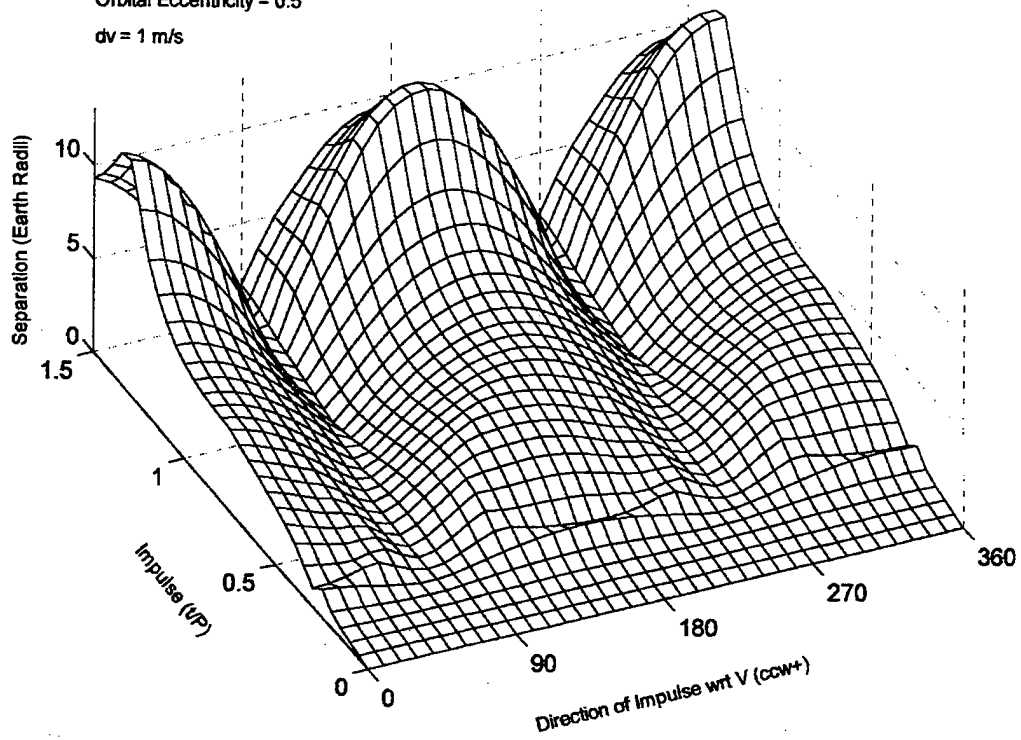




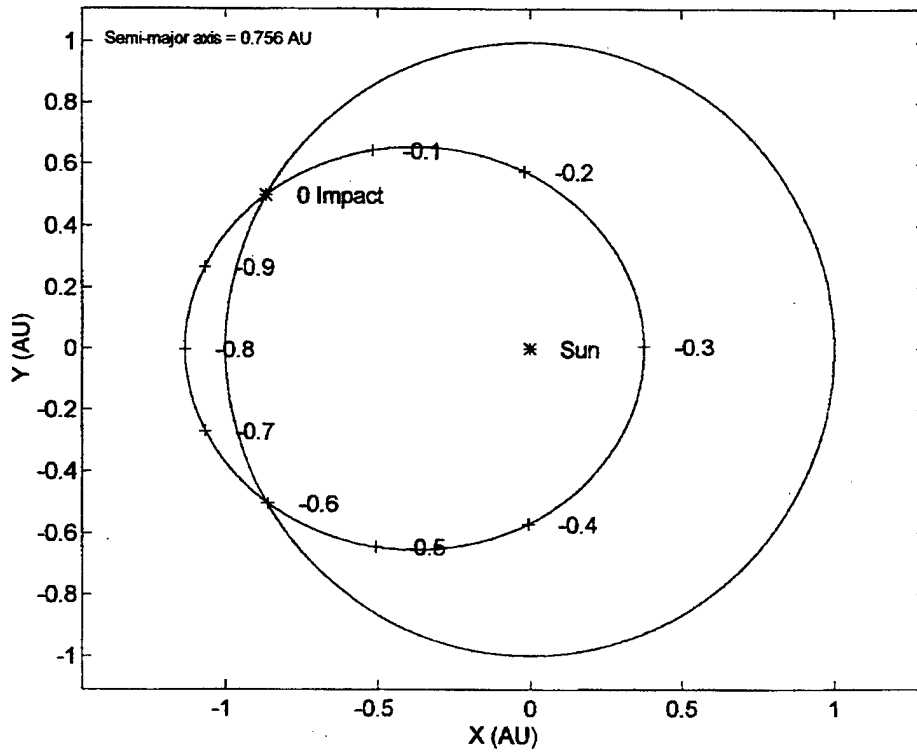
Impact True Anomaly = 150 deg

Orbital Eccentricity = 0.5

$dv = 1 \text{ m/s}$



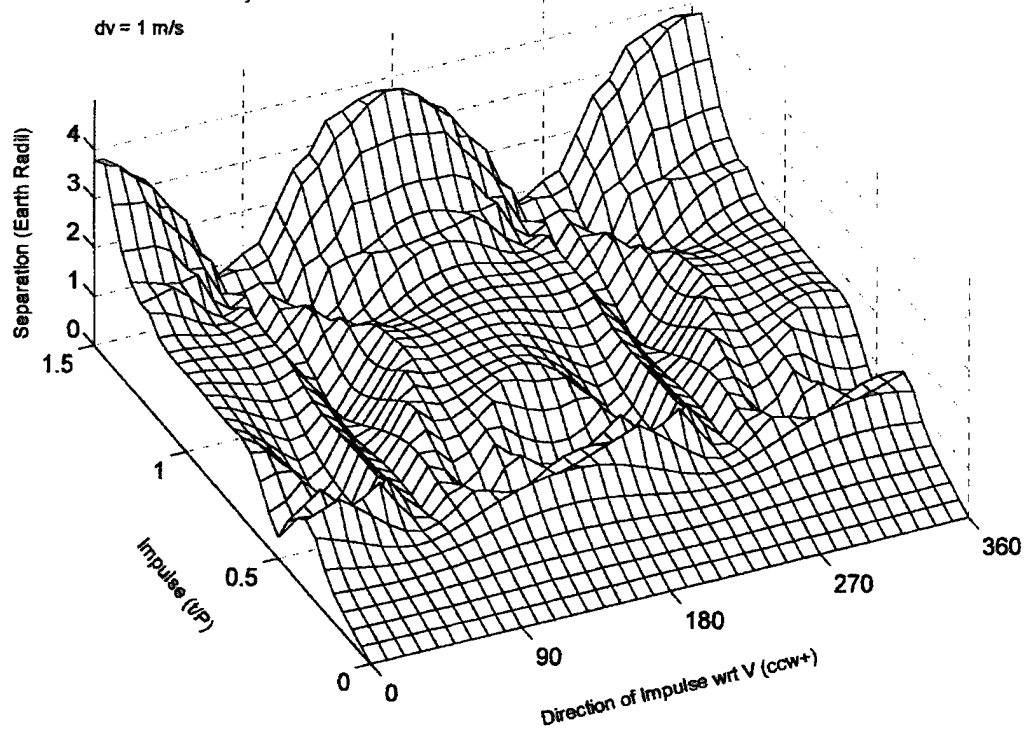
Impact True Anomaly = 150 Orbital Eccentricity = 0.5



Impact True Anomaly = 170 deg

Orbital Eccentricity = 0.5

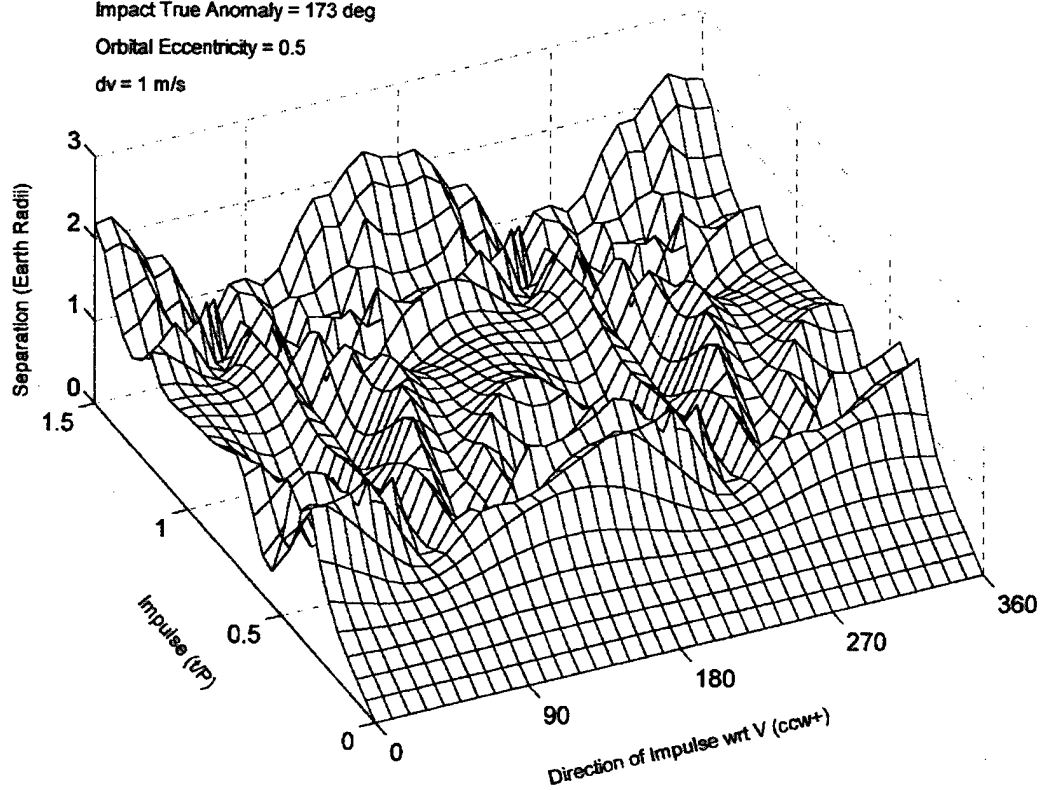
$dv = 1$ m/s



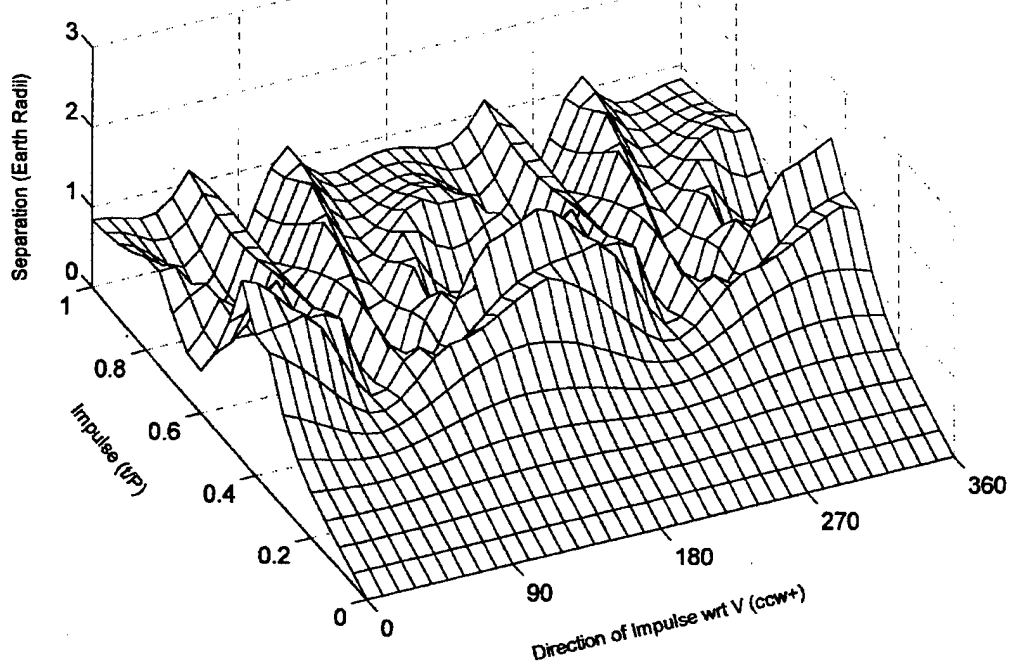
Impact True Anomaly = 173 deg

Orbital Eccentricity = 0.5

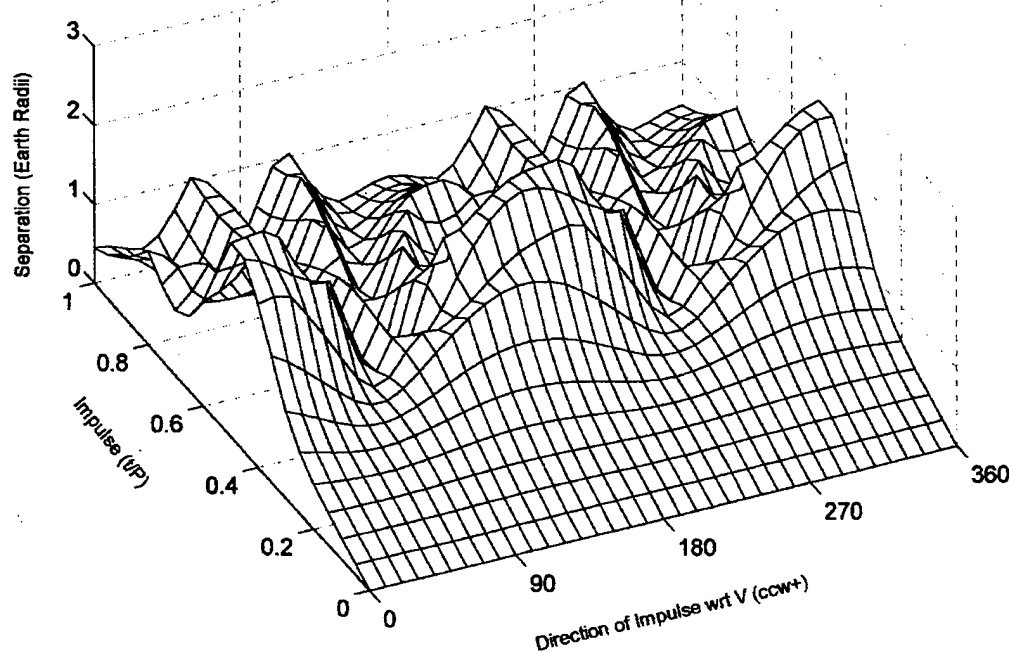
$dv = 1$ m/s

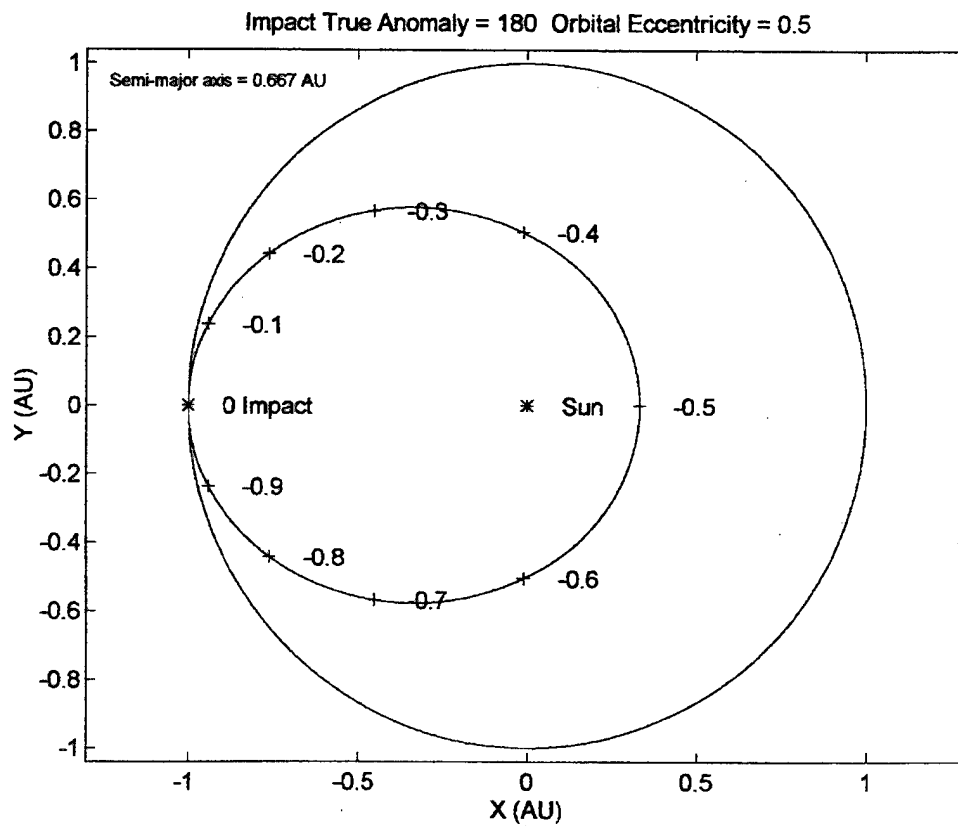
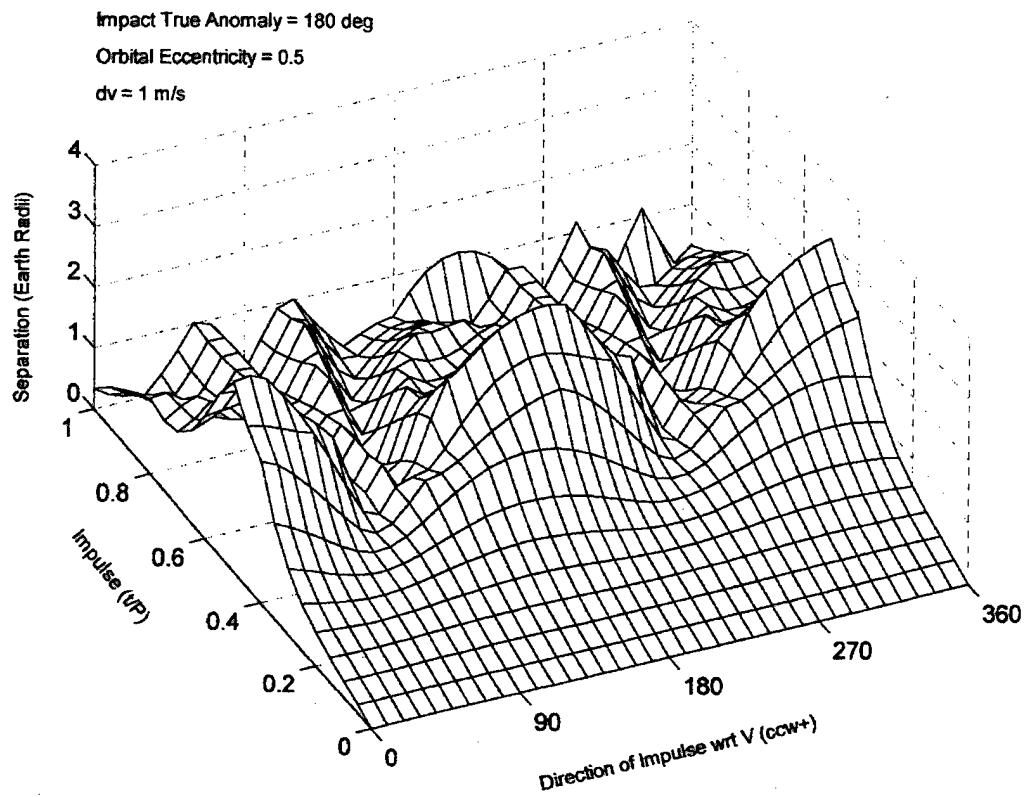


Impact True Anomaly = 175 deg
 Orbital Eccentricity = 0.5
 $dv = 1$ m/s

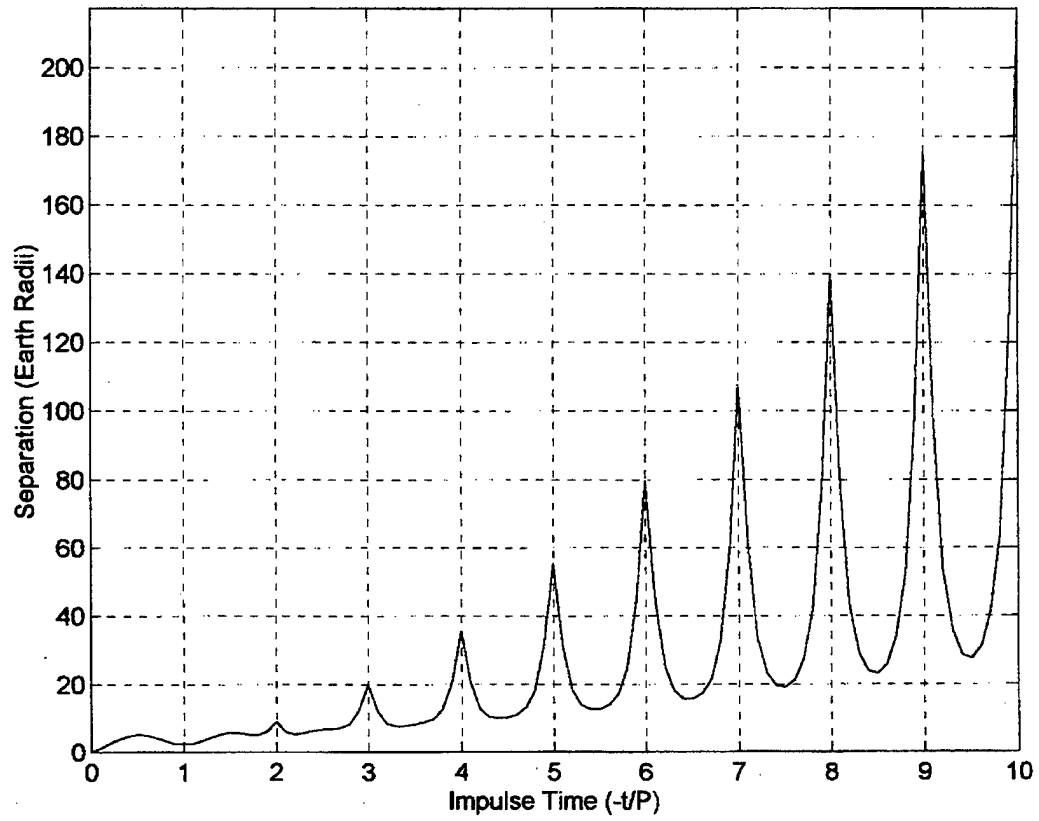


Impact True Anomaly = 178 deg
 Orbital Eccentricity = 0.5
 $dv = 1$ m/s





Impact True Anomaly = 0 deg, Orbital Eccentricity = 0.5, $dv = 1$ m/s



INITIAL DISTRIBUTION LIST

	Number of Copies
1. Defense Technical Information Center 8725 John J. Kingman Rd., STE 0944 Ft. Belvoir, Virginia 22060-6218	2
2. Dudley Knox Library Naval Postgraduate School 411 Dyer Rd. Monterey, California 93943-5101	2
3. Department Chairman, Code AA Department of Aeronautics and Astronautics Naval Postgraduate School Monterey, California 93943-5000	1
4. Department of Aeronautics and Astronautics Attn: Professor I. M. Ross, Code AA/Ro Naval Postgraduate School Monterey, California 93943-5000	5
5. Department Chairman, Code PH Department of Physics Naval Postgraduate School Monterey, California 93943-5000	1
6. Department of Physics Attn: Professor D. Cleary, Code PH/CI Naval Postgraduate School Monterey, California 93943-5000	2
7. Lieutenant Jeffrey T. Elder, USN 1 Cromwell Court Newport News, Virginia 23606	2